

# UC Berkeley

## SEMM Reports Series

### Title

Analysis and Design of Skew Box Girder Bridges

### Permalink

<https://escholarship.org/uc/item/7gc019n0>

### Authors

Comartin, Craig

Scordelis, Alex

### Publication Date

1972-11-01

REPORT NO.  
UCSESM 72-14

STRUCTURES AND MATERIALS RESEARCH  
DEPARTMENT OF CIVIL ENGINEERING

**ANALYSIS AND DESIGN  
OF SKEW  
BOX GIRDER BRIDGES**

by  
C. D. COMARTIN  
and  
A. C. SCORDELIS

IN COOPERATION WITH THE STATE OF CALIFORNIA,  
BUSINESS AND TRANSPORTATION AGENCY, DEPART-  
MENT OF PUBLIC WORKS, DIVISION OF HIGHWAYS AND  
U. S. DEPARTMENT OF TRANSPORTATION, FEDERAL HIGH-  
WAY ADMINISTRATION.

DECEMBER 1972

COLLEGE OF ENGINEERING  
OFFICE OF RESEARCH SERVICES  
UNIVERSITY OF CALIFORNIA  
BERKELEY CALIFORNIA

Structures and Materials Research  
Department of Civil Engineering  
Division of Structural Engineering  
and  
Structural Mechanics

UC-SESM Report No. 72-14

ANALYSIS AND DESIGN OF SKEW BOX GIRDER BRIDGES

by

C. D. Comartin  
Research Assistant

and

A. C. Scordelis  
Professor of Civil Engineering

In cooperation with  
State of California  
Business and Transportation Agency  
Department of Public Works  
Division of Highways  
Under Research Technical Agreement  
No. 13945-14648  
and  
U. S. Department of Transportation  
Federal Highway Administration

College of Engineering  
Office of Research Services  
University of California  
Berkeley, California

December 1972

### ABSTRACT

A detailed presentation is given of the reduction, analysis and interpretation of theoretical results obtained using a finite element computer program CELL to analyze a series of single span, simply supported, four cell, skew box girder bridges having varying angles of skew and span lengths. These theoretical results are compared with experimental results from a previous study on aluminum model bridges of identical dimensions. This investigation of the behavior of the skew box girder bridges includes a study of reactions, internal longitudinal stresses, external and internal total section moments, transverse distribution of the total moment to each girder, and the effects of the addition of a midspan diaphragm. Both point live loads and dead load on the bridges are considered. On the basis of these results, an approximate simplified method of analysis is proposed. Finally some tentative recommendations for the design of skew box girder bridges are made.

### KEYWORDS

Skew box girder bridges; finite element method; computer program; bridge analysis; bridge design; bridge model; theoretical study; experimental study; approximate analysis

TABLE OF CONTENTS

	<u>Page</u>
ABSTRACT . . . . .	i
KEYWORDS . . . . .	i
TABLE OF CONTENTS . . . . .	ii
LIST OF TABLES . . . . .	v
LIST OF FIGURES . . . . .	vii
1. INTRODUCTION . . . . .	1
1.1 Purpose of the Study . . . . .	1
1.2 Experimental Work . . . . .	2
1.3 Scope of the Study . . . . .	8
2. THEORETICAL ANALYSES . . . . .	10
2.1 General . . . . .	10
2.2 Finite Element Solution . . . . .	12
2.3 Mesh Sizes and Computer Times . . . . .	16
2.4 Theoretical Results . . . . .	19
2.4.1 Statics Checks . . . . .	22
2.4.2 Reactions . . . . .	23
2.4.3 $N_{xx}$ Forces in Top and Bottom Plates . . . . .	23
2.4.4 Deflections . . . . .	23
2.4.5 Total Longitudinal Moment at Midspan . . . . .	23
2.4.6 Distribution of Total Moment to Individual Girders . . . . .	24
2.5 Self-Consistency of Theoretical Results . . . . .	25
3. COMPARISON OF THEORETICAL AND EXPERIMENTAL RESULTS . . . . .	28
3.1 General . . . . .	28
3.2 Deflections . . . . .	28

	<u>Page</u>
3.3 Reactions . . . . .	41
3.4 External Midspan Moments . . . . .	49
3.5 Longitudinal Plate Forces $N_{xx}$ . . . . .	52
3.6 Distribution of Longitudinal Moment to Individual Girders . . . . .	64
3.7 Transverse Bending Moments . . . . .	75
3.8 Summary . . . . .	82
4. GENERAL BEHAVIOR AND PROPOSED APPROXIMATE ANALYSIS . . . . .	84
4.1 General . . . . .	84
4.2 Reactions and Total Midspan Moment for Point Loads at Midspan . . . . .	85
4.3 Reactions and Total Moment for Point Loads along the Longitudinal Centerline of Bridge . . . . .	90
4.4 Approximate Analysis for Arbitrary Point Loads . . . . .	94
4.5 Transverse Distribution of Total Longitudinal Moment . . . . .	97
4.6 Effect of Midspan Diaphragm . . . . .	104
4.7 Dead Load Considerations . . . . .	105
4.8 Support Conditions . . . . .	109
5. DESIGN CONSIDERATIONS . . . . .	114
5.1 General . . . . .	114
5.2 Present Design Procedures . . . . .	114
5.3 Tentative Recommended Design Procedure for Live Loads . . . . .	120
5.3.1 Determination of Critical Total Design Moment at Any Section . . . . .	120
5.3.2 Transverse Distribution of Total Moment at a Section . . . . .	124
5.4 Design for Dead Load Moments . . . . .	125
5.5 Transverse Slab Moments . . . . .	126

	<u>Page</u>
5.6 Other Design Considerations . . . . .	127
6. CONCLUSIONS AND RECOMMENDATIONS FOR IMPLEMENTATION AND FURTHER STUDY . . . . .	130
7. ACKNOWLEDGEMENTS . . . . .	133
8. REFERENCES . . . . .	135

## APPENDIX A

Theoretical Results from CELL Program . . . . .	A1
MODEL 1A (45°/53.5") . . . . .	A3
MODEL 1B (45°/53.5") . . . . .	A6
MODEL 2A (30°/47.4") . . . . .	A10
MODEL 2B (30°/47.4") . . . . .	A13
MODEL 3A (45°/35.5") . . . . .	A17
MODEL 3B (45°/35.5") . . . . .	A20
MODEL 4A (30°/29.7") . . . . .	A24
MODEL 4B (30°/29.7") . . . . .	A27
MODEL 5A (0°/22.5") . . . . .	A31
MODEL OB (0°/69.0") . . . . .	A35

LIST OF TABLES

<u>Table</u>	<u>Title</u>	<u>Page</u>
1.1	Dimensions of Models and Prototypes . . . . .	4
2.1	Finite Element Solution Information . . . . .	17
3.1	Ratio of Theoretical to Experimental Midspan Deflections Under Webs 1, 3, and 5 for Midspan Point Load on Girders 3, 4, or 5 . . . . .	29
3.2	Comparison Between Theory and Experiment for External Midspan Moments and Reaction Couples for a Midspan Point Load on Girder 3 . . . . .	52
3.3	Ratio of Theoretical to Experimental External Moment at Midspan for all Load Positions . . . . .	53
3.4	Ratio of Theoretical to Experimental Values of Maximum Percentage of Total Moment at Section 0-0 Taken by Each Girder Due to a Point Load at the Midspan Section . . . . .	76
4.1	Comparison of Theoretical and Approximate Total Midspan Moment Coefficients for a Point Load W at Midspan Center. . . . .	88
4.2	Maximum Negative Reaction, R <sub>4</sub> , Due to Point Load W . . . . .	90
4.3	Comparison of Coefficients for Total Moment at Loaded Cross-section Due to a Point Load W on Skew Bridges and Straight Bridges . . . . .	91
4.4	Ratio of Approximate to Theoretical Total Moment at Midspan Section for All Point Load Positions. . . . .	98
4.5a	Percentage of Total Longitudinal Moment at Section 0-0 Taken by Each Girder for Equal Loads at All Five Points Shown . . . . .	100
4.5b	Percentage of Total Longitudinal Moment at Section 0-0 Taken by Each Girder for Equal Loads at All Five Points Shown . . . . .	101
4.5c	Percentage of Total Longitudinal Moment at Section 0-0 Taken by Each Girder for Equal Loads at All Three Points Shown . . . . .	102



<u>Table</u>	<u>Title</u>	<u>Page</u>
4.5d	Percentage of Total Longitudinal Moment at Section 0-0 Taken by Each Girder for Equal Loads at All Thirteen Points Shown . . . . .	103
4.6	Dead Load Reactions in Terms of Total Load, W, and Midspan Moments in Terms of WL . . . . .	109
4.7a	Comparison of Results for Model 1A(45°/53.5") for Supports at Corners vs. All Girders Supported . . .	111
4.7b	Comparison of Results for Model 3A(45°/35.5") for Supports at Corners vs. All Girders Supported . . .	112

LIST OF FIGURES

<u>Figure</u>	<u>Title</u>	<u>Page</u>
1.1	Dimensions of Prototype and 1/29th Scale Model Cross-section . . . . .	3
1.2	Plan Dimensions of Models 0 through 5 . . . . .	5
1.3	Typical Skew Bridge . . . . .	7
2.1	Displacements and Internal Forces on a Typical Element Taken from the Bridge . . . . .	11
2.2	Finite Element Representation of General Box Girder Bridge . . . . .	11
2.3	Deck Elements Used in CELL Program . . . . .	14
2.4	Web Elements Used in CELL Program . . . . .	14
2.5	Typical Finite Element Mesh Layout for Model 4 . . . . .	18
2.6	Division of Cross-section into Individual Girders . . . . .	25
3.1-3.5	Comparison of Theoretical and Experimental Deflec- tions at Midspan . . . . .	30-34
3.6	Component Test for Shear Slip . . . . .	38
3.7	Component Test for Moment Continuity . . . . .	40
3.8	Influence Lines for Reaction R1 for Model 1A (45°/53.5"), Loads on Girders 1, 3, and 5 . . . . .	42
3.9	Influence Lines for Reaction R2 for Model 1A (45°/53.5"), Loads on Girders 1, 3, and 5 . . . . .	43
3.10	Influence Lines for Reaction R1 (Coefficients of W), Loads Along Girder 3 . . . . .	44
3.11	Influence Lines for Reaction R2 (Coefficients of W), Loads Along Girder 3 . . . . .	45
3.12	Influence Lines for Reaction R1 (Coefficients of W), Loads on Right Transverse Sections MM and QQ . . . . .	46
3.13	Influence Lines for Reaction R2 (Coefficients of W), Loads on Right Transverse Sections MM and QQ . . . . .	47

<u>Figure</u>	<u>Title</u>	<u>Page</u>
3.14	Total Moment on Sections Normal to the Longitudinal Axis for a Load at Midspan Center . . . .	50
3.15	Influence Lines for Total Midspan Moment (Coefficients of WL) for Loads on Girders 3, 4, and 5 of Model 1A (45°/53.5") . . . . .	51
3.16-3.24	Transverse Distribution of Axial Forces Per Unit Width in Top and Bottom Plates (N <sub>xx</sub> ) at Section 0-0 .	55-63
3.25-3.34	Percentage of Total Moment at Section 0-0 Carried by Each Girder . . . . .	65-74
3.35-3.39	Theoretical and Experimental Transverse Plate Bending Moments (in.-lb./in.) in Top and Bottom Decks . . . . .	77-81
4.1	Total Moment at Midspan for a Point Load at Midspan Center of the Bridge . . . . .	87
4.2	Point Load on Longitudinal Centerline of Bridge . . . .	92
4.3	Point Load at Arbitrary Position on Skew Bridge . . . .	95
4.4	Deflection in Inches of Girders 1, 2, and 3 in Model 1A due to Dead Load . . . . .	107
4.5	Dead Load Midspan Moment Coefficient as a Function of the Angle of Skew, $\theta$ . . . . .	108
5.1	Standard HS 20-44 Truck of the American Association of State Highway Officials (AASHO) . . . . .	116
5.2	Typical Influence Surface for Midspan Moment in Model 4A . . . . .	123
A.1	Skew Box Girder Bridge Model No. 1, Span = 53.50 inches, Skew Angle = 45° . . . . .	A2
A.2	Skew Box Girder Bridge Model No. 2, Span = 47.43 inches, Skew Angle = 30° . . . . .	A9
A.3	Skew Box Girder Bridge Model No. 3, Span = 35.50 inches, Skew Angle = 45° . . . . .	A16
A.4	Skew Box Girder Bridge Model No. 4, Span = 29.66 inches, Skew Angle = 30° . . . . .	A23
A.5	Rectangular Box Girder Bridge Model No. 5, Span = 22.50 inches, Skew Angle = 0° . . . . .	A30
A.6	Rectangular Box Girder Bridge Model No. 0, Span = 69.00 inches, Skew Angle = 0° . . . . .	A34

## 1. INTRODUCTION

### 1.1 Purpose of the Study

The purpose of this investigation is to provide a better understanding of the structural behavior of simply-supported skew box girder bridges. The behavior of straight box girder bridges is reasonably well established [1, 2, 3, 4]. However, the information available on the behavior of skew box girder bridges is rather limited. As part of the present study, ten skew box girder bridge models were analyzed using a computer program, entitled CELL, based on the finite element method summarized in Chapter 2. These bridge models, with various spans and angles of skew, all had four cells and corresponded exactly to those used in a comprehensive experimental study conducted in 1971 at the University of California at Berkeley, the results of which have been previously reported [5]. These models were made from aluminum and are described in the following section.

In order to determine the validity of the analysis based on the finite element method, theoretical results obtained using the computer program CELL are compared in Chapter 3 to those found in the experimental study.

Once the general agreement between theory and experiment is established, some general observations about the behavior of four-cell skew bridges are made in Chapter 4. This investigation of the behavior of skew box girder bridges includes a study of reactions, internal longitudinal stresses, external and internal total section moments, transverse distribution of the total moment to each girder, and the effects of the addition of a midspan diaphragm or the changing of

reaction support conditions. Both point live loads and dead load on the bridge are considered. In light of this overall picture of skew box girder bridge behavior, an effort to develop some approximate methods of analysis, adequate for design purposes, is made in Chapter 4.

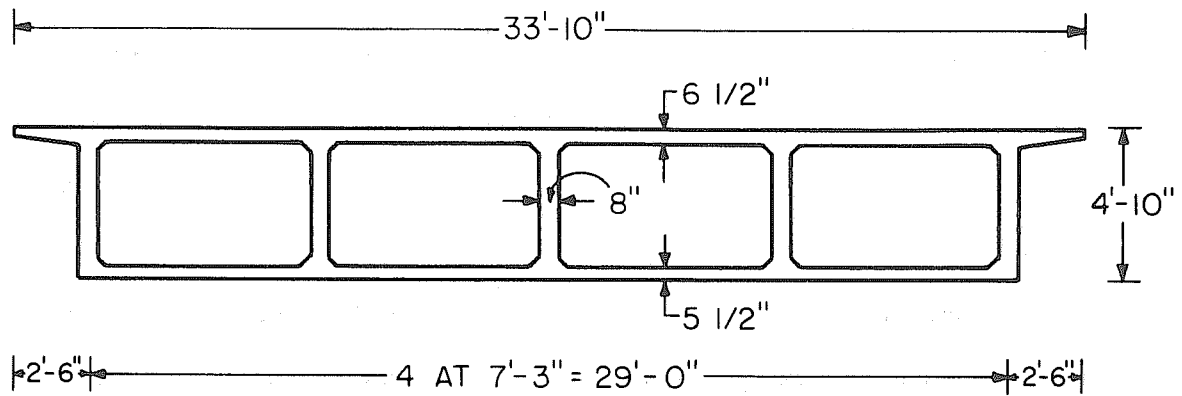
In Chapter 5, some tentative design recommendations are made based on the results of the investigation.

## 1.2 Experimental Work

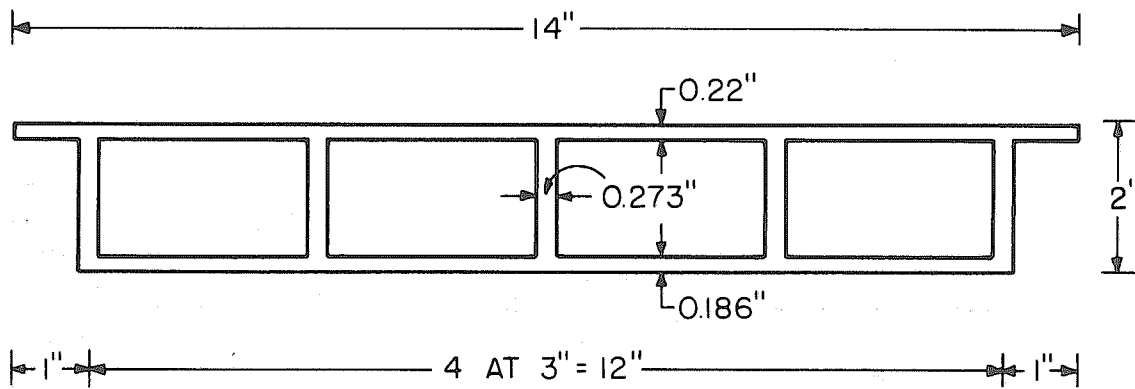
In an effort to provide adequate experimental data for the purpose of validating the proposed method of analysis, the previously mentioned study of aluminum box girder bridge models was undertaken. Results of this experimental investigation have been presented in detail in a previous report [5]. The utmost care was taken in the experiments to ensure the accuracy of the results. These results were presented in dimensionless form making them valid regardless of scale. This makes it possible for a series of bridges to be studied from the results of one basic model.

A linear scale of 1/29 was selected for the model study. The cross-sectional dimensions of the prototype and the model are shown in Figs. 1.1a, b. Fillets between the webs and top and bottom decks were eliminated in the models for simplicity in both the experimental study and the subsequent theoretical analysis performed in the present investigation. The thickness of the overhang was taken as constant and equal to that of the rest of the top deck.

The cross-sectional geometry of all ten models tested was the same. The parameters which were varied were the angle of skew and the span. It was also considered desirable to observe the effect



(a) PROTOTYPE



(b) MODEL

**FIG. 1.1 DIMENSIONS OF PROTOTYPE AND  $1/29$ TH SCALE MODEL CROSS-SECTION**

of a midspan transverse diaphragm. Therefore, the aluminum plates of which the models were made were fastened together using removable screws allowing each model to be tested with and without the diaphragm. The letter A following the model number indicates no midspan diaphragm existed. Conversely, the B series models all had the midspan diaphragm.

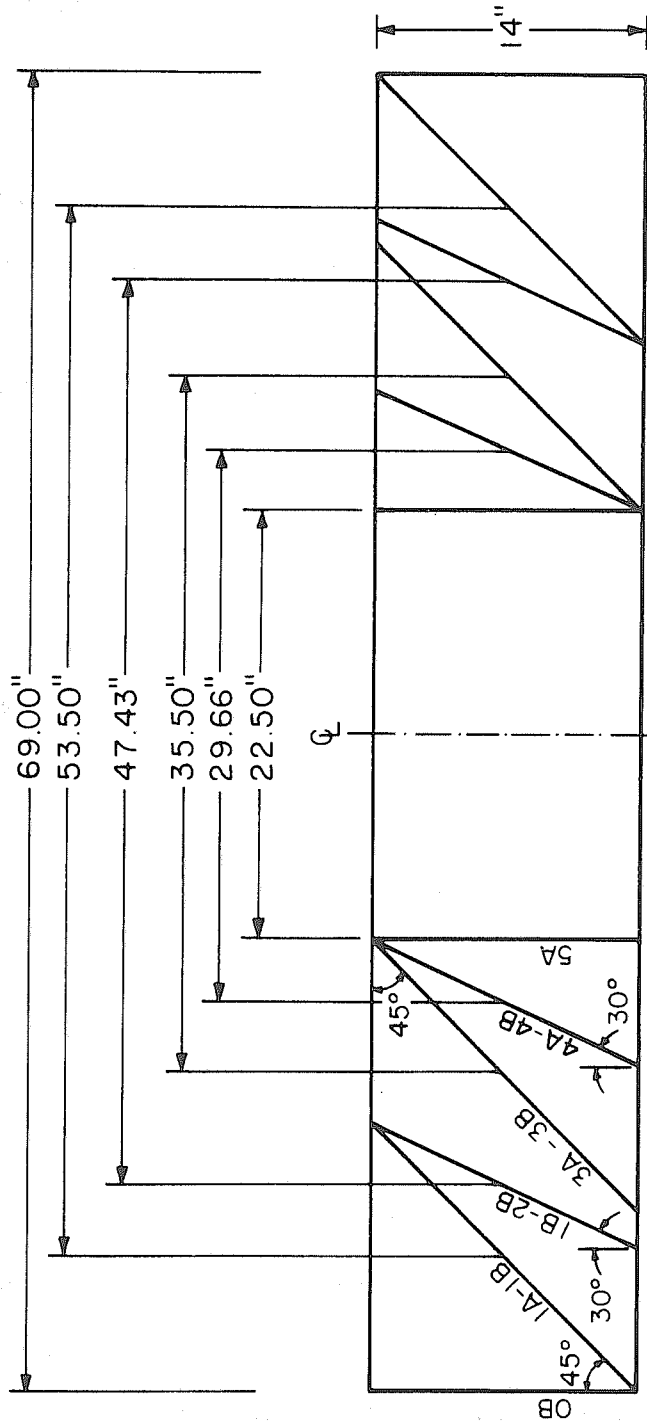
Starting with the longest span rectangular model OB with no skew, the model was cut back successively as shown in Fig. 1.2 yielding the models of varying span and angle of skew. The span in each case refers to the center-line distance, parallel to the webs, between the mid-thickness of each end diaphragm. This corresponds to the longitudinal span between points of support. The length of all models, as well as their prototypes, are summarized in Table 1.1.

TABLE 1.1 DIMENSIONS OF MODELS AND PROTOTYPES

Model	Skew Angle (deg)	Model Span (in.)	Prototype Span (ft.)	Aspect Ratio (b/L)	Depth-Span Ratio (d/L)
OB	0	69.00	168.0	.173	.029
1A, 1B	45	53.50	129.3	.224	.037
2A, 2B	30	47.43	114.6	.253	.042
3A, 3B	45	35.50	85.8	.338	.056
4A, 4B	30	29.66	71.7	.405	.067
5A	0	22.50	54.4	.533	.089

A refers to models without midspan diaphragm.

B refers to models with midspan diaphragm.



NOTE: ALL DIMENSIONS ARE TO THE CENTER OF END DIAPHRAGM  
 ALL BRIDGES SKEW SYMMETRIC ABOUT MIDSPAN

FIG. 1.2 PLAN DIMENSIONS OF MODELS 0 THROUGH 5



Each model was subjected to a series of vertical point loads at various locations on the top deck of the bridge. For each model and each load case the measured quantities were the same and may be summarized as follows.

(1) Boundary Reactions:

In all cases the bridge was supported on four point supports R1 through R4 located at the intersection of the outside webs and the end diaphragms - the intersection of the mid-thickness planes in each case, Fig. 1.3. All four reactions were measured by load-cells, and a static check was applied to ensure that the sum of the four reactions equalled the applied vertical load.

(2) Internal Strains:

The right transverse section designated 0-0 in Fig. 1.3 which is located 1 in. from the midspan was closely instrumented with strain rosettes on top and bottom plates and on all five webs. This enabled a complete experimental stress distribution to be derived for this section. Two static checks were then applied to the stress data. First, the integrated compressive and tensile forces along Section 0-0 were compared as these should be equal. Second, the integrated internal moment on Section 0-0 derived from the measured strains was compared with the external moment computed both to the left and right of Section 0-0 from the external forces (applied loading and end reactions). These should be equal; the comparison of left and right external moments was a further check on the accuracy of the measured reactions, and the comparison of internal and external moments being a precise check on the value of E of the material.

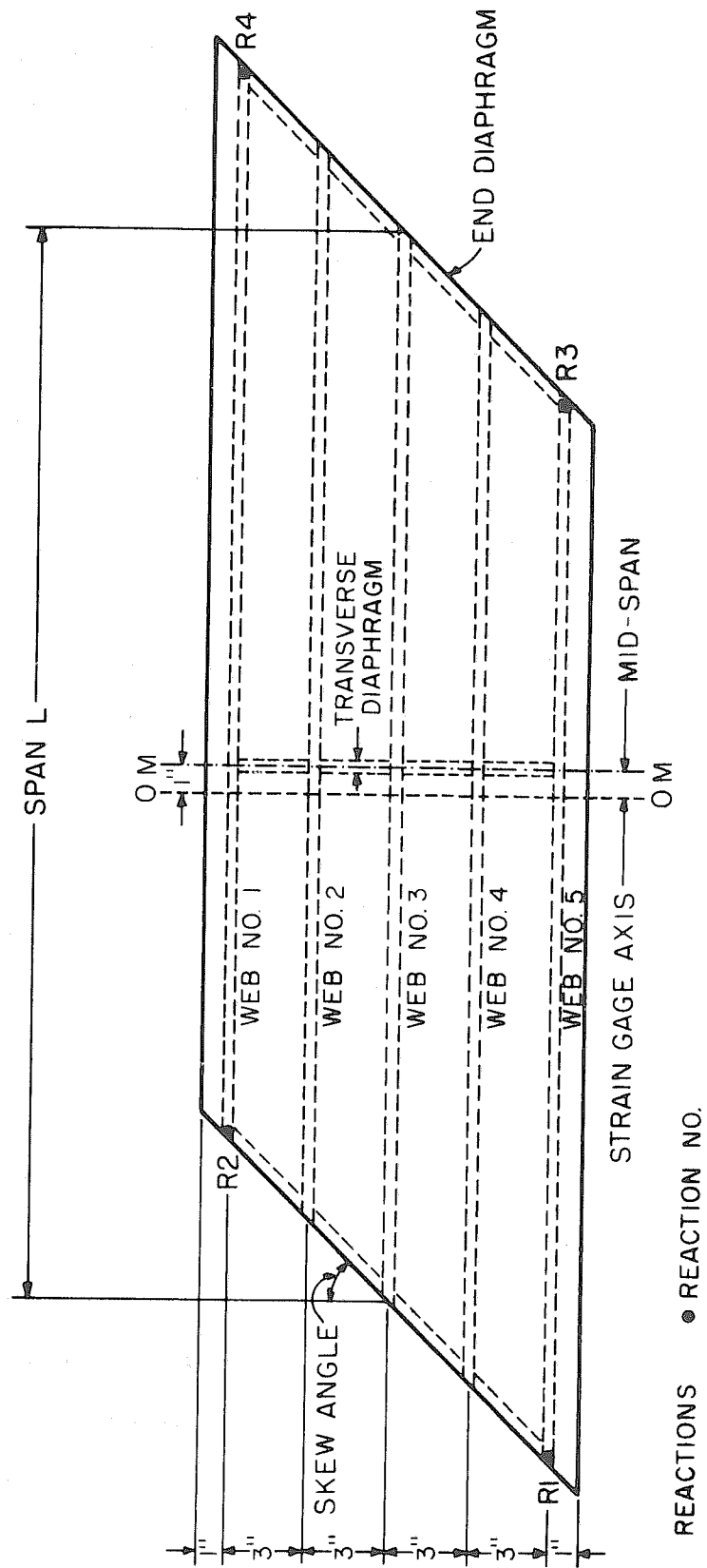


FIG. 1.3 TYPICAL SKEW BRIDGE

This value was determined to be  $10.1 \times 10^6$  psi. Poisson's Ratio,  $\mu$ , was assumed as 0.332.

In addition to the above-mentioned self consistency checks, symmetrical load positions were selected so that symmetry of response could also be checked.

(3) Deflections:

These were measured at selected points along all five webs. The self consistency checks on the measured deflections were based on conditions of symmetry and reciprocity. The latter of these also provided a check on the linearity of the system as reciprocal displacements are only equal in linear systems.

Figures giving the detailed dimensions of each model separately are presented with the theoretical results in Appendix A. In these figures the load positions and dial gage locations are also shown as well as the plan geometry of each model.

1.3 Scope of the Study

The scope of this investigation is meant to include only the four cell models which were analyzed. Any results which emerge from the study are, in the strictest sense, valid only for bridges similar to the prototypes of these models. This is especially true with regard to the plan aspect ratio (width to span) and the depth to span ratio of any bridge in question. Preliminary studies of bridges with fewer cells and smaller aspect ratios indicate they behave quite similarly to the four cell bridges discussed in this report. However, preliminary studies of six and eight cell bridges with larger aspect ratios than the four cell models indicate that these bridges might

behave somewhat differently. Further study of these bridges must be made before additional conclusions can be made concerning their structural behavior.

## 2. THEORETICAL ANALYSES

### 2.1 General

An analytical solution of the true response of a concrete box girder bridge is complicated by factors common to many structural systems. A reinforced concrete bridge experiences cracking under increasing load and a subsequent redistribution of internal forces occurs. In addition, the internal forces are time-dependent because of creep and shrinkage in the concrete. Nevertheless, as for other reinforced concrete systems, such as frames, slabs, and shells, it is generally accepted that for design purposes, the distribution of internal forces, moments and displacements in a box girder bridge due to applied loads can be based on an elastic analysis of an uncracked homogeneous concrete system.

In a complete analysis of multi-cell box girder bridge, all of the internal forces and displacements shown on a typical element in Fig. 2.1 taken from a deck or web plate of the bridge should be determined. The internal forces  $N_{xx}$ ,  $N_{yy}$ , and  $N_{xy}$  are termed membrane forces while  $M_{xx}$ ,  $M_{yy}$ ,  $M_{xy}$ ,  $Q_{xx}$  and  $Q_{yy}$  are internal forces due to plate bending. In many approximate analyses certain internal forces are assumed to be negligible and are thus taken as zero.

Many analytical models and methods have been developed for analyzing box girder bridges. Among these are approximate methods based on simplified structural behaviour such as the use of an equivalent beam grillage or anisotropic slab to represent the system; exact and approximate methods based on folded plate theory; and numerical solutions based on finite element or finite difference methods. No

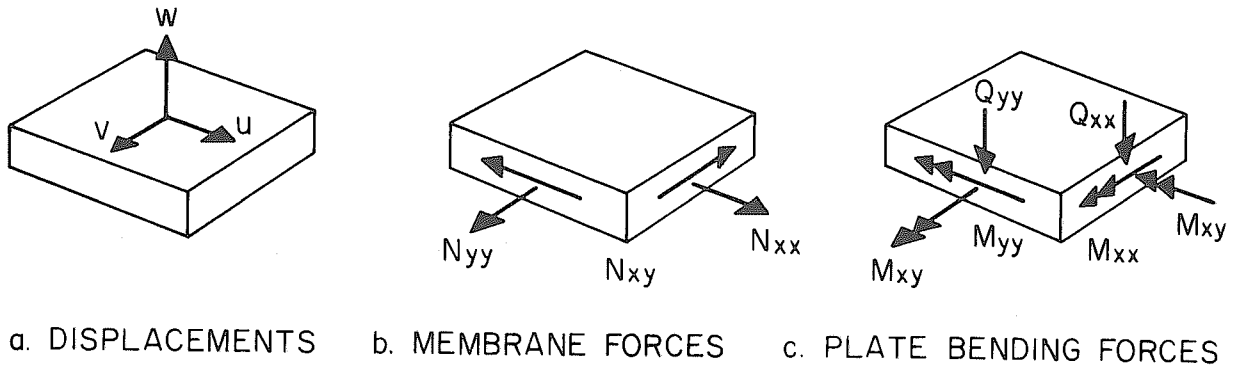


FIG. 2.1 DISPLACEMENTS AND INTERNAL FORCES ON A TYPICAL ELEMENT TAKEN FROM THE BRIDGE

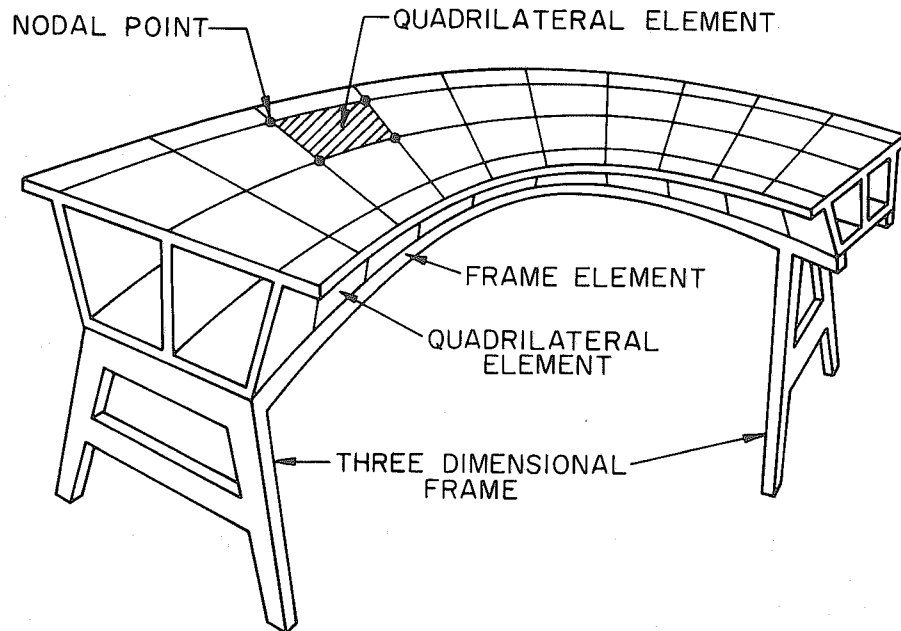


FIG. 2.2 FINITE ELEMENT REPRESENTATION OF GENERAL BOX GIRDER BRIDGE

attempt will be made to review all of these methods here.

## 2.2 Finite Element Solution

The finite element method has been described extensively in the literature during the past decade. A comprehensive discussion of the theory and application of the method is given in the book by Zienkiewicz [6].

In the finite element method the actual continuum is replaced by an assembly of finite elements interconnected at nodal points (Fig. 2.2). For a general box girder bridge system, the finite elements may consist of two dimensional shell or plate elements and transverse or longitudinal one dimensional frame type elements. Stiffness matrices which approximate the behavior in the continuum, are developed for the finite elements based on assumed displacement or stress patterns, after which an analysis based on the direct stiffness method may be performed to determine nodal point displacements and thence the internal stresses in the finite elements. It should be recognized that the accuracy obtained is dependent on the assumptions used in deriving the stiffness matrices and on the fineness of mesh used in subdividing the structure. As generally applied, the results obtained closely satisfy compatibility, but not necessarily equilibrium in the continuum until a sufficiently fine mesh is used.

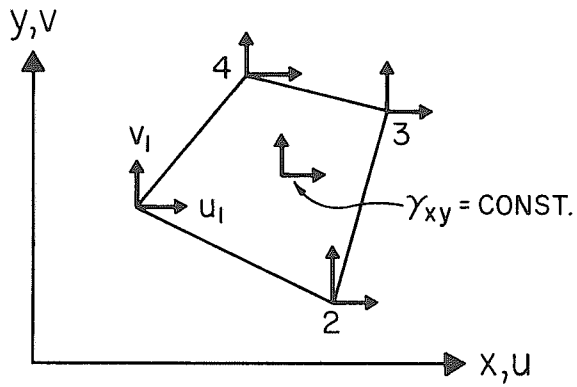
A number of investigators have developed general shell programs which could be used for analyzing box girder bridges. However, if available, it is better to use special purpose programs which take

advantage of the repetitive and special nature of these structures. These should provide the required accuracy in the results with a minimum of the following: (1) required amount of input preparation; (2) execution time and core storage in the computer; and (3) amount of output data reduction necessary for meaningful interpretation.

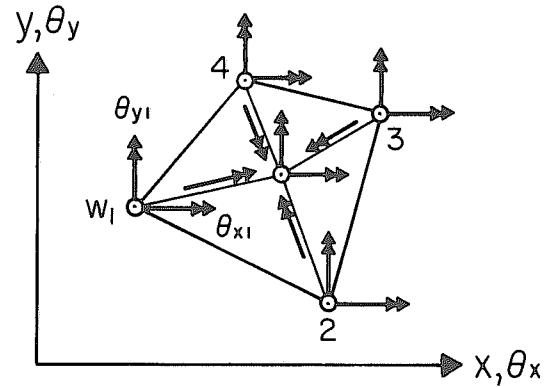
Thus, because of the complexities of the skew box girder bridge system, the finite element method was selected to obtain an analytical solution for the models described in the previous chapter. The desired features were found to be incorporated in a program named CELL developed in 1970 at the University of California, Berkeley [7, 9]. Detailed information on the program CELL including input-output specifications and a FORTRAN listing may be found in reference [7]. This program analyzes cellular structures of constant depth with arbitrary plan geometry. The structure must be made up of top and bottom decks and vertical webs. Two different finite element types are used to capture the main behavior of the deck and web components. Orthotropic plate properties and arbitrary loadings and boundary conditions can be treated. Automatic element and coordinate generation options minimize the required input data.

The deck slabs are idealized by quadrilateral elements having a total of 5 degrees of freedom (DOF) per node, 3 translations and 2 rotations (Fig. 2.3). The in-plane action of the quadrilateral elements is represented by the plane stress mixed model Q8D11 having 2 translation DOF at each external corner node and 3 internal DOF (Fig. 2.3a). The mixed model is constructed using separate expansions for the displacement and strain fields. The variations of the  $u$  and  $v$



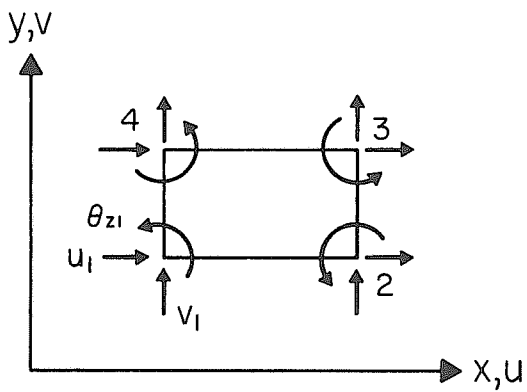


a) PLANE STRESS Q8DII

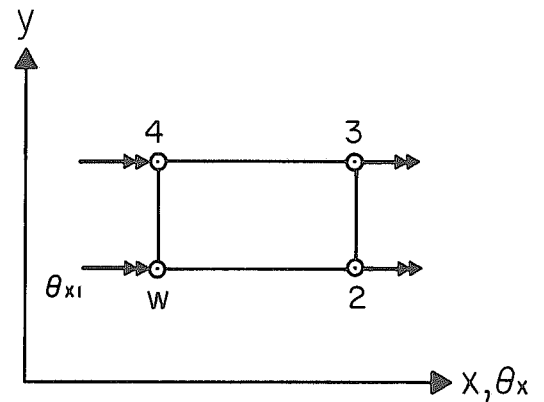


b) PLATE BENDING Q19

FIG. 2.3 DECK ELEMENTS USED IN CELL PROGRAM



a) PLANE STRESS QUSPI2



b) PLATE BENDING ONEW

FIG. 2.4 WEB ELEMENTS USED IN CELL PROGRAM

components of the displacement field are approximated by the standard bi-linear expansion for the 8 corner node DOF and by bi-quadratic expansions for 2 of the internal DOF. The third internal DOF is used to enforce a constant shear-strain variation over the entire element, which produces a more flexible and better element. After the element stiffness is formed the 3 internal DOF are eliminated by an internal static condensation process. The quadrilateral plate bending element Q19 (Fig. 2.3b) used for the deck slabs has been described in detail by Clough and Felippa [10]. This compatible element is made up of four subtriangles, each of which has 11 DOF associated with full cubic expansions of the w-displacement field and an enforced linear variation of the normal slope along one edge. In combining the four sub-elements, a quadrilateral with 19 DOF is obtained. However, the 7 internal DOF are eliminated by static condensation leaving the essential 3 DOF at each corner node, 2 rotations and a translation (Fig. 2.3b).

The vertical webs of the bridge are idealized by special rectangular spar elements having a total of 5 DOF at each corner node, 3 translations and 2 rotations. A single element over the entire depth of the bridge can be used to capture the essential behavior of the web. The in-plane action of these elements is represented by the model QUSP12 (Fig. 2.4a). A bi-linear expansion for u and v is associated with the 2 translational DOF at each node and a cubic variation in the x-direction of v is defined by the rotation  $\theta_{zi} = \partial v / \partial x$  at each node. The plate bending is represented by a simple one-way bending element ONEW having 2 DOF

at each node, a rotation and a translation (Fig. 2.4b).

### 2.3 Mesh Sizes and Computer Times

Of particular interest in finite element solutions are the mesh size used and the computer time needed to obtain the solution. This information for the models analyzed in this study using a CDC 6400 computer is summarized in Table 2.1.

A typical top deck mesh layout for Model 4 is shown in Fig. 2.5. A different layout could have been used incorporating parallelogrammic elements only. However, studies have shown that more accurate results are obtained using rectangular elements with triangular elements only at the supports to accommodate the skew boundary. While arbitrary quadrilateral elements can be used with the CELL program, highly skewed elements should be avoided. Fig. 2.5 indicates that the element sizes are not constant along the length of the bridge. The mesh is finer near the reactions and at midspan. The finer mesh yields more accurate results in these regions of particular interest. Table 2.1 lists mesh sizes in the form "a x b". The number "a" refers to the total transverse number of elements in the top deck. The second number, "b", is twice the total longitudinal number of elements between an acute reaction point and midspan. Bottom deck elements correspond to top deck without the over-hangs. The two decks are connected by vertical web elements along each of the five longitudinal web lines and at the end and midspan diaphragms, Figs. 1.3 and 2.5.

The number of equations in Table 2.1 corresponds to the total number of degrees of freedom in the system. The bandwidth is

TABLE 2.1 FINITE ELEMENT SOLUTION INFORMATION

Model	Skew Angle (deg)	Span (in)	Mesh Size	Band Width	No. of Eqs.	No. of Load Cases	First Load Case		Subsequent Load Case		Total	
							CP	PP	CP	PP	CP	PP
OB	0	69.00	6 x 22	90	1610	10	4.1	3.8	.56	1.11	9.2	13.8
1A, 1B	45	53.50	6 x 28	90	1750	13	2.5	4.3	.56	1.62	9.3	23.7
1A, 1B	45	53.50	10 x 56	130	5370	13	15.0	22.7	1.72	4.23	35.6	73.5
2A, 2B	30	47.43	6 x 28	90	1750	13	2.8	3.8	.56	1.30	9.4	19.4
3A, 3B	45	35.50	6 x 24	90	1450	15	2.8	3.1	.42	1.21	8.7	20.0
4A, 4B	30	29.66	6 x 24	90	1470	15	2.1	5.7	.42	1.74	8.7	30.0
5A	0	22.50	6 x 16	90	1190	10	1.8	2.5	.40	1.44	5.3	11.9

1. All computer runs were made in a CDC 6400 computer.

2. CP = Central computer processing time in minutes

3. PP = Peripheral processing time in minutes

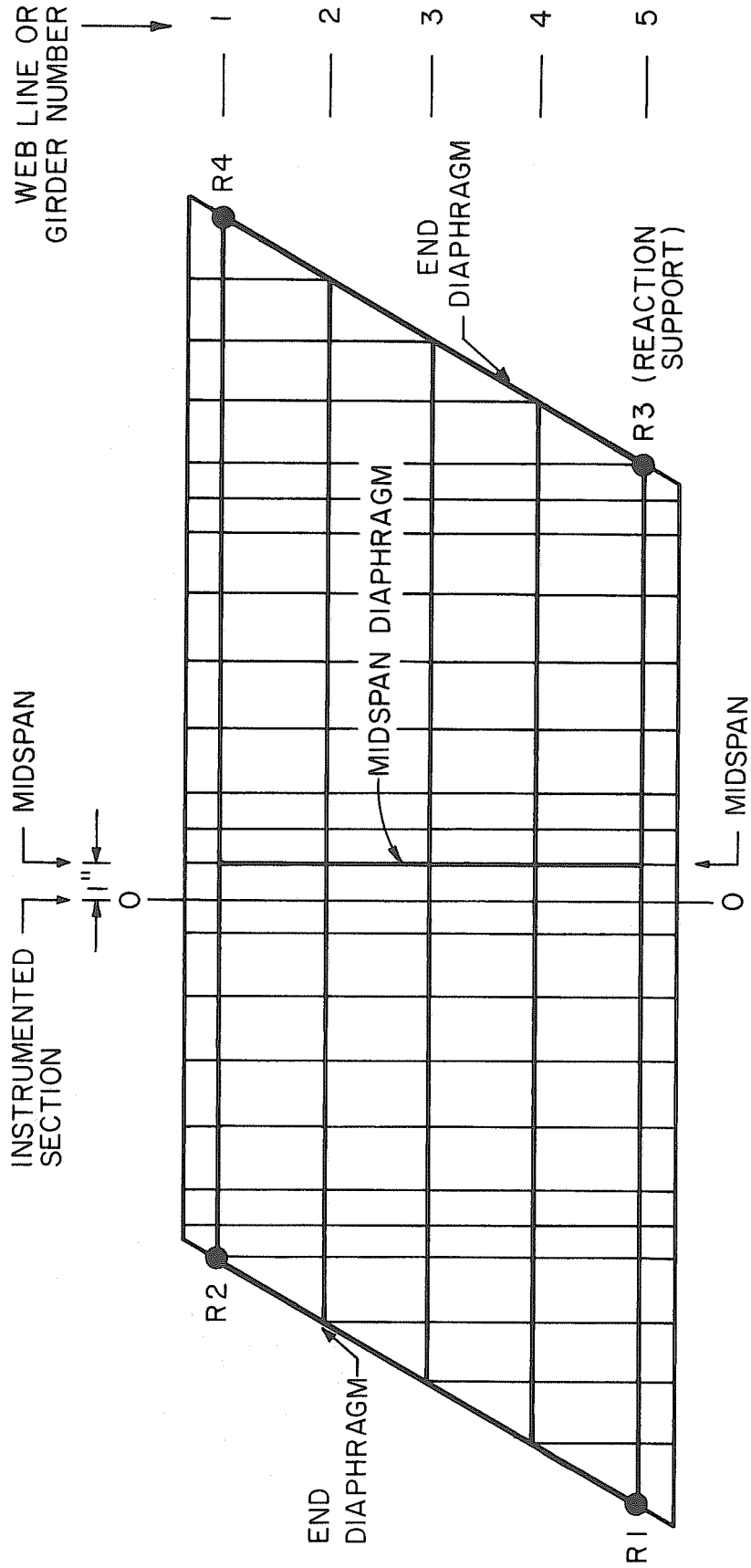


FIG. 2.5 TYPICAL FINITE ELEMENT MESH LAYOUT FOR MODEL 4

indicative of the coupling between these equations. The solution time is a function of both these factors. The CP (central processing) time is actual computation time in the central computer while PP (peripheral processing) is the time used for input and output of data. Notice that the solution of the first load case takes much more time than each of the subsequent load cases. The time taken for the first load case includes the input of all data, and the assembly and reduction of the global stiffness matrix to yield a solution of the equations for the first load vector. Thereafter, for each additional load case, only the input and solution for a new load vector, utilizing the reduced global stiffness matrix obtained in the solution of the first load case, takes place.

In Table 2.1 two sets of information are shown for models 1A and 1B. These models were run with both a coarse and a fine mesh. The difference in the results obtained with the fine mesh as compared to those with the coarse mesh was not significant. However, the cost was approximately four times as great. Approximate total costs using the University of California Computer Center CDC 6400 were \$110 for the coarse mesh run and \$400 for the fine mesh run. Both runs were made for a total of 13 load cases. Because of the cost factor all models other than 1A and 1B were analyzed using only the coarse mesh.

#### 2.4 Theoretical Results

The output produced by CELL for each problem is summarized as follows:

(1) Input Echo:

All input data is printed out and properly identified.

(2) Nodal Displacements:

All global displacements are output at the nodes of the top and bottom deck. The five components  $u$ ,  $v$ ,  $w$ ,  $\theta_x$  and  $\theta_y$  are listed sequentially for each node.

(3) Nodal Forces:

This information yields the reactions to the loading and gives an insight into the round-off error and the magnitude of the residual forces at all nodes.

(4) Internal Forces at Center of Deck Elements:

Both stresses and moments are computed and printed at the center of deck elements.

(5) Internal Forces at Nodes of Deck Elements:

Internal forces and moments at the node of each element, averages at a node from contributing elements and associated principal stresses and moments, and their directions are computed and output for specific nodes if the user desires.

(6) Internal Forces in Web Elements:

Again, the user may request the internal force contributions and their averages at specified nodes for both transverse and longitudinal web elements.

(7) Direction of Internal Forces (for deck elements only):

This feature allows the user to obtain the values of the normal stress resultants for any specified angle from the global  $x$  - axis. This capability simplifies arbitrary equilibrium checks, e.g. for

skewed box girders at a section parallel to skewed supports.

(8) Log of Problem:

Each problem is terminated with a summary listing of execution times in various sections of the program, number of degrees freedom, bandwidth, etc.

(9) Punched Output:

In addition to the printed output for each problem the user may request that pertinent data be punched on cards.

For all the models analyzed in this study the punched output was further processed for the purpose of simplified interpretation and easy comparison with the previously mentioned experimental results. These final results are presented in Appendix A in the form of computer output tables from the data processing program. In addition, the presentation of each specific result in Appendix A is explained below.

In order to preserve the most general applicability of the results, the data is presented in dimensionless form. Thus, it is possible to utilize these results for any value of loading, elastic modulus, or span of bridge. However, it must be re-emphasized here that the data should be applied only to box girder bridges of similar geometry to the prototypes of the models. In the tables in Appendix A, any response quantity which involves the size of the bridge is referenced to the length,  $L$ . This refers, for convenience, to the center-line span of the bridge. This variable controls all other dimensions of the bridge. If, for example, one wishes to apply the results from a model of a certain span to another bridge of longer span, the cross-sectional geometry of the longer bridge must correspond by the same



proportion as the span to that of the model.

#### 2.4.1 Statics Checks

Three independent checks of the static equilibrium of each model were tabulated in the data processing program.

##### 1) Vertical Forces:

The vertical reactions were extracted from the nodal force vector and compared to the total applied load which in all cases was unity. Thus the sum of the reactions R1 through R4 would also ideally be unity. A measure of this accuracy is presented as a ratio of applied load to the sum of the reactions. Perfect agreement yields a ratio of unity.

##### 2) Internal Longitudinal Forces at Section 0-0:

Since there were no applied external horizontal loads in any of the cases, the sum of the tensile forces at section 0-0, Fig. 1.3, should be exactly equal to the sum of compressive forces. Values for compressive or tensile forces were available as the nodal averages of element forces. A linear distribution was assumed between nodes and an integration procedure was used to obtain the total tension and compression forces at section 0-0. The ratio of total longitudinal compression force to longitudinal tension force is tabulated for each load case. Again, in the ideal case, this ratio approaches unity.

##### 3) Moments:

The total longitudinal moment at section 0-0 can be computed in two different ways. First, the total internal moment is found by multiplying the distance between the longitudinal tensile and compressive resultants by the average value of these two forces. Secondly,

the external moment can be found as the sum of the reactions and the applied load either on the "right" or "left" of section 0-0 times their respective lever arms. The data processing program averages the "right" and "left" moments to obtain the external moment at section 0-0. The ratio of the internal to external moment is tabulated and perfect agreement is signified by a value of unity.

#### 2.4.2 Reactions

Each reaction, R1 through R4, is expressed as a coefficient of the applied load, W, and tabulated for each load case. The sum of the reactions is also shown.

#### 2.4.3 $N_{xx}$ Forces in Top and Bottom Plates:

The  $N_{xx}$  forces in the top and bottom plates are the longitudinal forces per unit width and are calculated at the nodes from the average of the adjacent element forces as mentioned previously. These values are tabulated for each load case. The transverse location of the various  $N_{xx}$  values is expressed as the distance, S, in inches from the edge of the top slab divided by B, the total width of the top slab. All values of  $N_{xx}$  are expressed as coefficients of W/L.

#### 2.4.4 Deflections

The deflections at points corresponding to dial gage positions shown in Appendix A are given. Downward deflection is considered positive and all values are in terms of 1000 W/EL.

#### 2.4.5 Total Longitudinal Moment at Midspan

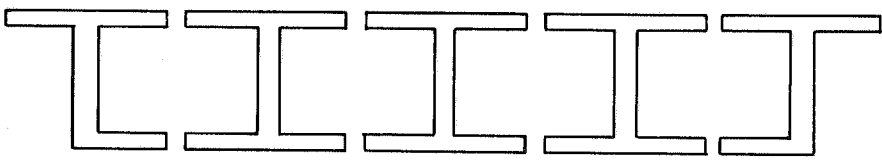
Values expressed in terms of WL were obtained from the average

of the "right" and "left" external moment computed from the applied load and reactions.

#### 2.4.6 Distribution of Total Moment to Individual Girders:

In order to determine the transverse distribution of the total longitudinal moment at section 0-0, the actual box girder bridge cross-section is first divided into a number of similar interior I girders plus two exterior girders. Each interior girder consists of a web and a top and bottom flange equal in width to the web spacing, while each exterior girder consists of an exterior web with a top flange extending from the midpoint between girder webs to the edge of the cantilever overhang and the bottom flange being equal in width to half of the web spacing. Thus the bridge model, shown in Fig. 2.6, has three interior girders 2, 3 and 4 and two exterior girders 1 and 5.

The girder moment at any section taken by an individual girder can be found by integrating the longitudinal membrane stresses, over the proper slab and web areas to obtain forces and then multiplying these forces by their respective lever arms to the neutral axis of the gross uncracked section. The small contribution of the longitudinal slab moments is also included. The girder moments, at a particular section, can then be summed to determine the total moment on an entire cross-section. Each girder moment can then be divided by the total moment at a section to determine the percentage distribution to each girder. These values are given in Appendix A for each case studied.



GIRDER NUMBER	①	②	③	④	⑤	TOTAL
MOMENT OF INERTIA (in <sup>4</sup> )	0.753	1.086	1.086	1.086	0.753	4.764
% OF TOTAL I	15.8	22.8	22.8	22.8	15.8	100.00

**FIG. 2.6 DIVISION OF CROSS-SECTION INTO INDIVIDUAL GIRDERS**

Fig. 2.6 shows the individual moments of inertia for the various girders. Further, the percentage of the total moment of inertia of the entire cross-section contributed by each girder is tabulated. These percentages correspond to the ideal load distribution of the total moment on a section to each girder which would exist if the longitudinal stresses on the section had a uniform transverse distribution.

### 2.5 Self-Consistency of Theoretical Results

The first step in determining the accuracy of the theoretical results is to check their self-consistency. This procedure involves two independent checks:

(1) Statics Checks

The three statics checks tabulated in Appendix A for each model ensure that the theoretical results satisfy equilibrium. The ratio of applied load to reactions is unity for all models and load cases. Internal longitudinal tension and compression forces balance to within 2.5% as do internal and external moments. Indeed, most values agree within 2%. Since the finite element method utilizes a displacement model it only approximately satisfies equilibrium of forces across element interfaces. In general, as the mesh size is refined greater and greater accuracy is obtained.

(2) Reciprocity Checks

In any linear analysis the law of reciprocal displacements should be satisfied. Most simply, this law states: a unit load at point "i" produces a displacement at "j" which is identical to the displacement at "i" due to a unit load at "j". In all models this check can be performed for load positions 1, 3, and 5 indicated in the figures in Appendix A. In models 2 through 5 load positions 6, 8, 10 and 13 may also be utilized. Checking the theoretical results reveals that this condition is simulated very well by the finite element model. In general, agreement is within 1%.

In determining the self-consistency of the experimental results an additional check of symmetry was made. All the models possess geometric symmetry about an axis normal to the plane of the bridge passing through midspan center. Thus, load position 3 should produce symmetrical forces and displacements. Also, load positions 1 and 5, as well as 2 and 4, are a symmetrical pair and should render exactly

the same results on corresponding symmetrical points on the models. The experimental results satisfied the conditions of symmetry very well. Since the finite element mesh is also symmetrical the theoretical results automatically reflect the requirements of symmetry. Consequently, this condition can only be used to detect input errors in the theoretical analysis and is not otherwise significant.

The statics and reciprocity checks reveal no serious inconsistencies in the theoretical results. This fact in itself, however, does not effectively validate the overall applicability of the method to skew box girder bridges. The finite element model only simulates reality. The accuracy of this representation will be studied in the next chapter by comparing the theoretical results to the experimental results found in testing the aluminum models.

### 3. COMPARISON OF THEORETICAL AND EXPERIMENTAL RESULTS

#### 3.1 General

In this chapter the theoretical results are compared with the experimental model results. Perfect agreement, of course, cannot be expected. The finite element method utilizes an idealized analytical model, which can only simulate the true skew box girder bridge behavior. The experimental model also only simulates a true bridge and the experimental results are dependent on the accuracy with which the physical model is made. The results are also subject to human error in the setting up, gaging and performing of the model tests. Thus, the purpose of this chapter will be to show that theory and experiment exhibit generally good agreement for each of the particular models in their predictions of external reactions, internal forces and longitudinal moments. However, significant differences between theory and experiment exist for deflections and the causes of these discrepancies will be discussed. Also, general trends in the behavior of skew bridges will become apparent and are scrutinized in the following chapter.

#### 3.2 Deflections

The most significant disagreement between theoretical and experimental results occurred in the comparison of deflection values. This comparison is given in Figs. 3.1 to 3.5 and also in Table 3.1 for midspan point loads acting on Girders 3, 4 or 5. It is evident that the experimental model was more flexible than the theoretical model, with the percentage difference between deflection values

TABLE 3.1 RATIO OF THEORETICAL TO EXPERIMENTAL MIDSPAN DEFLECTIONS UNDER WEBS 1, 3, AND 5 FOR MIDSPAN POINT LOAD ON GIRDERS 3, 4 OR 5

Model	Load on Girder 3			Load on Girder 4			Load on Girder 5		
	$\Delta 1$	$\Delta 3$	$\Delta 5$	$\Delta 1$	$\Delta 3$	$\Delta 5$	$\Delta 1$	$\Delta 3$	$\Delta 5$
1A(45°/53.4")	.86	.84	.87	.87	.81	.81	.89	.83	.77
2A(30°/47.4")	.89	.86	.88	.92	.87	.84	.94	.87	.82
3A(45°/35.5")	.78	.77	.74	.86	.75	.73	1.25	.78	.75
4A(30°/29.7")	.80	.78	.81	.87	.79	.78	.99	.80	.76
5A(0°/22.5")	.76	.80	.76	.85	.75	.73	4.33	.81	.77
0B(0°/69.0")	—	.91	.92	—	.92	.95	—	.92	.91
1B(45°/53.5")	.85	.82	.84	.85	.82	.80	.82	.80	.73
2B(30°/47.4")	.92	.86	.89	.92	.87	.84	.91	.88	.81
3B(45°/35.5")	.79	.76	.79	.83	.79	.73	.71	.77	.74
4B(30°/29.7")	.82	.76	.83	.89	.78	.75	1.08	.87	.76



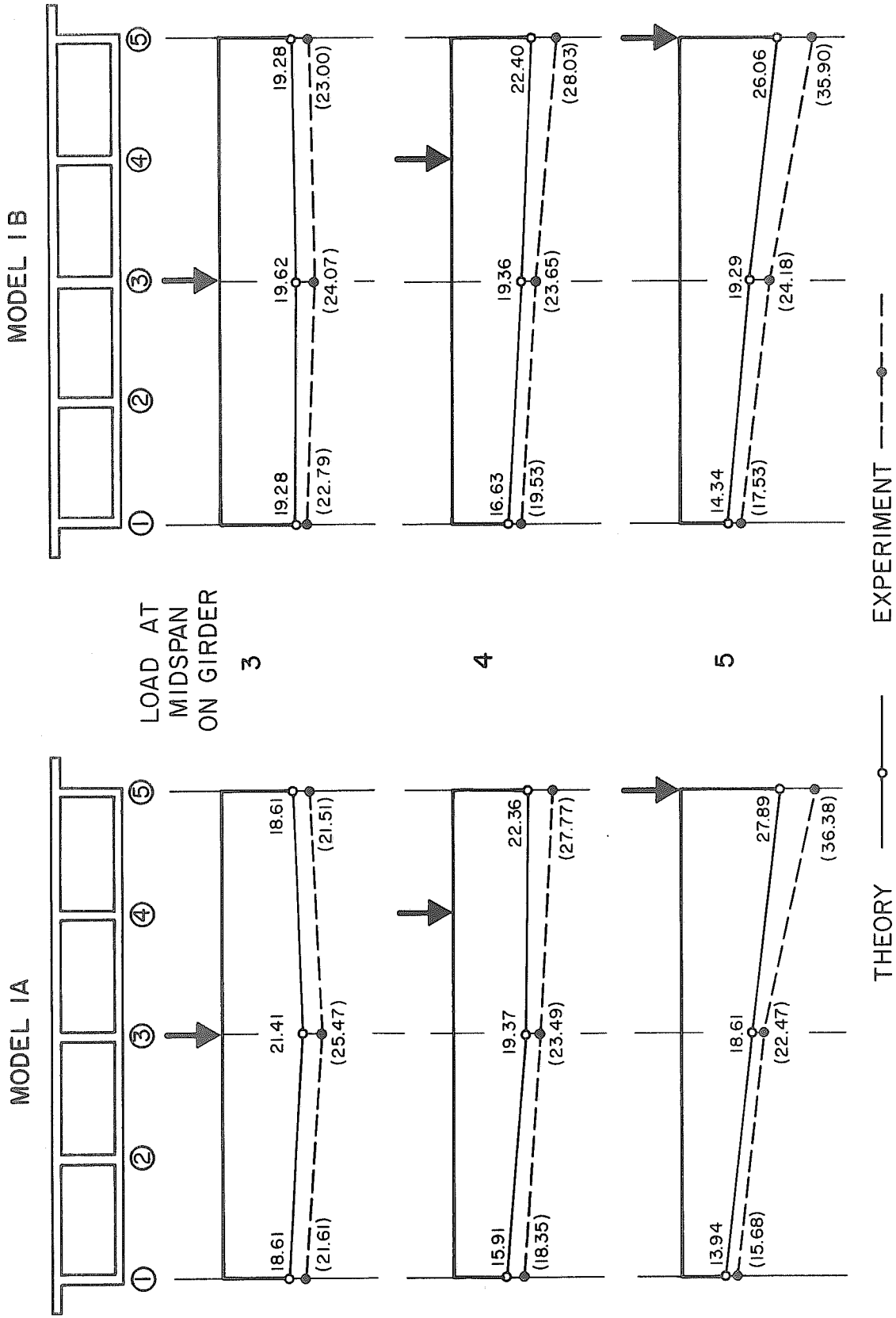


FIG. 3.1 COMPARISON OF THEORETICAL AND EXPERIMENTAL DEFLECTIONS AT MIDSPAN

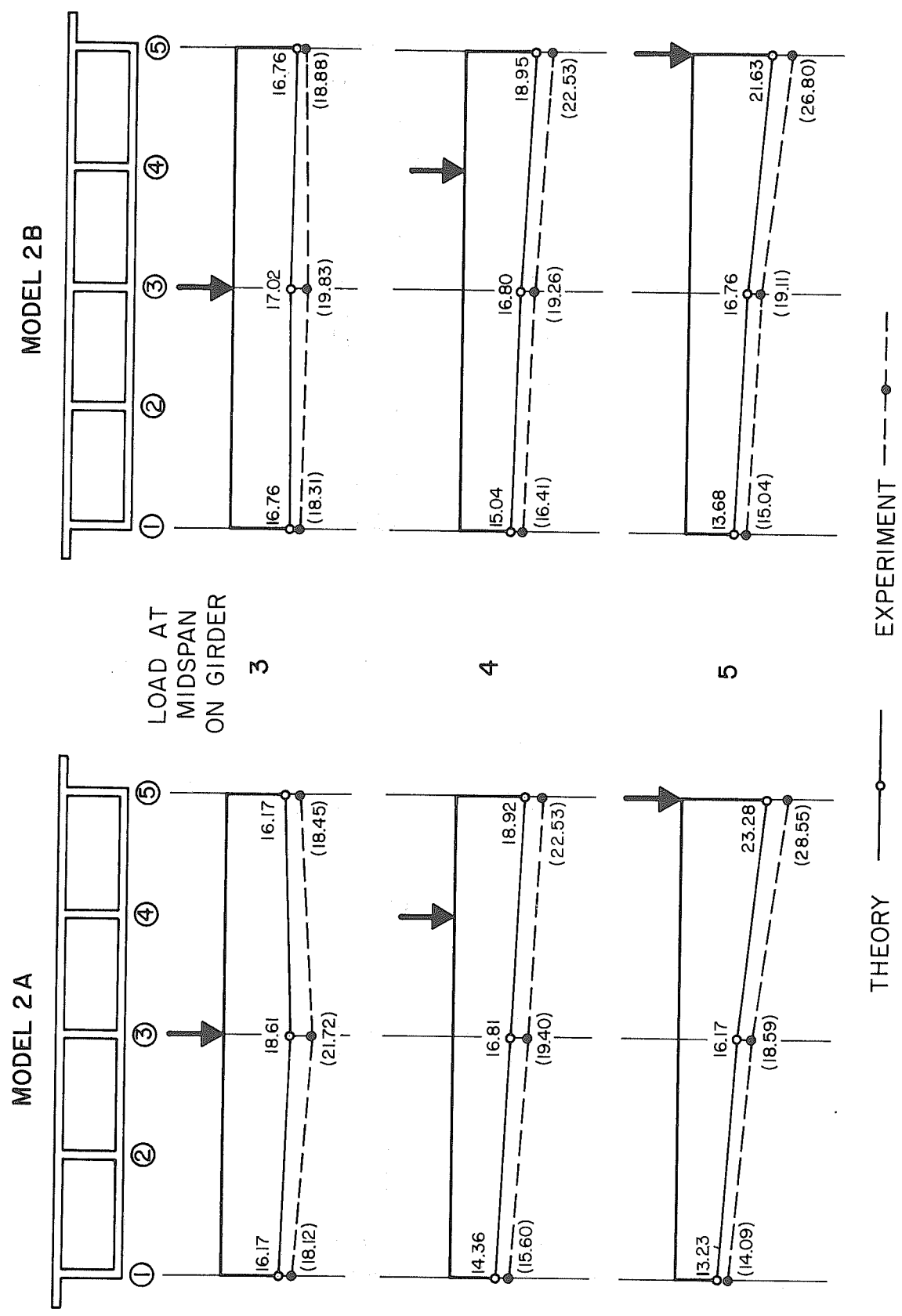


FIG. 3.2 COMPARISON OF THEORETICAL AND EXPERIMENTAL DEFLECTIONS AT MIDSPAN

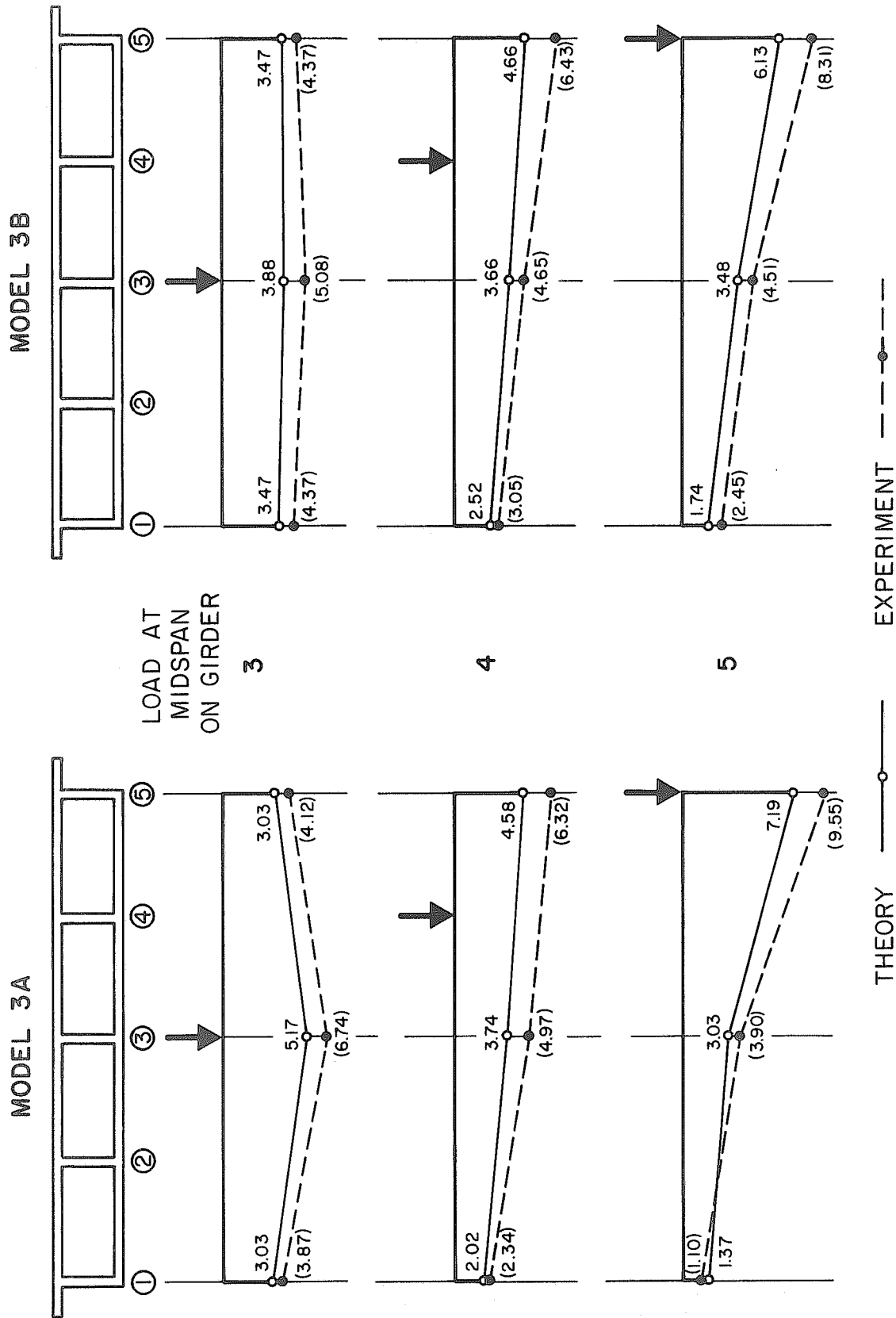


FIG. 3.3 COMPARISON OF THEORETICAL AND EXPERIMENTAL DEFLECTIONS AT MIDSPAN

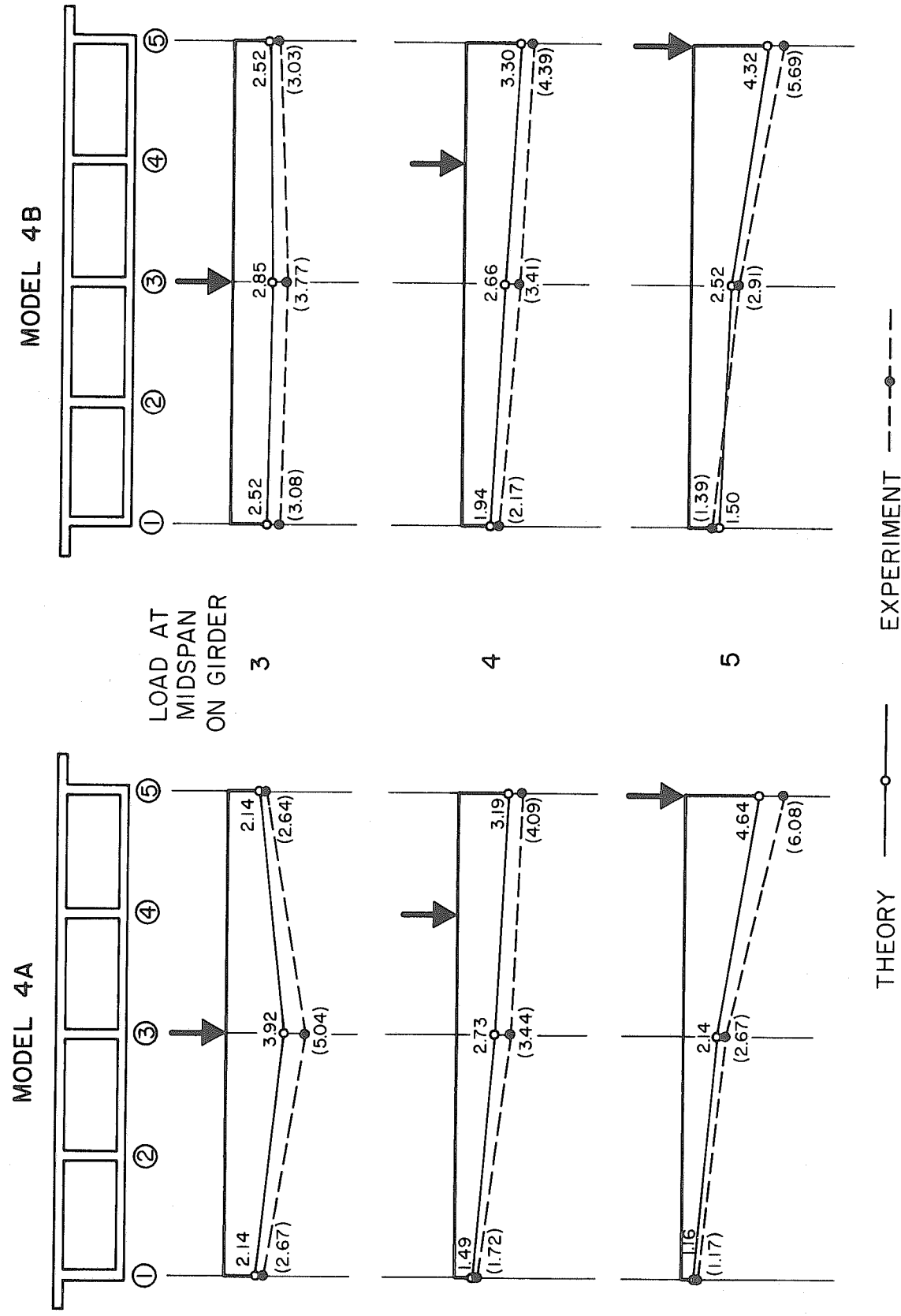


FIG. 3.4 COMPARISON OF THEORETICAL AND EXPERIMENTAL DEFLECTIONS AT MIDSPAN

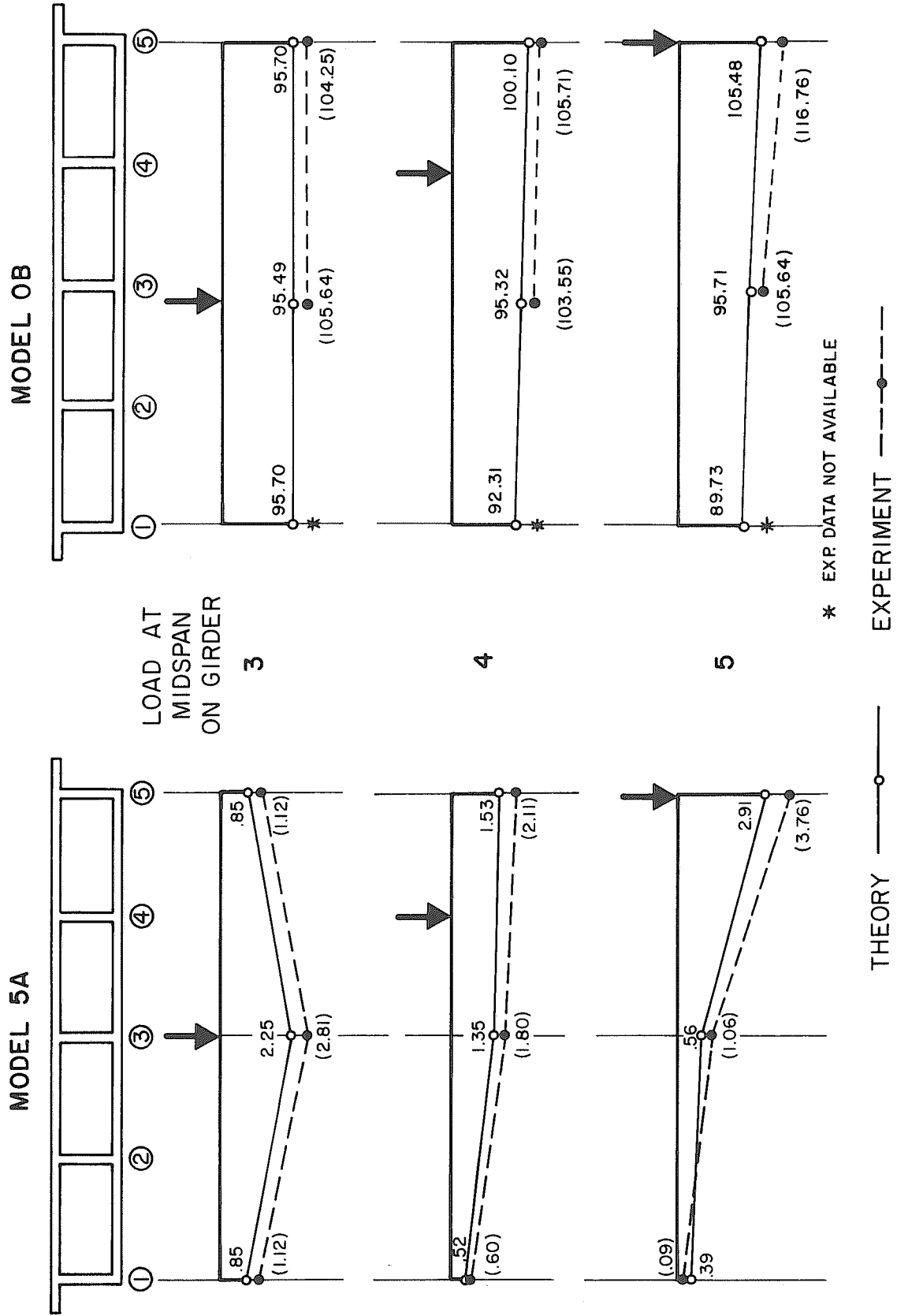


FIG. 3.5 COMPARISON OF THEORETICAL AND EXPERIMENTAL DEFLECTIONS AT MIDSPAN

generally increasing as the span becomes shorter or the angle of skew is increased. For deflections on the loaded half of the cross-section, therefore  $\Delta_3$  and  $\Delta_5$  in Figs. 3.1 to 3.5 and Table 3.1, which are the values of significant magnitude, Table 3.1 shows that the discrepancy ranges from 8% in the longest model OB to 27% in the shortest model 5A, with values for all other bridges falling somewhere in between these extremes.

Figures 3.1 to 3.5 compare, side by side, the results for each particular model without (A models) and with (B models) a midspan diaphragm. It can be seen that the addition of a diaphragm decreases the deflection under the loaded girder with the effect being most pronounced as the span becomes shorter or the skew angle is increased. Comparing theoretical and experimental values for the B models it again appears that the diaphragm in the experimental model is more flexible than in the theoretical model.

Deflections in a box girder bridge under arbitrary point loads are due to a complex mixture of the contributions from deformations due to longitudinal bending, transverse bending, shear and torsion. For a long span box girder bridge, the longitudinal bending stiffness and to a lesser degree the torsional stiffness of the overall cross-section play the dominant roles in the deflection response of the bridge. The bridge tends to behave somewhat like an ordinary longitudinal beam. However, as the span gets shorter, the transverse bending stiffness and shear stiffness become increasingly important to the deflection response. The load distribution and correspondingly the deflections in box girder bridge under an arbitrary point load

are highly dependent on the ratio of the transverse to longitudinal stiffnesses of the bridge. An increase in this ratio, such as occurs if the span is increased or if the plate thicknesses are increased, improves the load distribution in the bridge resulting in a more uniform distribution of deflections across the width of the bridge.

Since the experimental model yielded higher deflections than the theoretical model with differences ranging from 8% for the longest span to 27% for the shortest span, it would appear from the preceding discussion that a significantly greater difference must have existed between the transverse stiffnesses than between the longitudinal stiffnesses in the experimental and theoretical models.

At the time of publishing the report [5] on the experimental studies, it could not be determined whether the difference was due to an undesired increased flexibility in the screwed experimental model or due to an undesired increased stiffness in the theoretical finite element model. Subsequent, to the publication of reference [5] and in preparation for a similar experimental study on a curved aluminum model, some important evidence pertinent to the discrepancy between theoretical and experimental deflections for the skew bridge models was uncovered. The curved bridge model was to be constructed using a special cement (Aerobond 3041) to fasten the top and bottom deck to the webs instead of the screws used in the skew model. Several tests were conducted to compare the two methods of connection to the theoretical response of a homogeneous specimen.

Figure 3.6 presents the results of a component test on a simple span I-beam specimen similar in cross-section to an individual girder taken from the bridge. The glued specimen and the screwed specimen are both somewhat more flexible than theory. Both flexural and shear deformations were included in calculating the theoretical deflection. For the 20 in. span used in Fig. 3.6 the contributions were 88% due to flexure and 12% due to shear. These percentages would, of course, change if the span were varied. It can be seen in Fig. 3.6 that the upper portion of the glued specimen curve is nearly parallel to the theoretical curve. The bottom portions of both the glued and screwed specimen curves are slightly non-linear suggesting some initial slippage of the supporting testing frame used in the experiment. A so-called preload was applied to eliminate this "slack" in the testing system. The nonlinearity of the two experimental curves indicates that this preload should have been larger. If the linear portions of the experimental curves are extended downward to the deflection axis, the net deflection due to system slack can be found as the distance from the point of intersection with the horizontal axis to the origin. If the slack is deducted from the experimental values the glued specimen is about 4% more flexible than theory. The screwed specimen, however, differs from the theoretical curve by about 9% which approximates the difference between experiment and theory found in the long span box girder bridge models.

These results indicate not only that the screwed test models in the bridge were considerably more flexible than theory, but also that



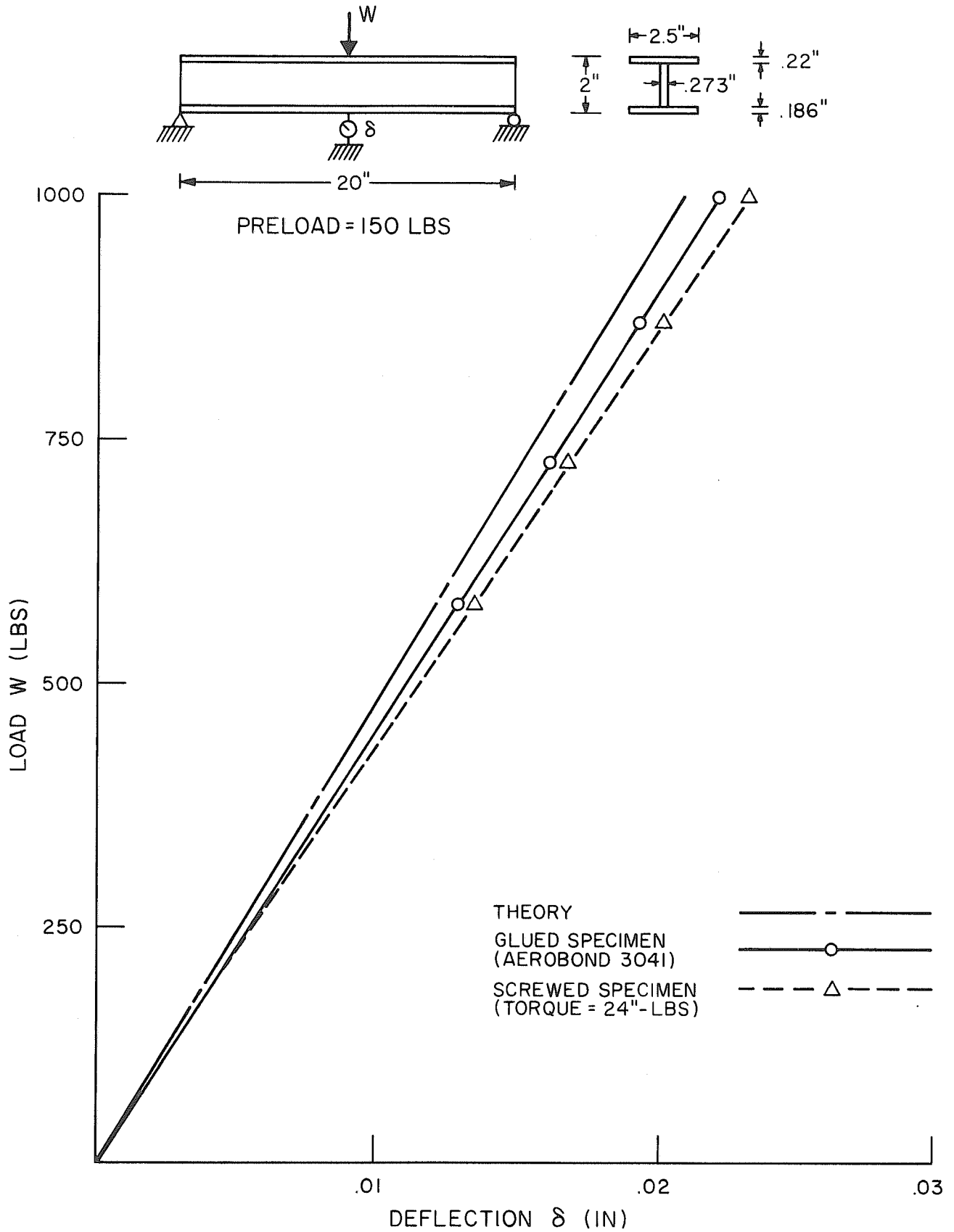


FIG. 3.6 COMPONENT TEST FOR SHEAR SLIP

a part of the observed experimental deflections may have been due to initial slippage of the testing frame. A preload of 100 lbs. was used for all models tested. This preload may have been too small to eliminate the slack. This slack would be independent of span and would constitute a larger percentage of the deflection in the shorter bridges. This might also partially explain the changing percentage difference between theory and experiment as the span was shortened.

A second component test to compare transverse stiffnesses was performed as illustrated in Fig. 3.7. Here a 1.5 in. long strip of the bridge cross-section was tested as a vierendeel rigid frame spanning transversely between simple supports under the two exterior edges of the bridge. Once again a theoretical analysis was made, with the aid of a computer frame analysis program, assuming a homogeneous system and the results compared with those found experimentally for a glued specimen and a screwed specimen. Results from the glued specimen compared almost exactly with theory. However, comparing theory with experiment for the screwed specimen which was similar to that used in the skew model, the ratio of theoretical to experimental deflection is about 0.68 or a 32% difference. This indicates as postulated earlier that a much greater difference between theory and experiment existed for transverse stiffness than for longitudinal stiffness. Despite the great care exercised in the experimental study, the screwed connections prevented a true simulation of the homogeneous and monolithic system assumed in the theoretical model resulting in the observed discrepancy between theoretical and experi-

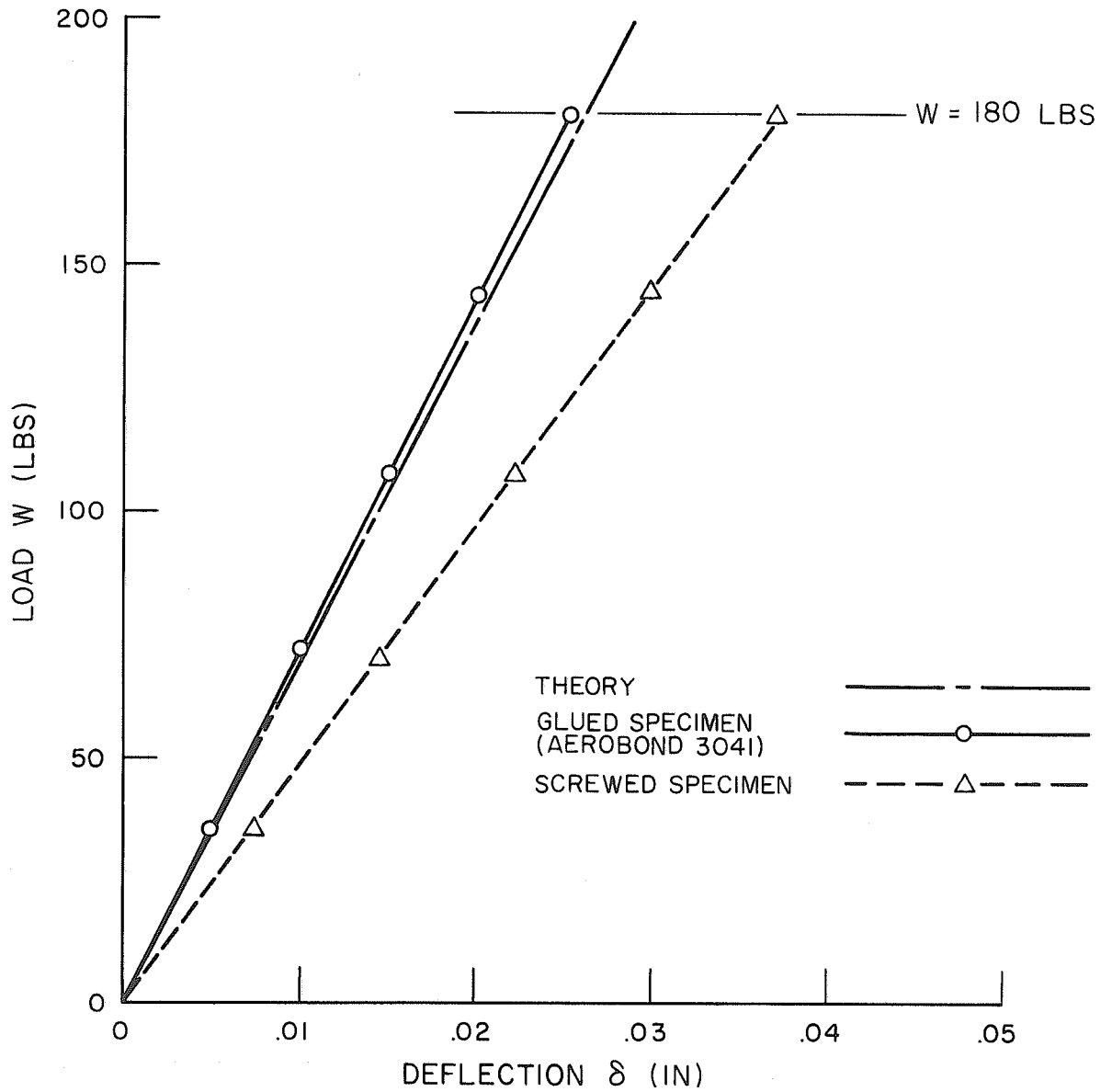
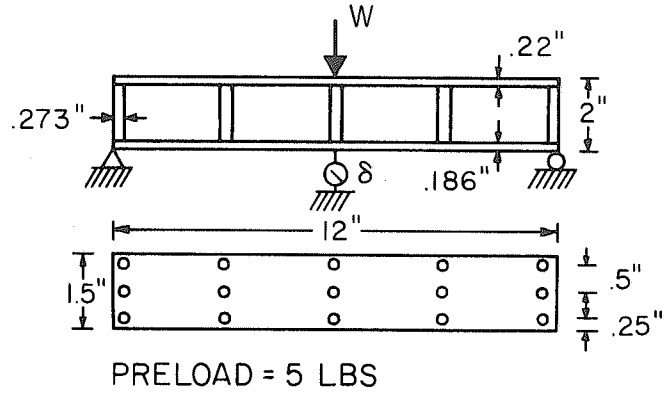


FIG. 3.7 COMPONENT TEST FOR MOMENT CONTINUITY

mental deflections. It is concluded that if a glued system had been used, the agreement in deflections would have been much better. Preliminary results from the curved bridge model study seem to verify this conclusion and thus it is felt that the finite element program CELL can be used to adequately predict the deflections of skew box girder bridges.

### 3.3 Reactions

The theoretical and experimental reactions for all models and load cases compare relatively well. In both theory and experiment no difference in reactions between models with and without diaphragms was found. Therefore, results only for models without diaphragms are presented in Figs. 3.8 to 3.13 and are discussed further in this section.

It can be seen in Figs. 3.8 and 3.9 that there is very little difference between theoretical and experimental influence lines for reactions in Model 1A for loads on girders 3 and 5. The differences are somewhat larger when the load moves along girder 1. The influence lines for the other models are very similar and are partially illustrated in Figs. 3.10 to 3.13. Some indication of the behavior of skew box girder bridges can be seen in Figs. 3.10 and 3.11 by comparing the influence lines for skew models 1A through 4A to the straight model 5A. The sum of reactions R1 and R2 is always given by taking moments about an axis through R3 and R4. Thus, for a load on girder 3 on the straight bridge, 5A, the reactions R1 and R2 are always equal. With the supports skewed, however, the reaction R2 at the obtuse corner is larger than R1 at the acute corner. The difference between R2 and R1 becomes greater as the angle of skew increases. Figs. 3.12 and 3.13

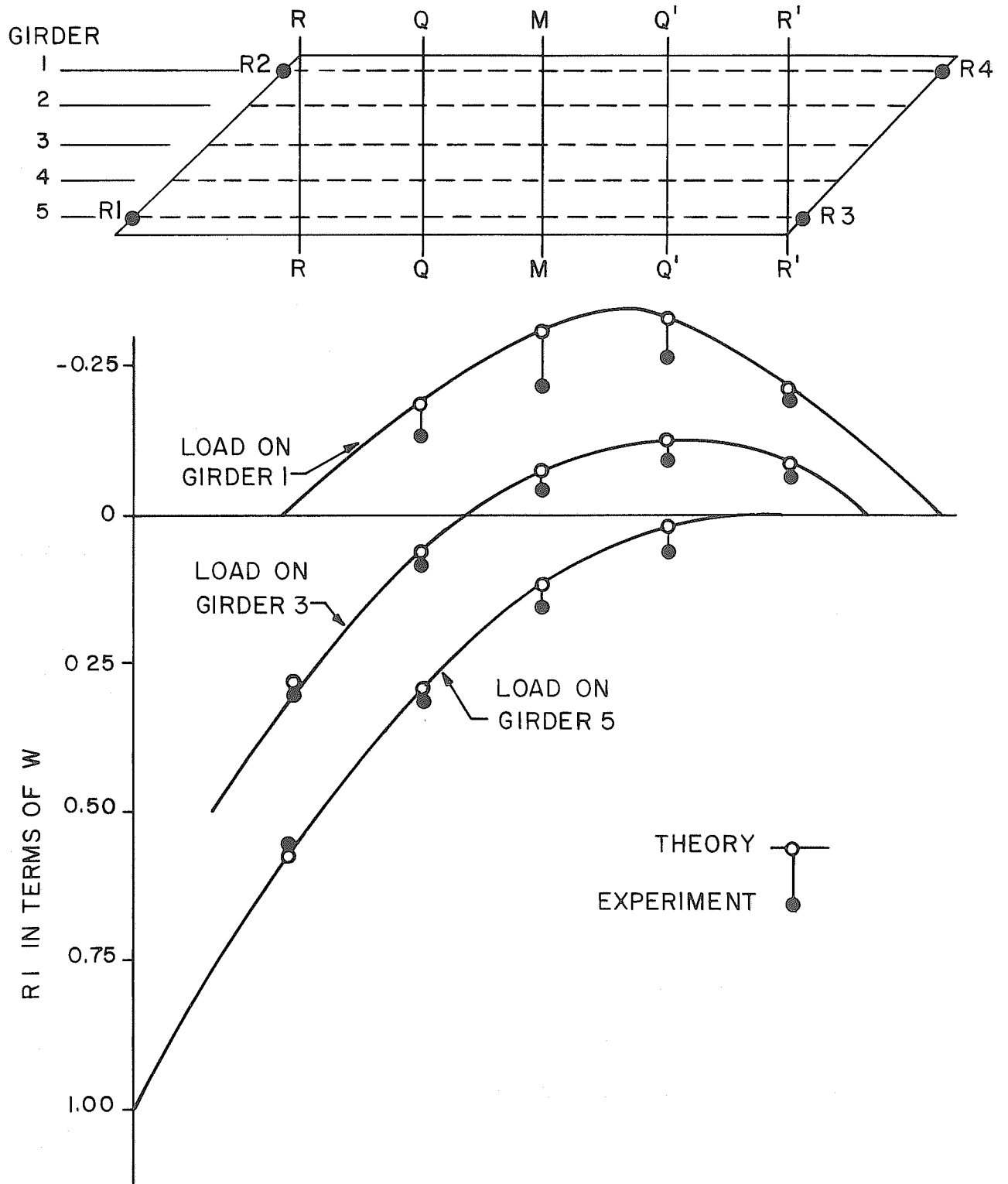


FIG. 3.8 INFLUENCE LINES FOR REACTION R1 FOR MODEL 1A (45°/53.5°), LOADS ON GIRDERS 1, 3, AND 5

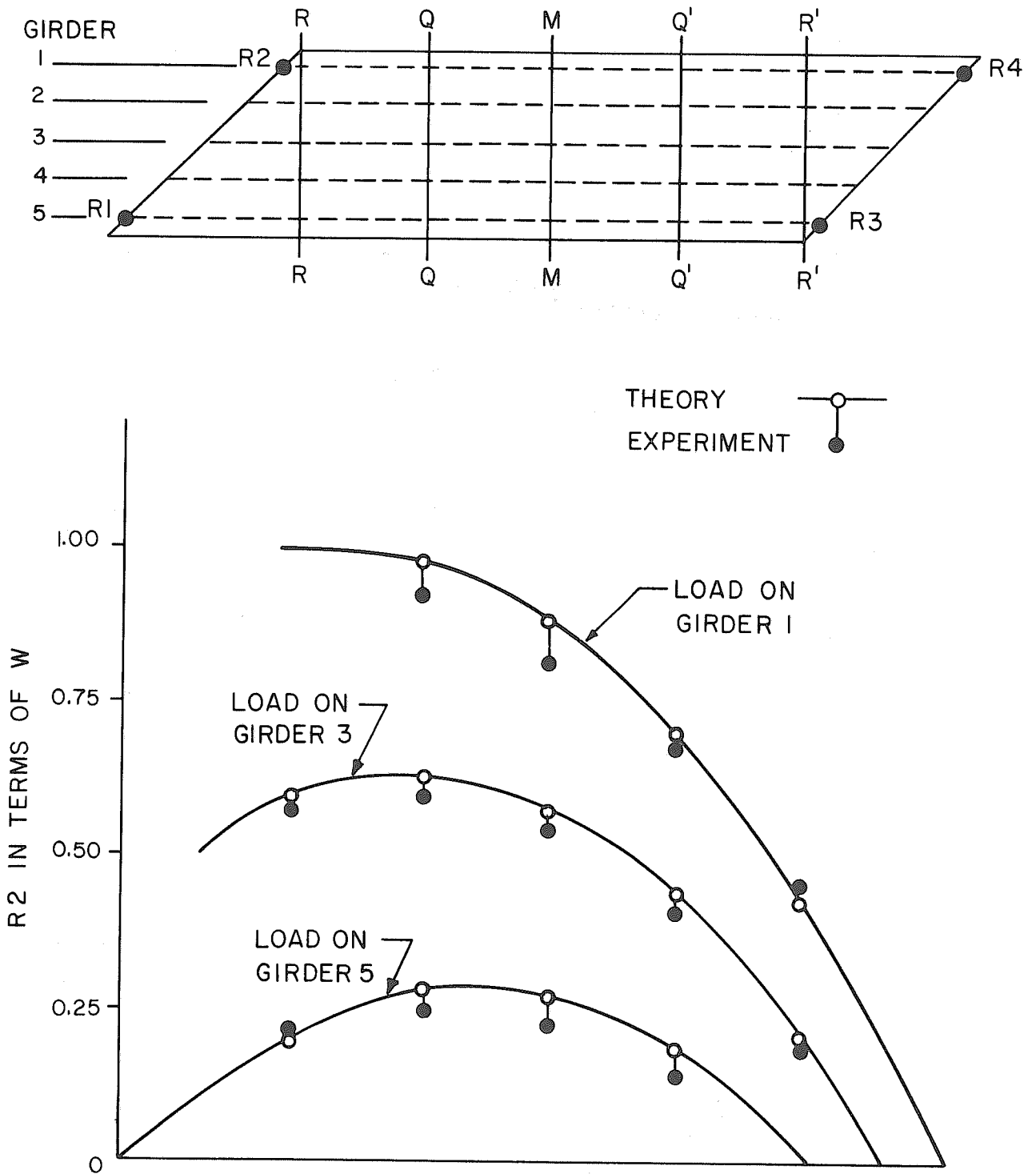


FIG. 3.9 INFLUENCE LINES FOR REACTION R2 FOR MODEL 1A (45°/53.5°), LOADS ON GIRDERS 1, 3, AND 5

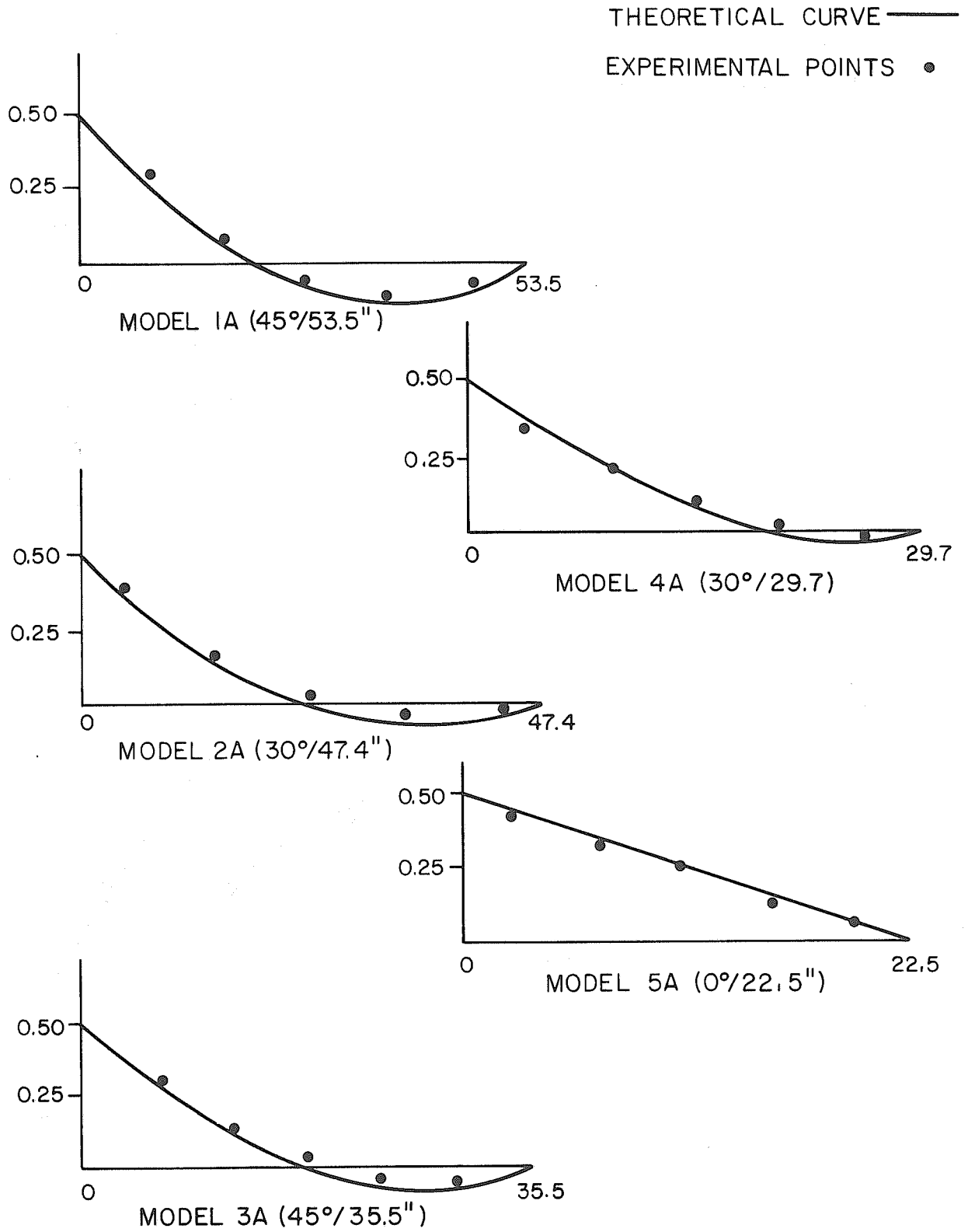


FIG. 3.10 INFLUENCE LINES FOR REACTION R1 (COEFFICIENTS OF W), LOADS ALONG GIRDER 3

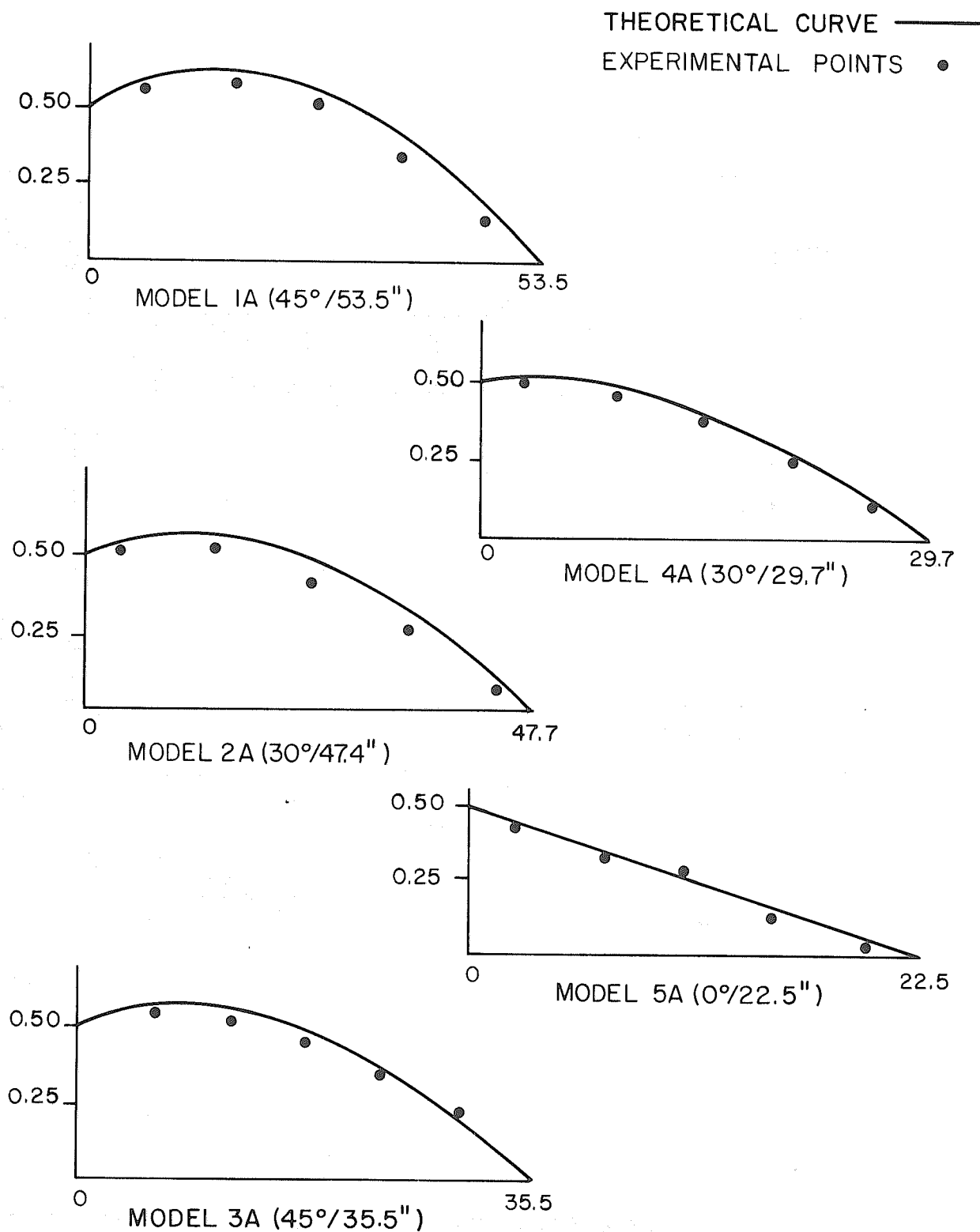


FIG. 3.11 INFLUENCE LINES FOR REACTION R2 (COEFFICIENTS OF W), LOADS ALONG GIRDER 3



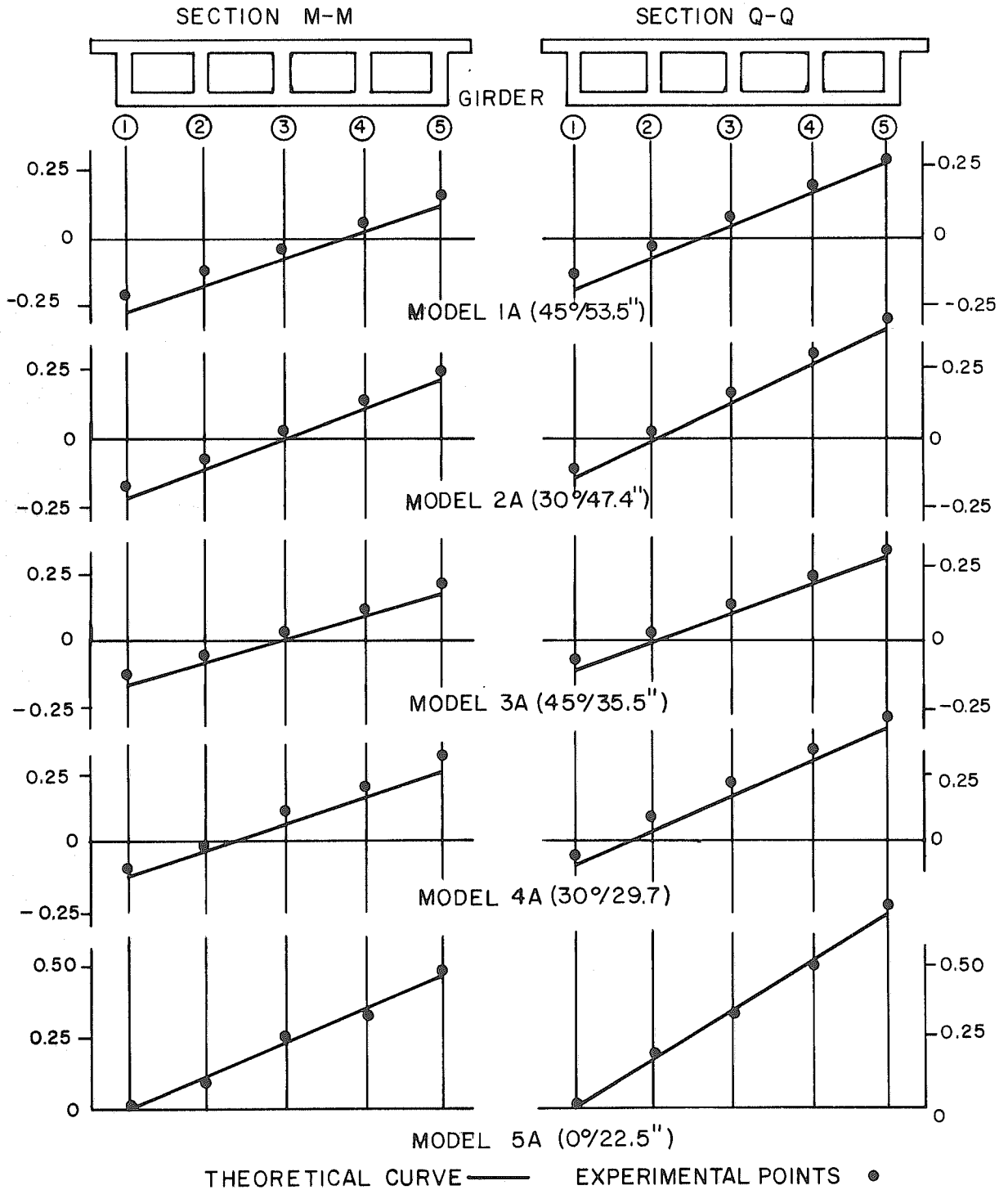


FIG. 3.12 INFLUENCE LINES FOR REACTION R1 (COEFFICIENTS OF W), LOADS ON RIGHT TRANSVERSE SECTIONS MM AND QQ

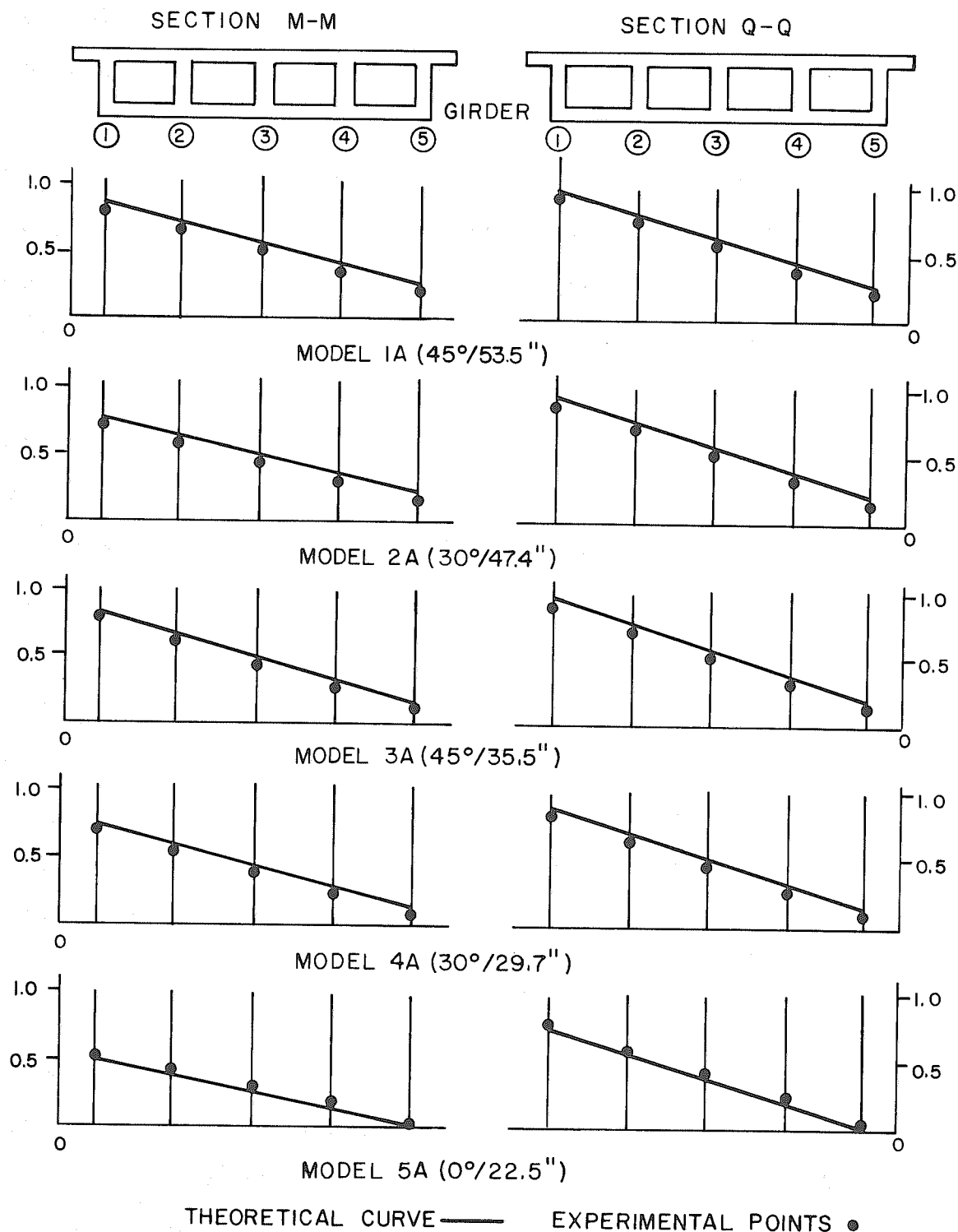
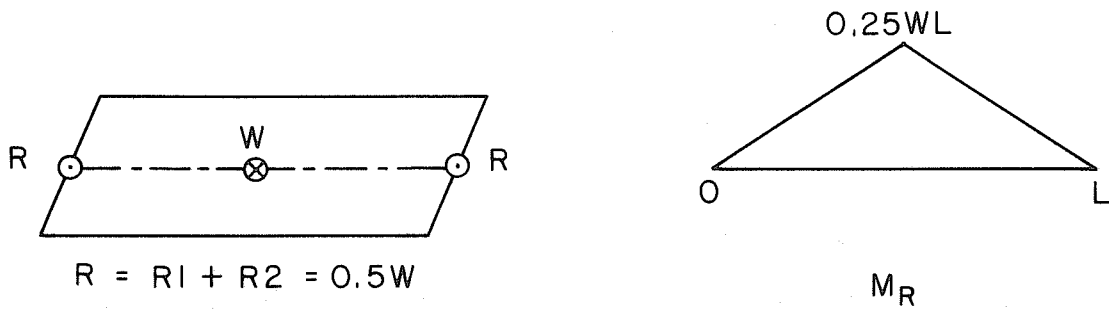
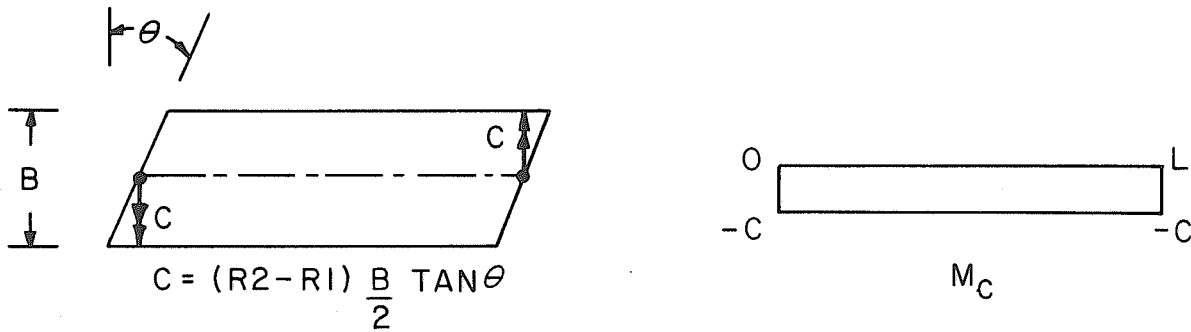


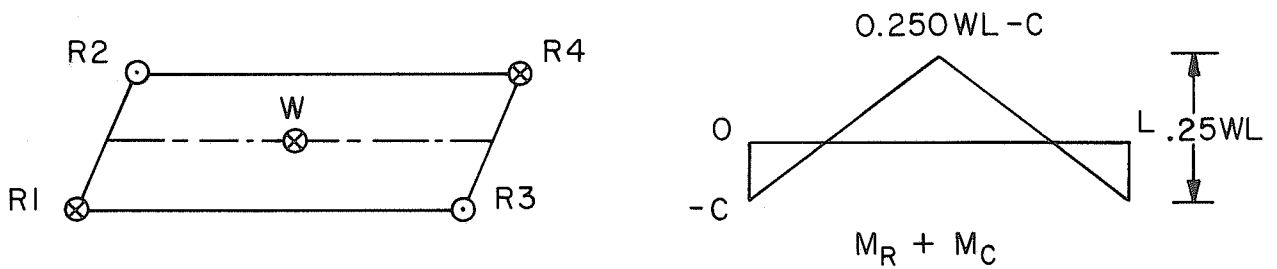
FIG. 3.13 INFLUENCE LINES FOR REACTION R2 (COEFFICIENTS OF W), LOADS ON RIGHT TRANSVERSE SECTIONS MM AND QQ



a) EFFECT OF RESULTANT VERTICAL REACTION R



b) EFFECT OF RESULTANT COUPLE C



c) SUPERPOSITION OF EFFECTS R+C

FIG. 3.14 TOTAL MOMENT ON SECTIONS NORMAL TO THE LONGITUDINAL AXIS FOR A LOAD AT MIDSPAN CENTER

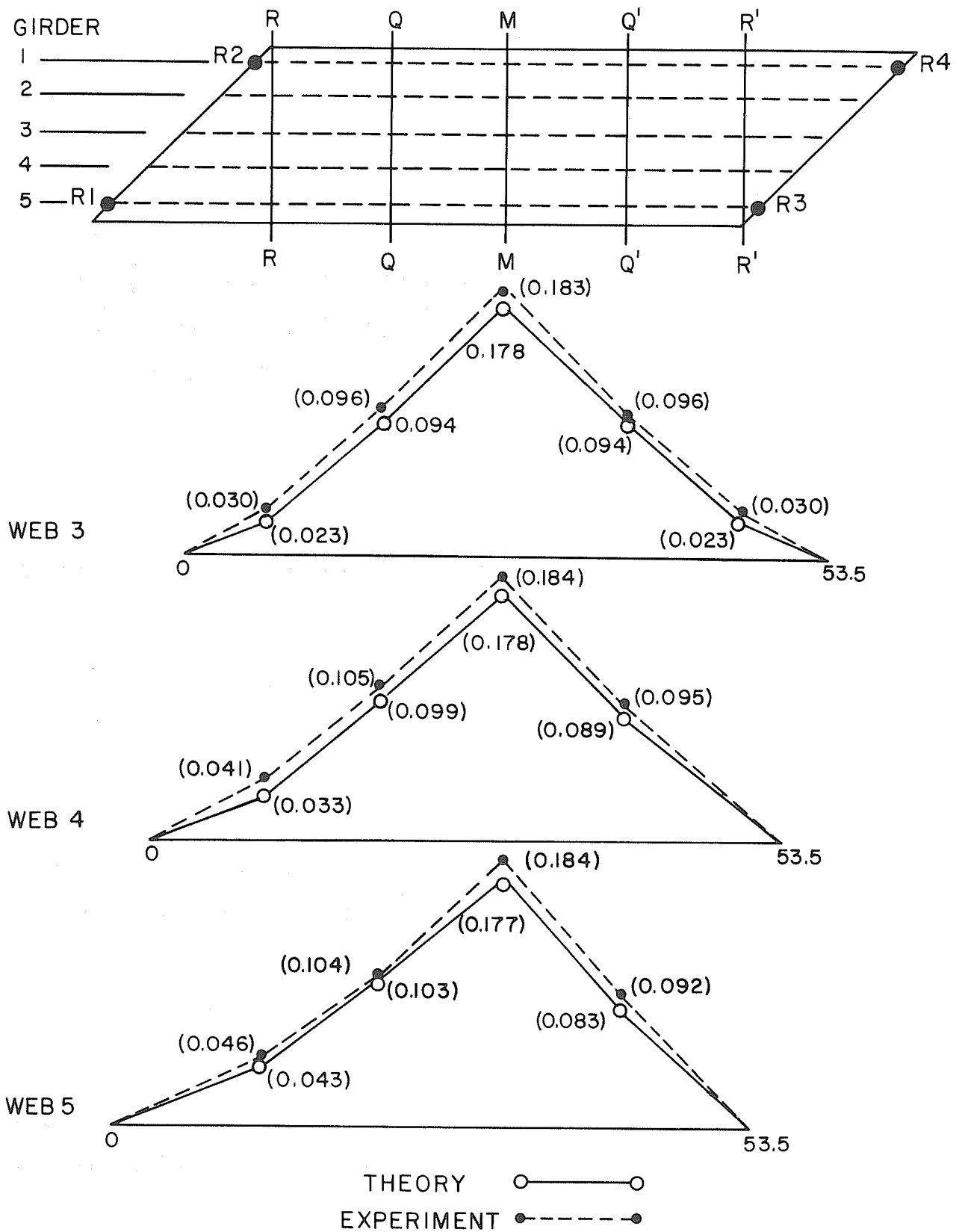


**FIG. 3.15 INFLUENCE LINES FOR TOTAL MIDSPAN MOMENT (COEFFICIENTS OF WL) FOR LOADS ON GIRDERS 3, 4, AND 5 OF MODEL 1A (45°/53.5")**

TABLE 3.2 COMPARISON BETWEEN THEORY AND EXPERIMENT FOR EXTERNAL MIDSPAN MOMENTS AND REACTION COUPLES FOR MIDSPAN POINT LOAD ON GIRDER 3

Model	$M_T$	$M_E$	$C_T$	$C_E$	$M_E - M_T$	$C_E - C_T$
1A (45°/53.5")	.178	.183	-.072	-.065	.005	.007
2A (30°/47.4")	.214	.217	-.036	-.032	.003	.004
3A (45°/35.5")	.168	.179	-.081	-.071	.011	.010
4A (30°/29.7")	.209	.218	-.041	-.034	.009	.007
5A (0°/22.5")	.250	.252	0	0	.002	0

$M_T$  = Theoretical midspan moment;  $M_E$  = Experimental midspan moment

$C_T$  = Theoretical reaction couple;  $C_E$  = Experimental reaction couple

\* All values in terms of WL

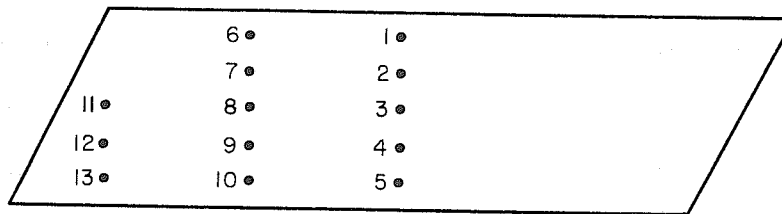
Notice that the difference between theoretical and experimental external moments at midspan is essentially the same as between the corresponding reaction couples as would be expected.

Table 3.3 shows that this trend extends to most other load cases. It can be seen that the difference between theory and experiment in the prediction of the external midspan moment is generally very small.

### 3.5 Longitudinal Plate Forces $N_{XX}$

As previously noted in Section 2.5 on the self-consistency of theoretical results, the correspondence between internal and external

TABLE 3.3 RATIO OF THEORETICAL TO EXPERIMENTAL EXTERNAL  
MOMENT AT MIDSPAN FOR ALL LOAD POSITIONS



Model	Load Position at Midspan Section				
	1	2	3	4	5
1A (45°/53.5")	.93	.97	.97	.98	.96
2A (30°/47.4")	.96	.99	.99	.99	.99
3A (45°/35.4")	.93	.94	.94	.96	.96
4A (30°/29.7")	.97	.95	.96	.96	.98
5A (0°/22.5")	1.00	1.00	.99	.99	.98
Model	Load Position Near Quarter Span				
	6	7	8	9	10
1A (45°/53.5")	.90	.94	.98	.94	.99
2A (30°/47.4")	.94	.96	.97	.99	.98
3A (45°/35.4")	.87	.89	.91	.95	.94
4A (30°/29.7")	.93	.92	.93	.95	.97
5A (0°/22.5")	.98	.98	.97	.96	.96
Model	Load Position Near Supports				
			11	12	13
1A (45°/53.5")			.77	.80	.93
2A (30°/47.4")			.92	1.00	1.00
3A (45°/35.4")			.82	.92	.93
4A (30°/29.7")			.88	.91	.97
5A (0°/22.5")			-	-	-

theoretical moments at midspan was very close. This comparison for experimental values was also very good. Consequently, theoretical and experimental internal moments should exhibit a comparison similar to that already described for the external moments at midspan. Figures 3.16 to 3.24 show computer plots of theoretical and experimental  $N_{xx}$  forces at Section 0-0. While this section is not directly at midspan it is close enough to reflect the response at midspan very well. It can be concluded from studying Figs. 3.16 to 3.24 that the agreement between theory and experiment for  $N_{xx}$  is generally very good. As might be expected in light of the comparison between theory and experiment for external moment at midspan, the experimental plate forces are slightly higher than theory in most cases. The corresponding theoretical and experimental curves for all models without diaphragms under the same point load position are of the same general shape with some differences in magnitude near the load point. The theoretical plate forces at the load point seem to be consistently higher than experimental. This slight difference is probably due to the coarse mesh used in the finite element analysis. However, when averaged over the width of the top and bottom deck the experimental forces are higher by approximately the same percentages as the experimental external moments.

Notice that in models with the midspan diaphragm the curves are much flatter indicating the improved distribution of internal forces which one would expect. The experimental results still show a slight peaking in the loaded region. This indicates that the experimental diaphragm was more flexible than its counterpart in theory. Similar

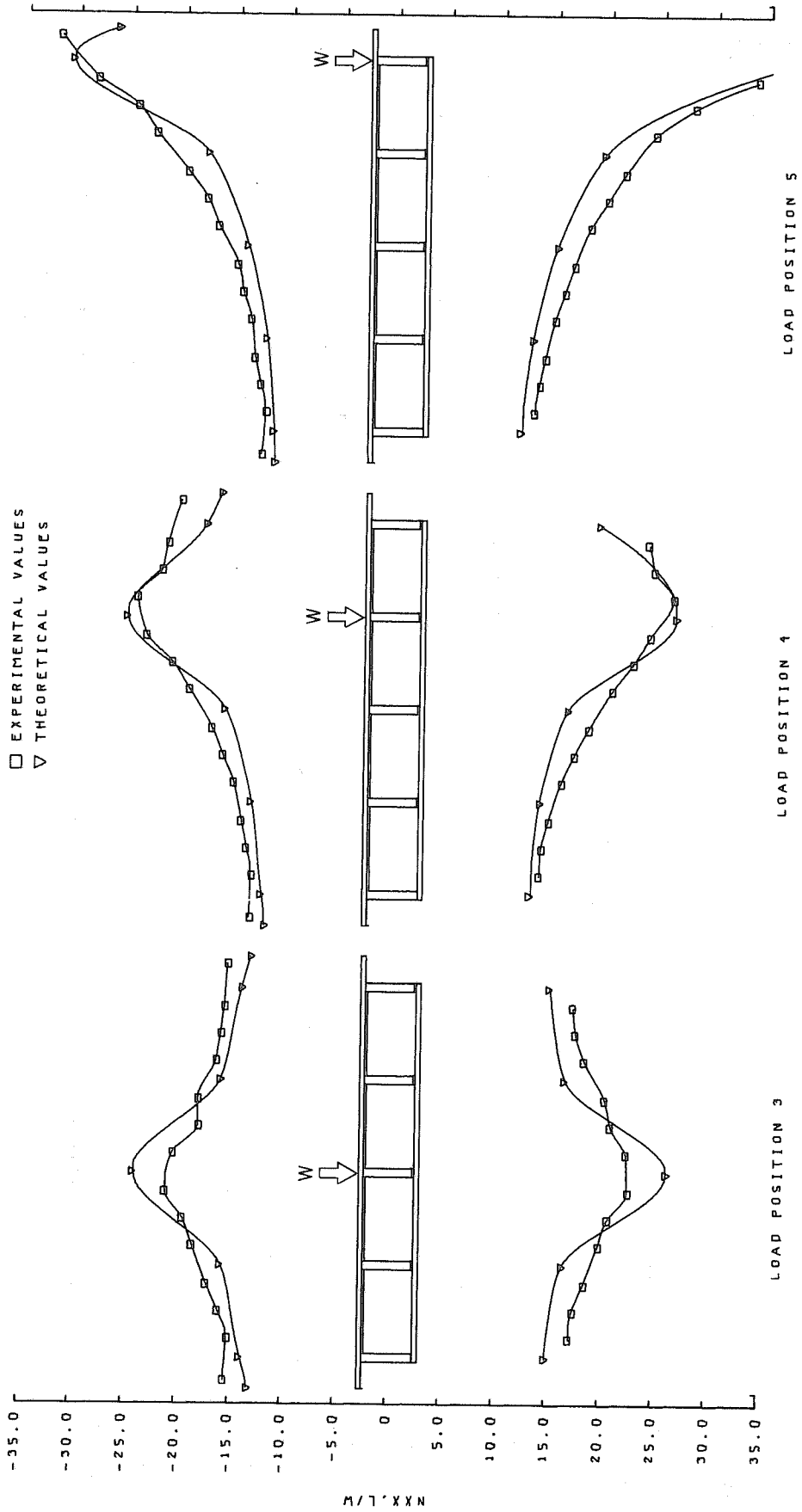


FIG. 3.16 TRANSVERSE DISTRIBUTION OF AXIAL FORCES PER UNIT WIDTH IN TOP AND BOTTOM PLATES (NXX) AT SECTION 0-0

MODEL 1A (45°/53.5")



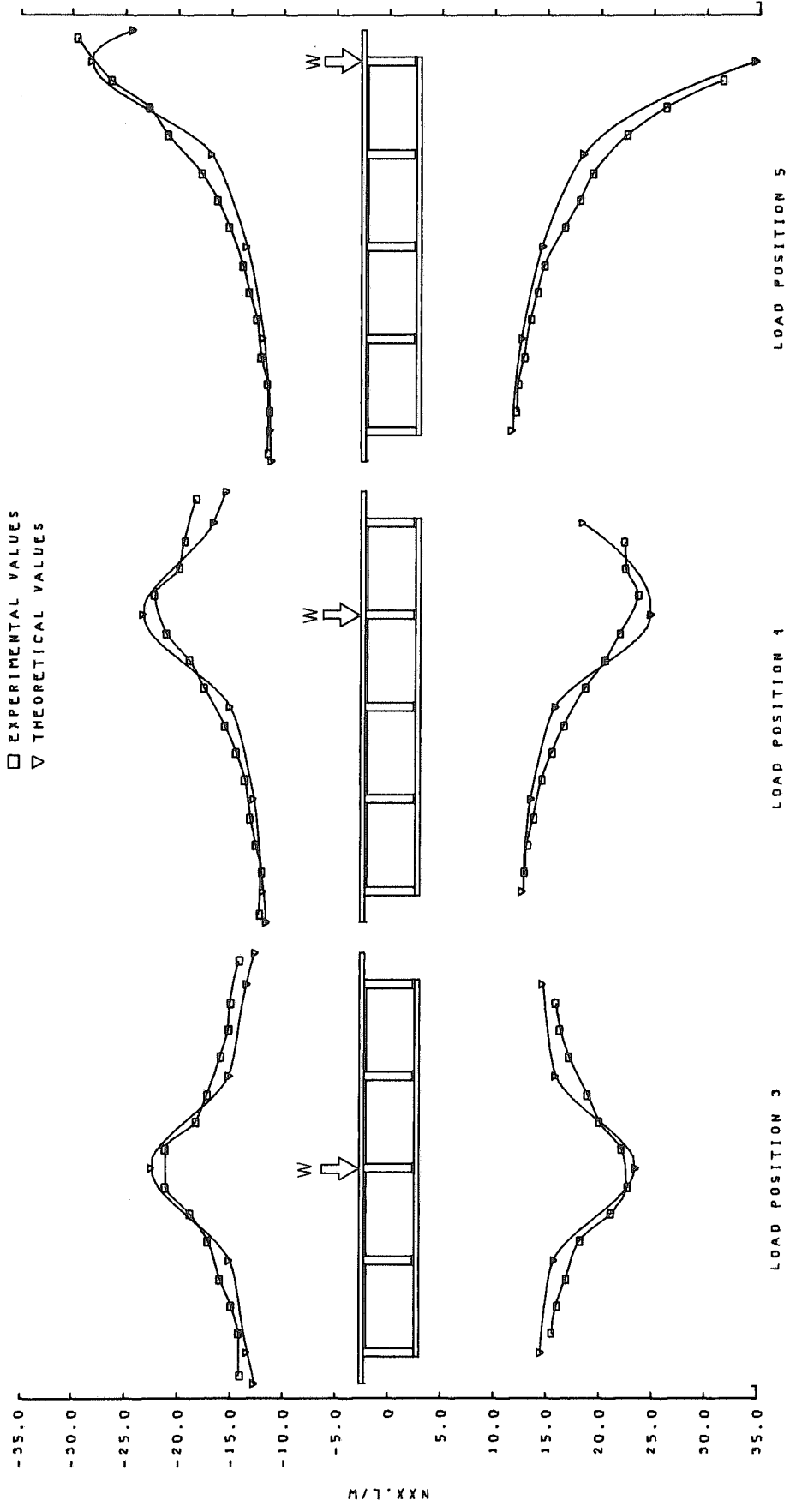


FIG. 3.17 TRANSVERSE DISTRIBUTION OF AXIAL FORCES PER UNIT WIDTH IN TOP AND BOTTOM PLATES (NX) AT SECTION 0-0  
 MODEL 2A (30°/47.4")

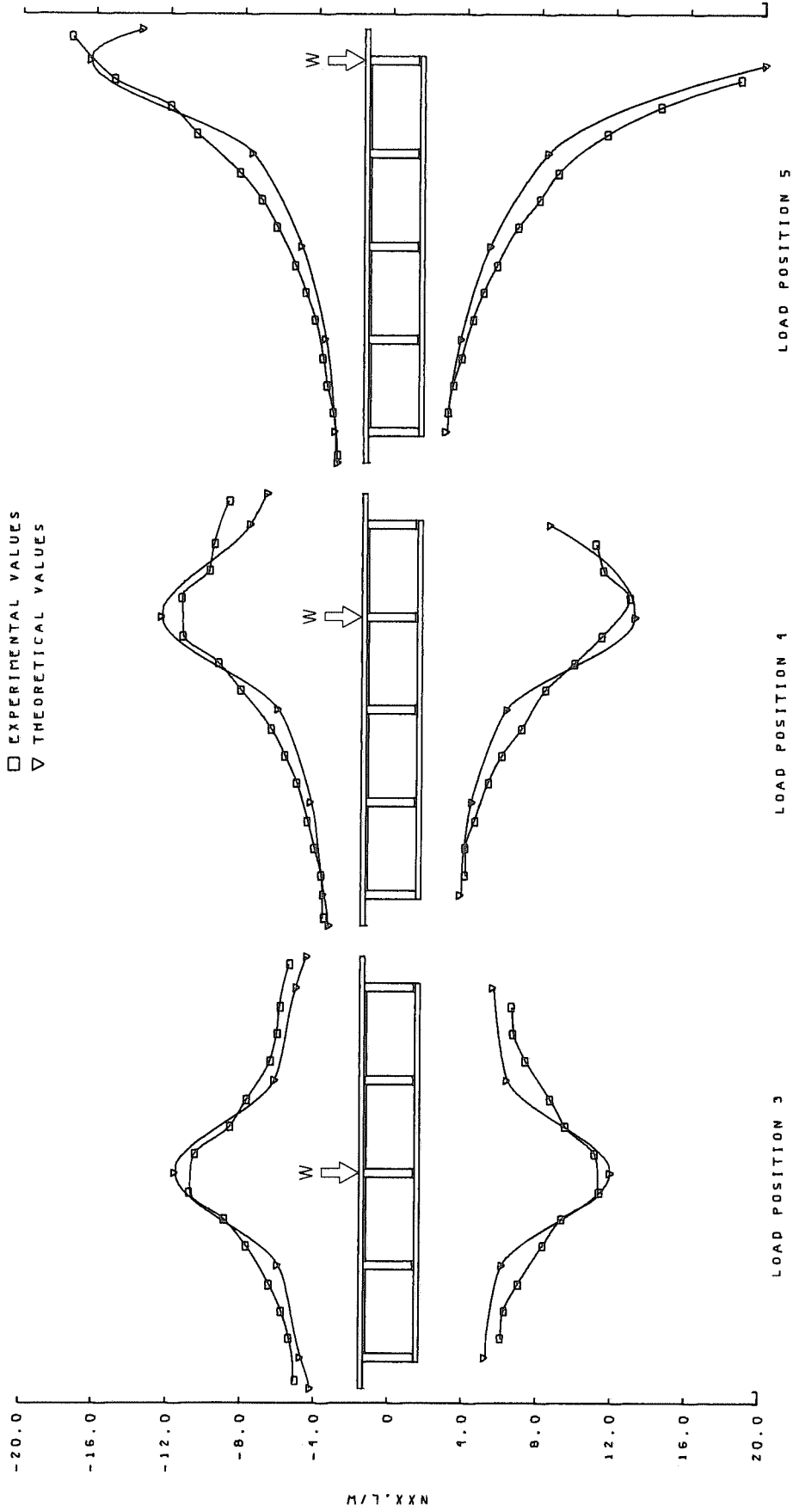


FIG. 3.18 TRANSVERSE DISTRIBUTION OF AXIAL FORCES PER UNIT WIDTH IN TOP AND BOTTOM PLATES (NXX) AT SECTION 0-0

MODEL 3A (45°/35.5'')

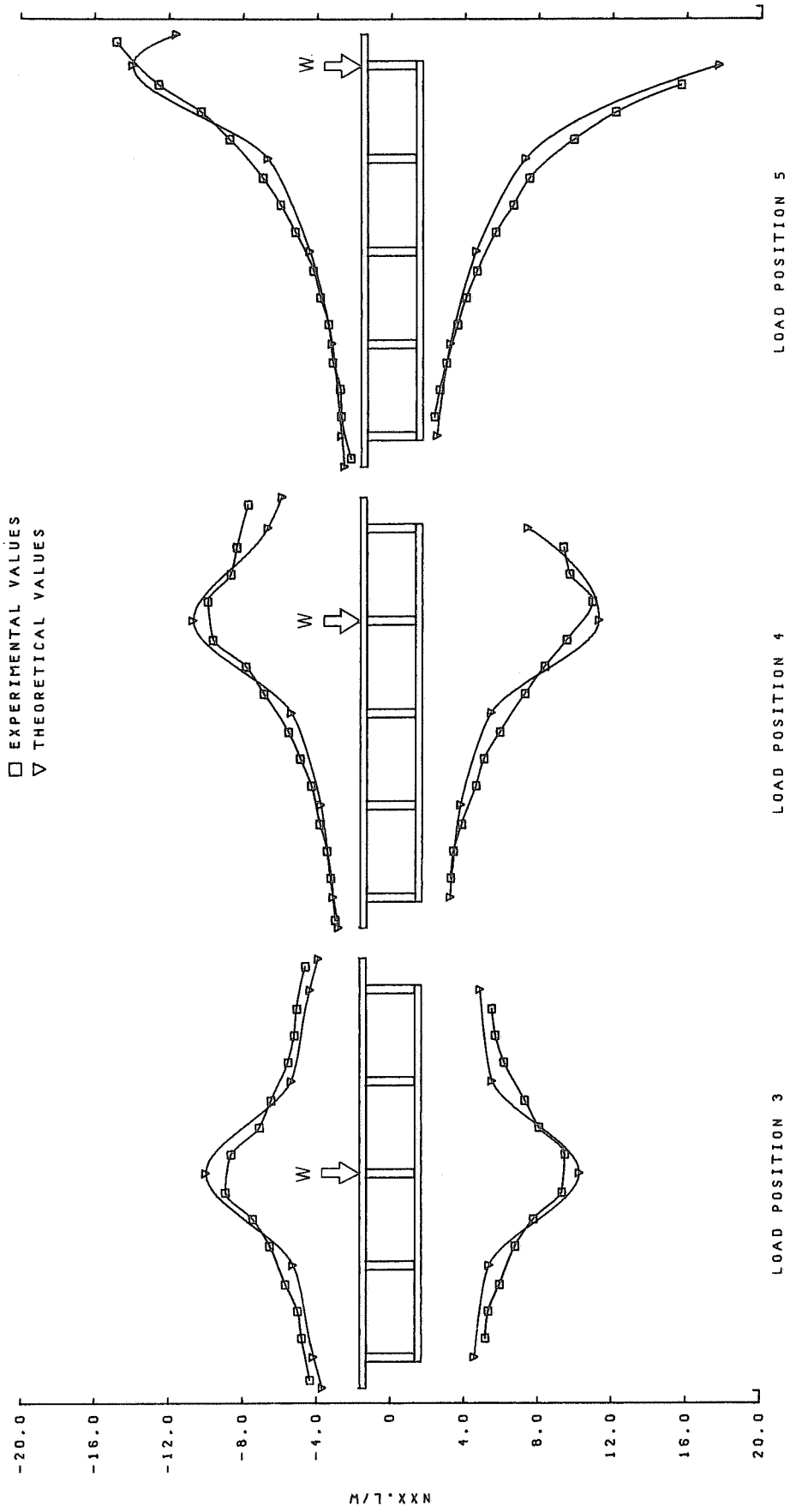


FIG. 3.19 TRANSVERSE DISTRIBUTION OF AXIAL FORCES PER UNIT WIDTH IN TOP AND BOTTOM PLATES (NXX) AT SECTION 0-0 MODEL 4A (30°/29.7")

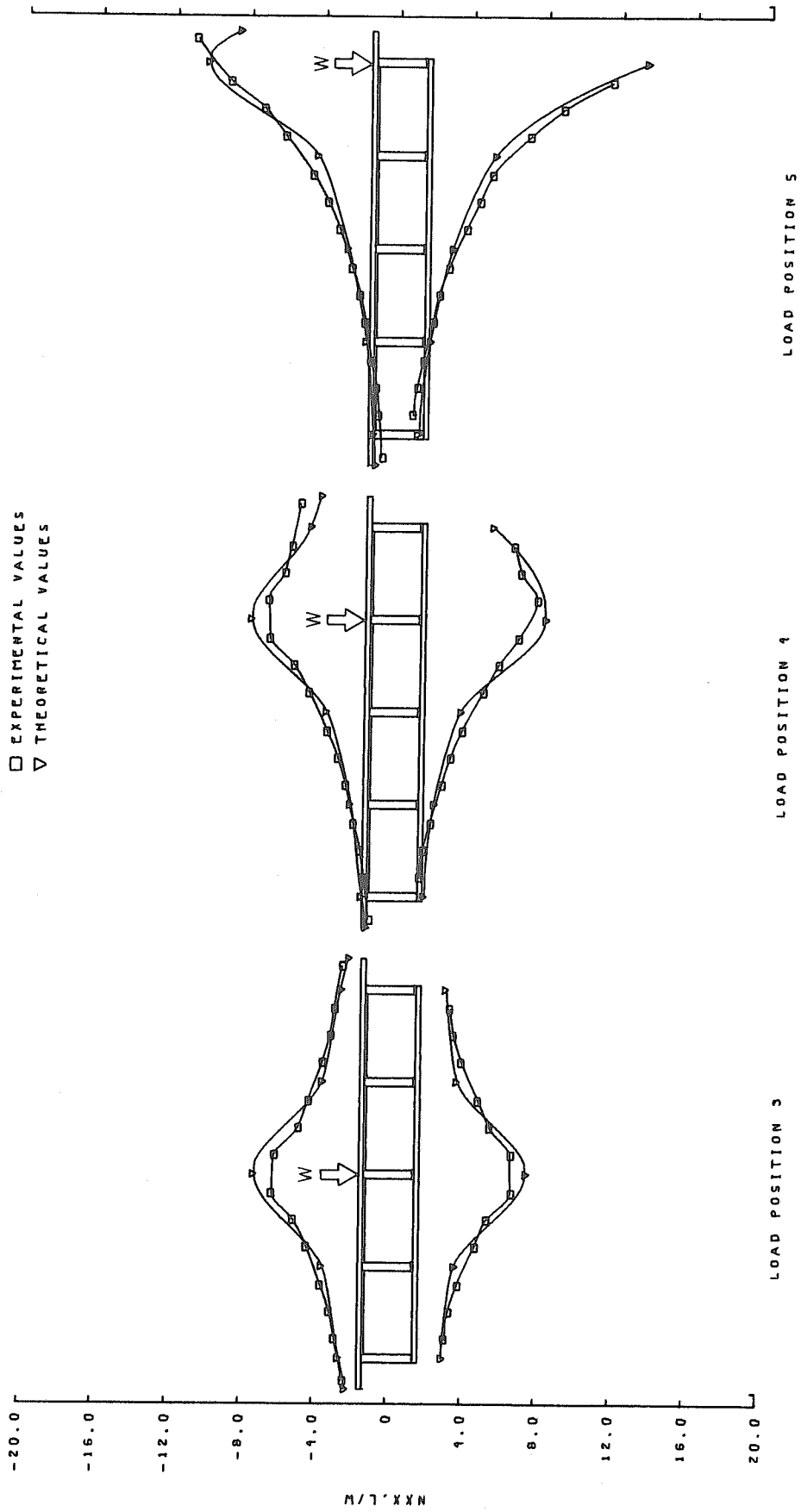


FIG. 3.20 TRANSVERSE DISTRIBUTION OF AXIAL FORCES PER UNIT WIDTH IN TOP AND BOTTOM PLATES (NXX) AT SECTION 0-0

MODEL 5A (0°/22.5°)

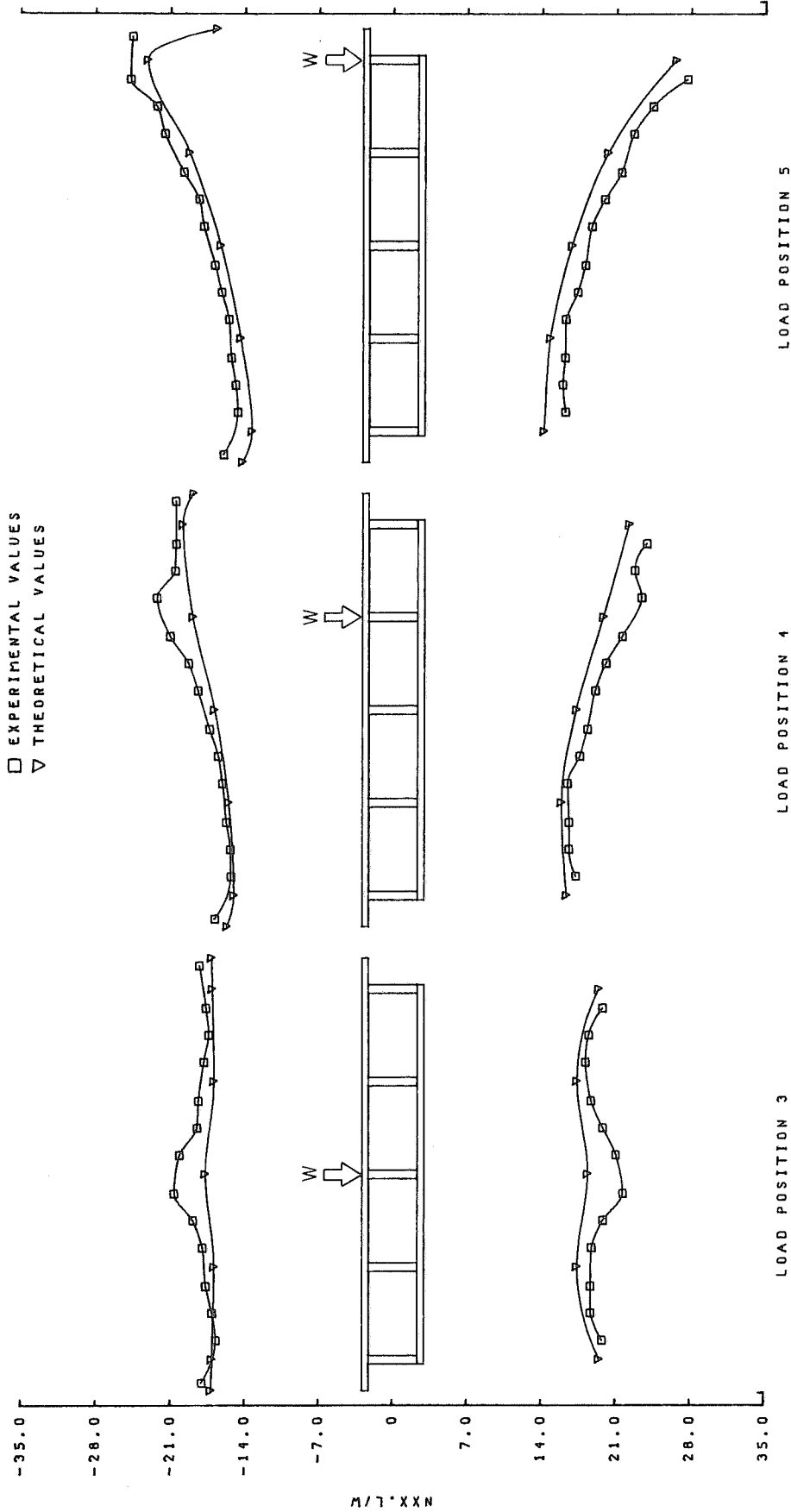


FIG. 3.21 TRANSVERSE DISTRIBUTION OF AXIAL FORCES PER UNIT WIDTH IN TOP AND BOTTOM PLATES (NXX) AT SECTION 0-0  
 MODEL 1B (45°/53.5")

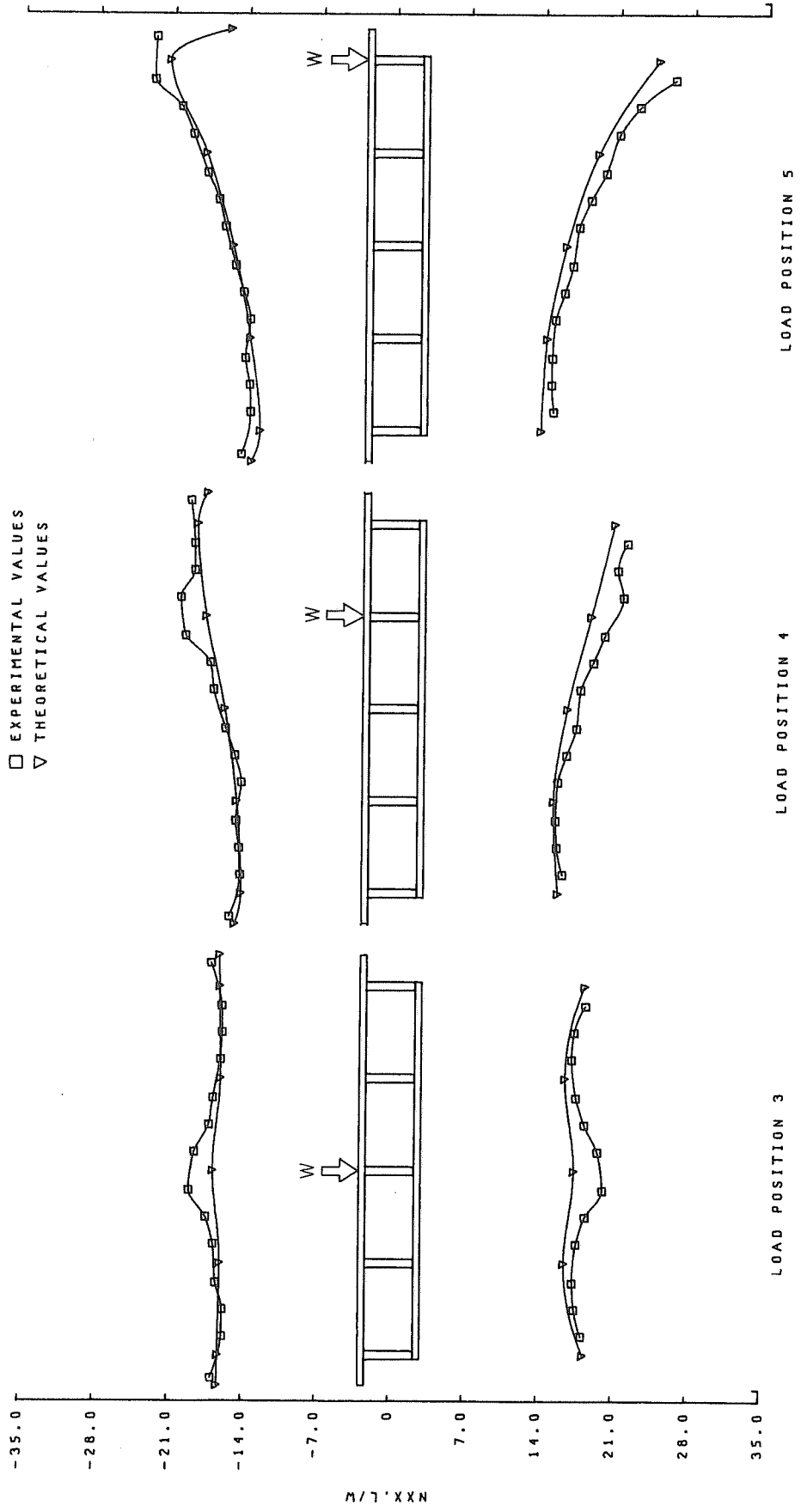


FIG. 3.22 TRANSVERSE DISTRIBUTION OF AXIAL FORCES PER UNIT WIDTH IN TOP AND BOTTOM PLATES (NXX) AT SECTION 0-0

MODEL 2B (30°/47.4")

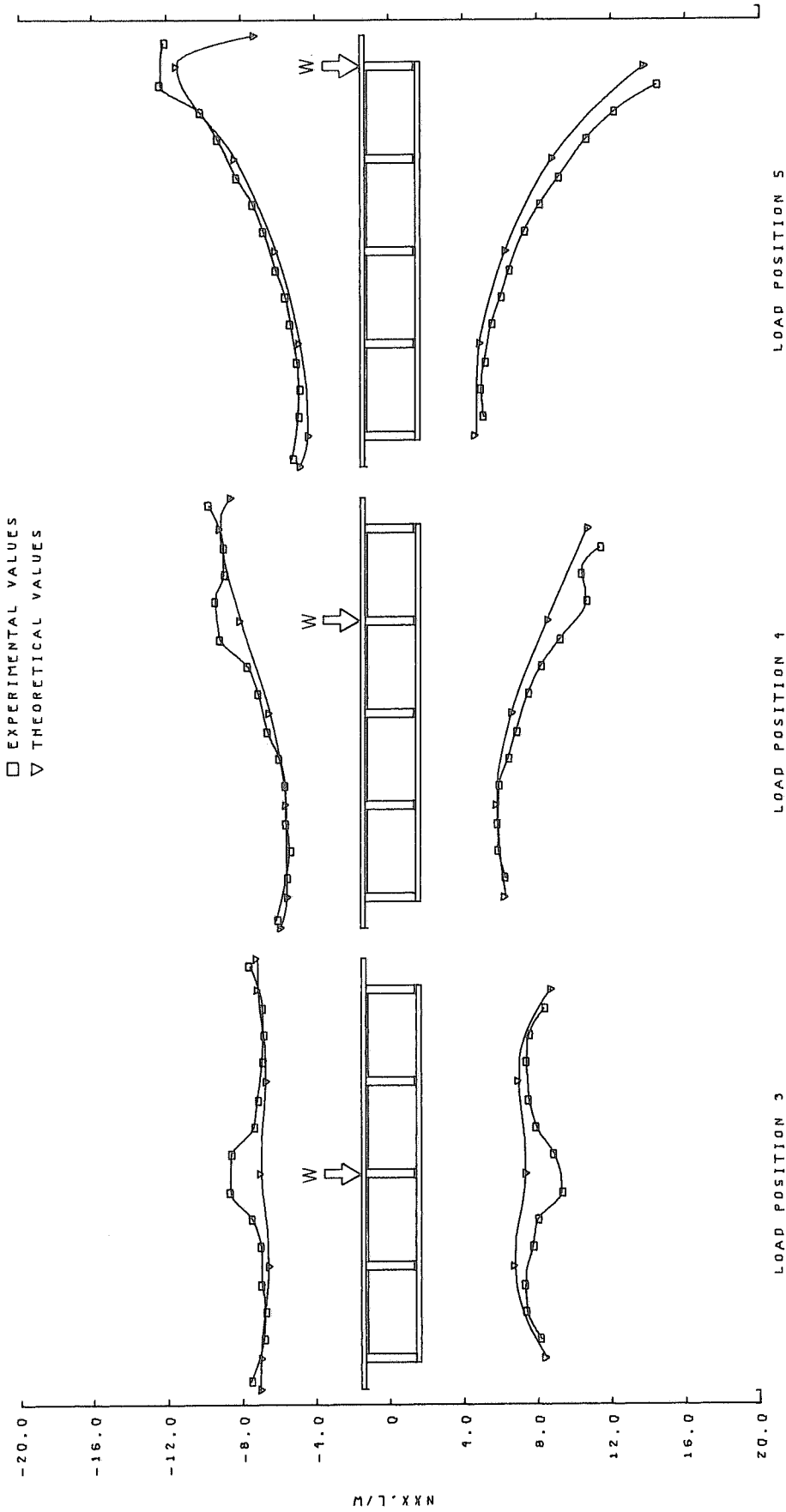


FIG. 3.23 TRANSVERSE DISTRIBUTION OF AXIAL FORCES PER UNIT WIDTH IN TOP AND BOTTOM PLATES (NXX) AT SECTION 0-0

MODEL 3B (45°/35.5")

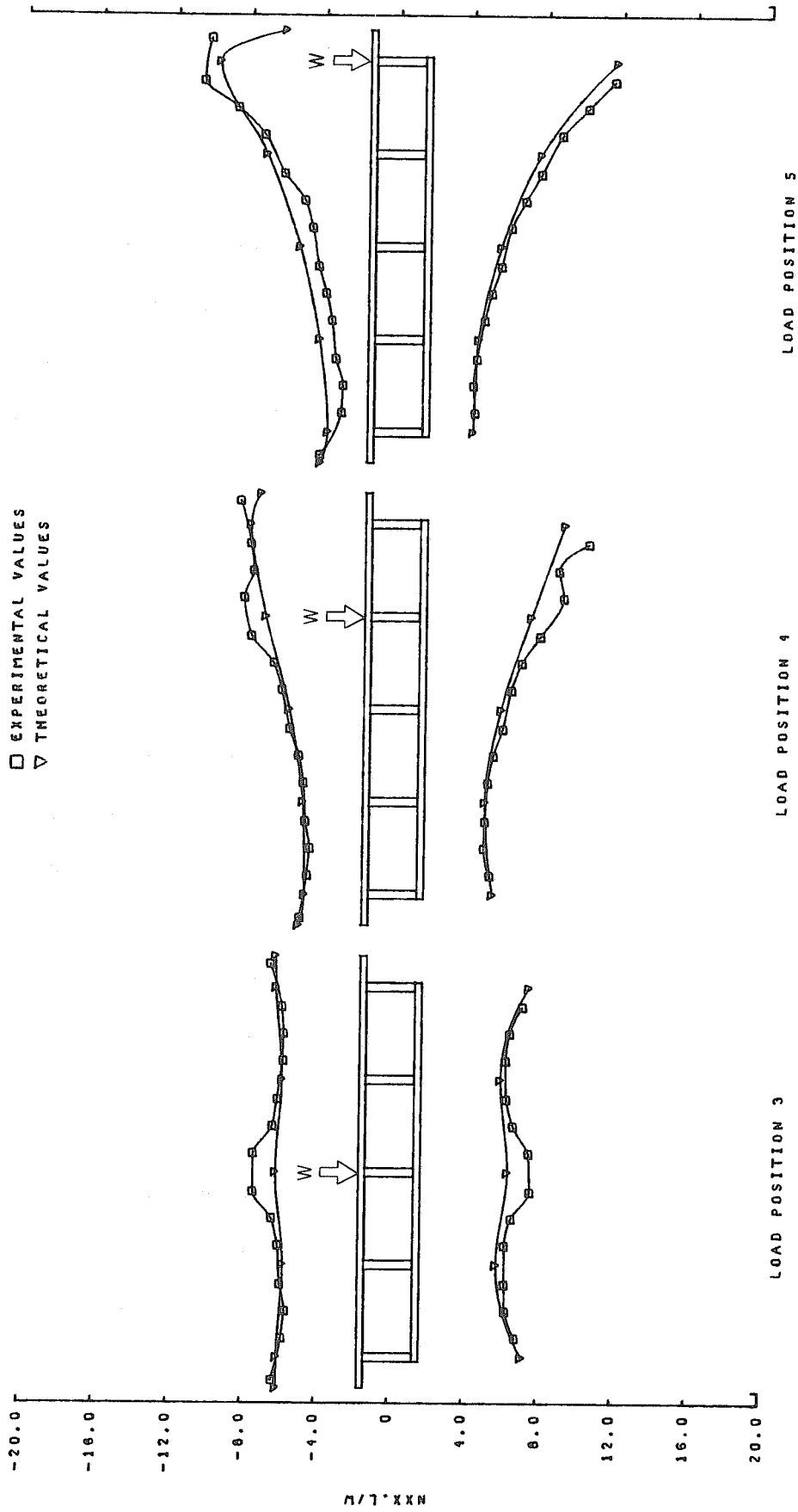


FIG. 3.24 TRANSVERSE DISTRIBUTION OF AXIAL FORCES PER UNIT WIDTH IN TOP AND BOTTOM PLATES (NXX) AT SECTION 0-0  
MODEL 4B (309/29.7")



to the A series models without diaphragms, the averaged plate forces for the B series models with diaphragms show the same comparison between theory and experiment as the external moments.

It is interesting to note that for a given load position the shape of the transverse distribution curve for  $N_{xx}$  seems to be nearly independent of span and angle of skew. The curve merely shifts upward or downward as the span or skew increases or decreases. The curves for the various models remain roughly parallel. This is especially true for loads near the center of the bridge. Thus, the departure of the curve from a uniform transverse distribution is primarily due to local bending effects and not the span or angle of skew as might have been expected.

### 3.6 Distribution of Longitudinal Moment to Individual Girders

Of particular interest, especially for design purposes, are the percentages of the total moment at a section carried by each girder in the box section (see Fig. 2.6). These percentages are directly related to the transverse distribution of longitudinal plate forces just discussed. Again, for the purpose of comparison with experimental results, these percentages were theoretically determined for section 0-0 which was one inch from midspan. Fig. 3.25 to 3.34 illustrate the general agreement between theory and experiment for loads at midspan. The difference between theory and experiment is rarely greater than 2% of the total moment at the section. It should be pointed out, however, that a difference of 2% with respect to the total moment could cause a difference of up to 10% in the actual moment carried by an individual girder. Nevertheless, the agreement is more than

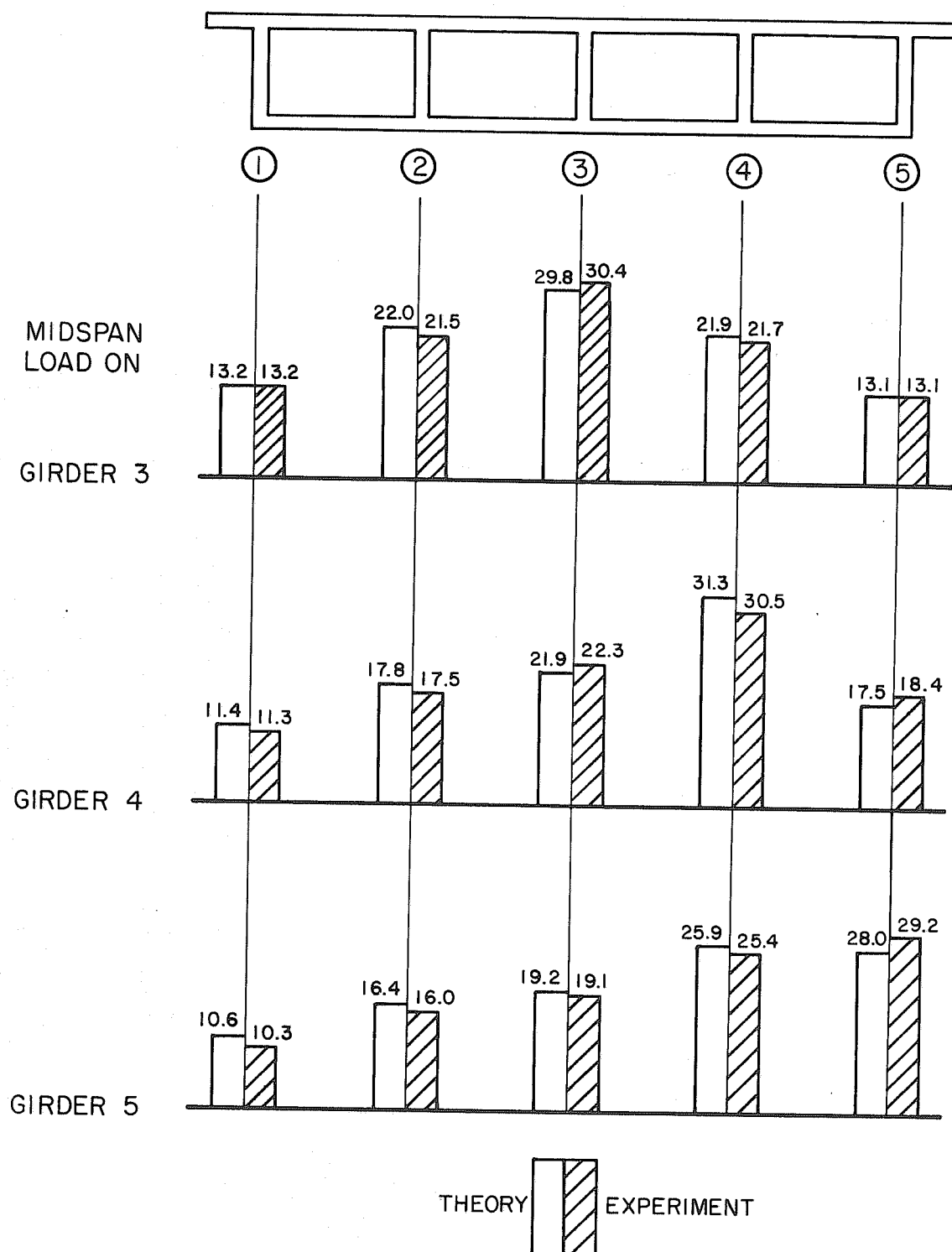


FIG. 3.25 PERCENTAGE OF TOTAL MOMENT AT SECTION 0-0 CARRIED BY EACH GIRDER, MODEL 1A (45°/53.5")

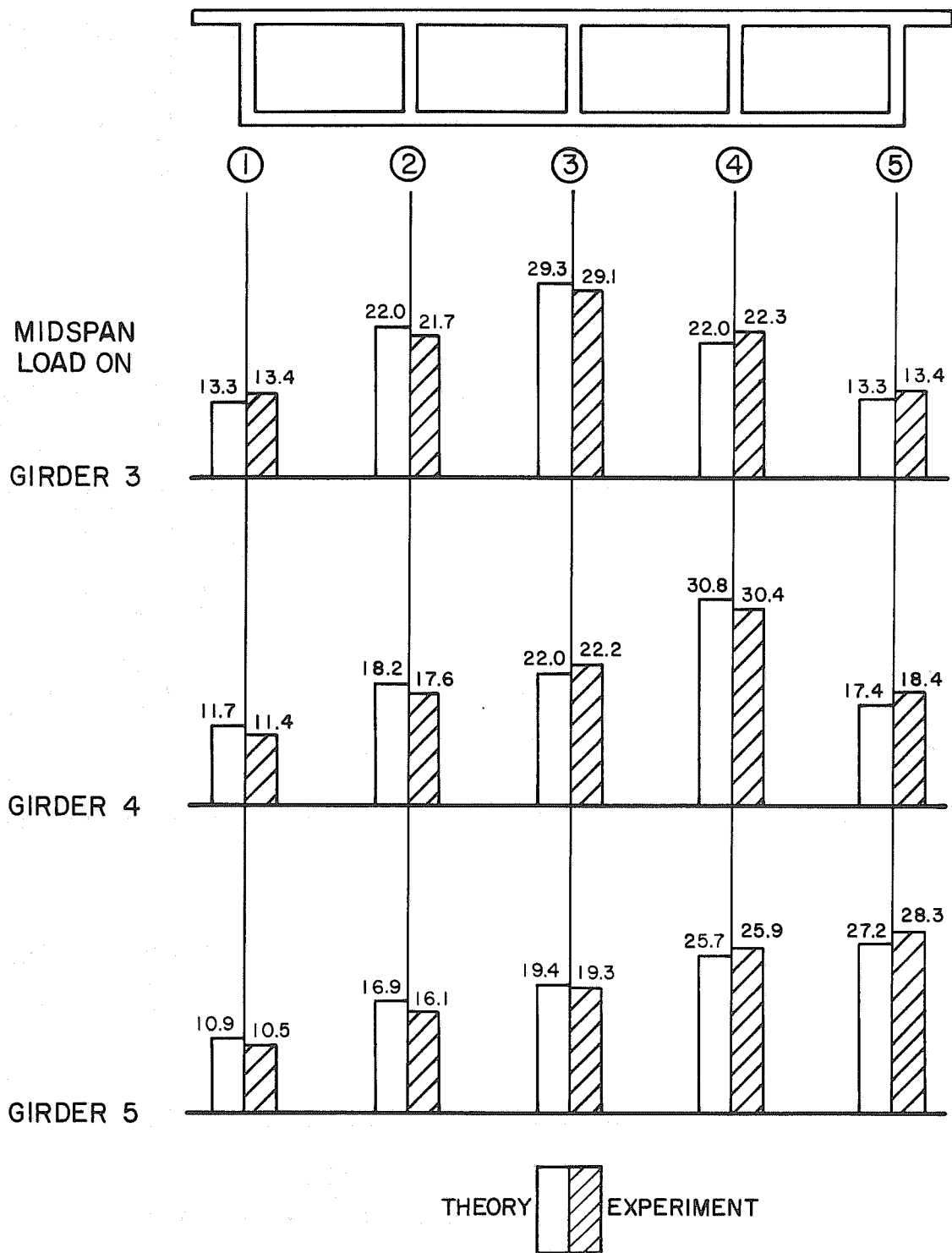


FIG. 3.26 PERCENTAGE OF TOTAL MOMENT AT SECTION 0-0 CARRIED BY EACH GIRDER, MODEL 2A (30°/47.4")

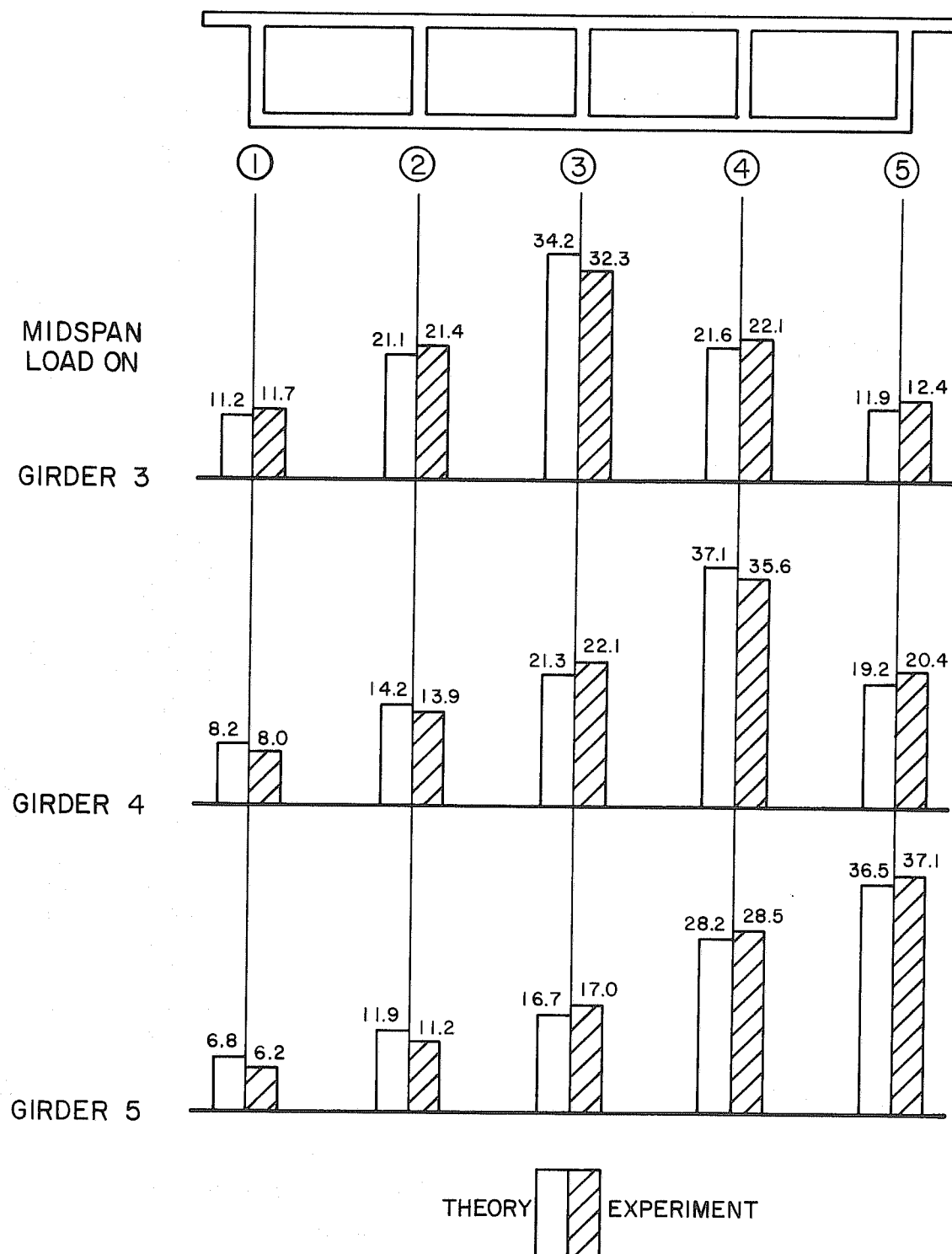


FIG. 3.27 PERCENTAGE OF TOTAL MOMENT AT SECTION 0-0 CARRIED BY EACH GIRDER, MODEL 3A (45°/35.5")

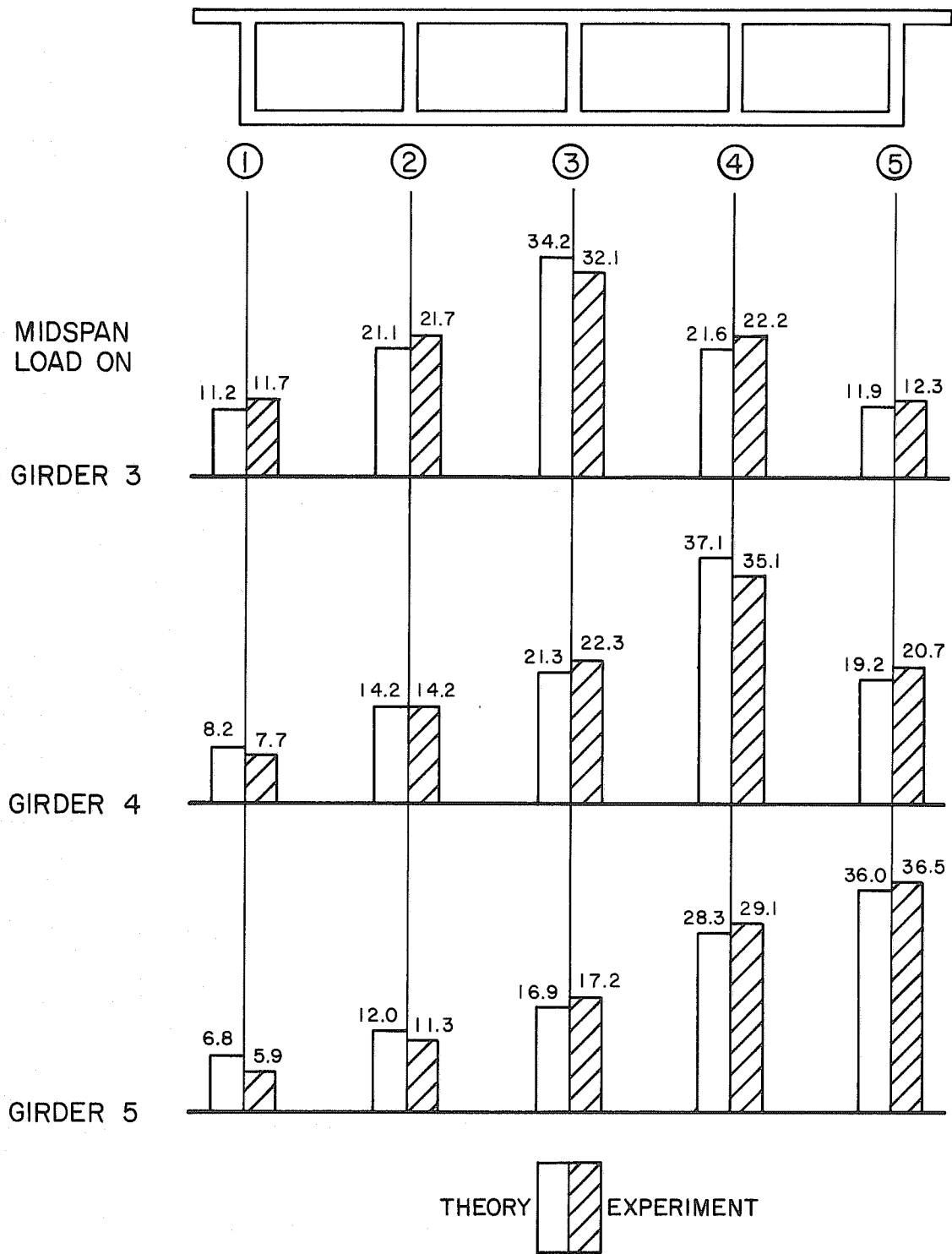


FIG. 3.28 PERCENTAGE OF TOTAL MOMENT AT SECTION 0-0 CARRIED BY EACH GIRDER, MODEL 4A (30<sup>0</sup>/29.7")

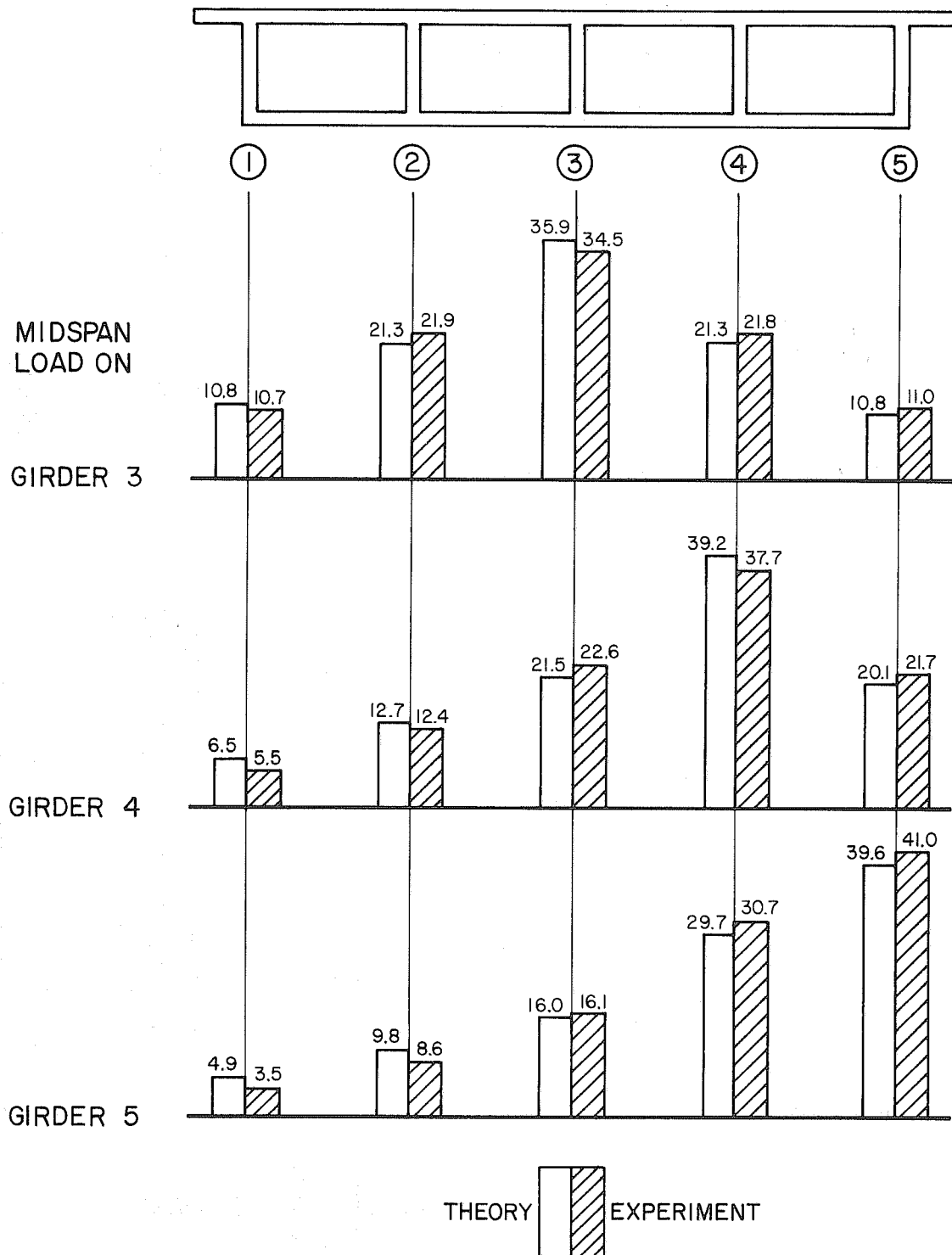


FIG. 3.29 PERCENTAGE OF TOTAL MOMENT AT SECTION 0-0 CARRIED BY EACH GIRDER, MODEL 5A (0°/22.5°)

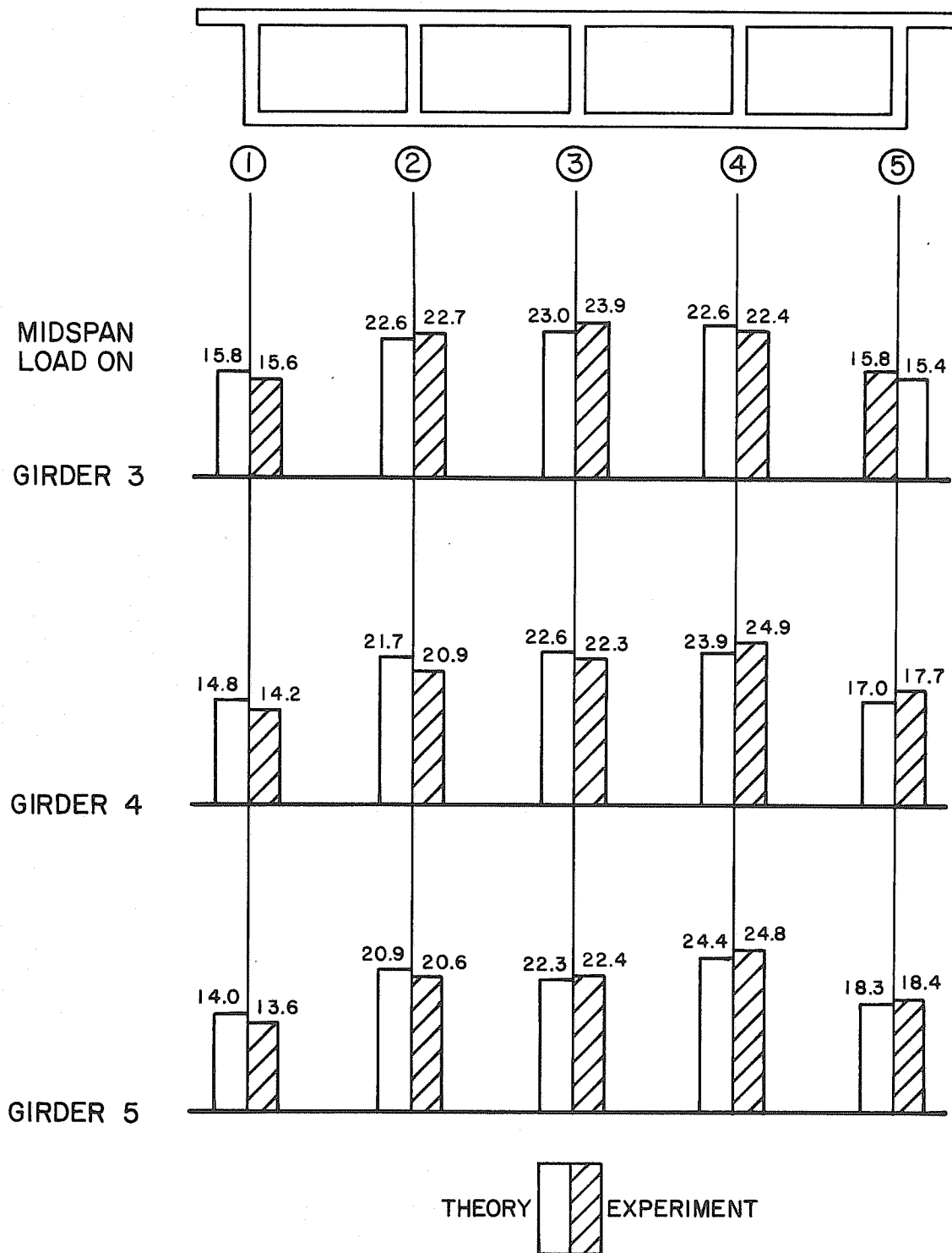


FIG. 3.30 PERCENTAGE OF TOTAL MOMENT AT SECTION 0-0 CARRIED BY EACH GIRDER, MODEL OB (0<sup>0</sup>/69.0")

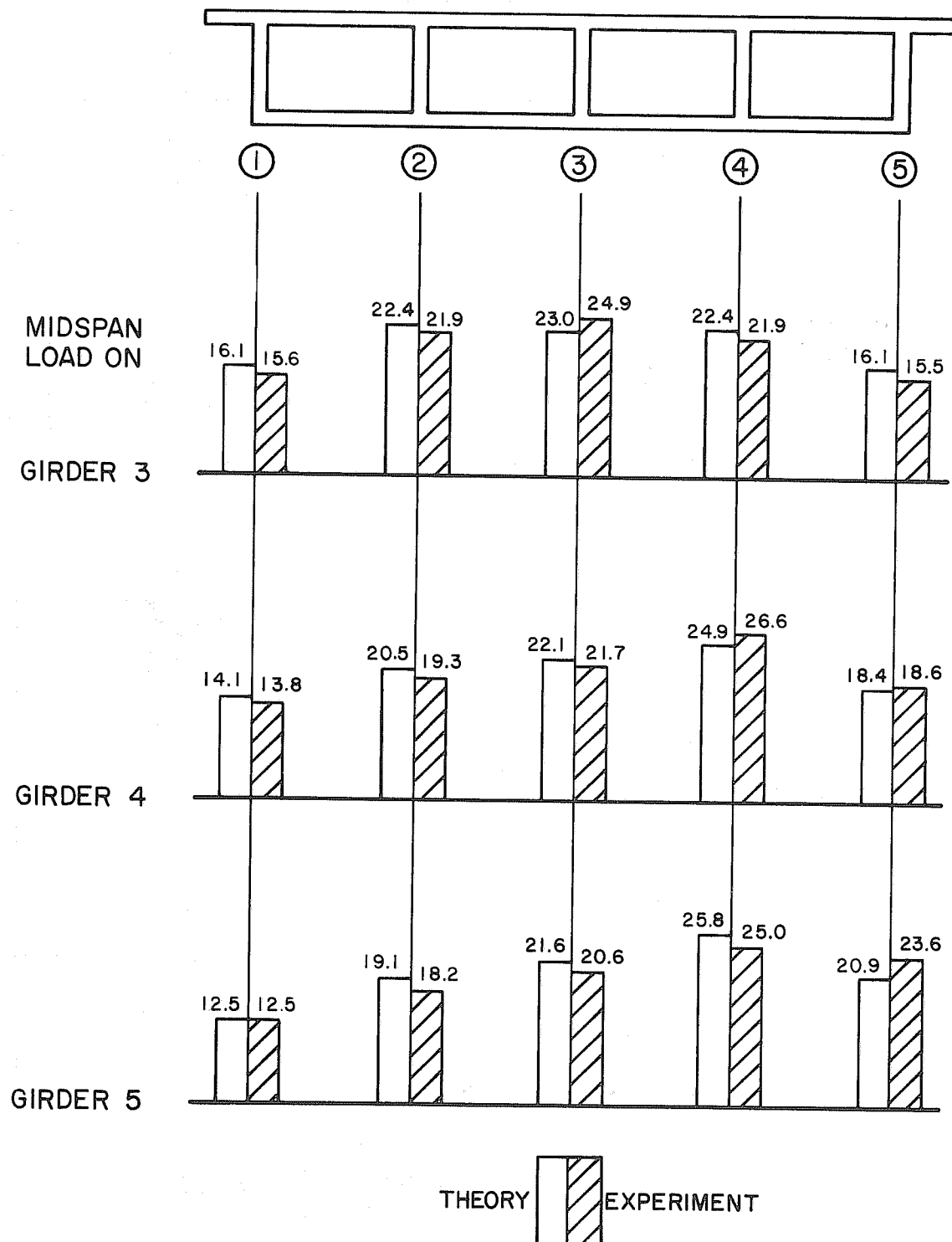


FIG. 3.31 PERCENTAGE OF TOTAL MOMENT AT SECTION 0-0 CARRIED BY EACH GIRDER, MODEL 1B (45°/53.5°)



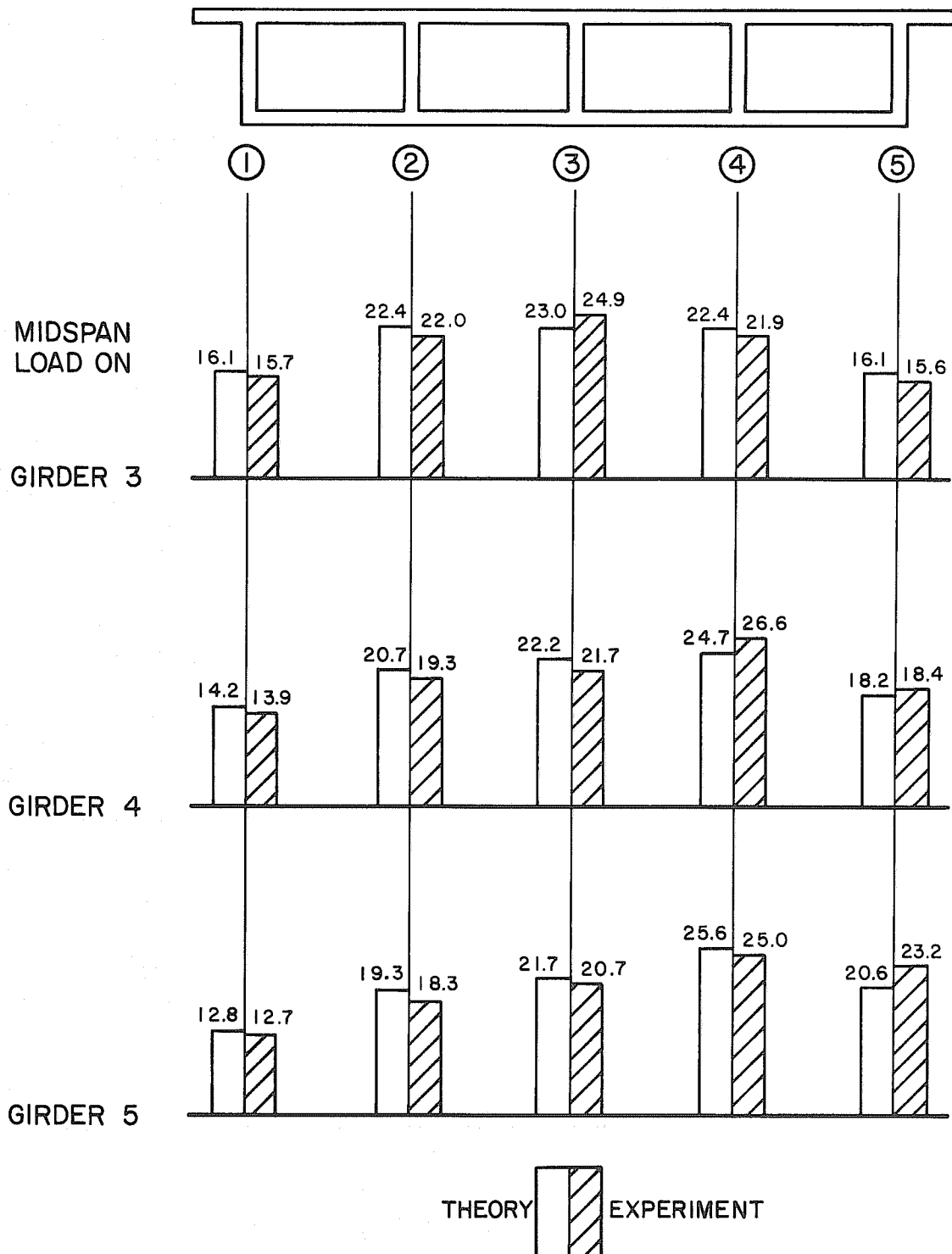


FIG. 3.32 PERCENTAGE OF TOTAL MOMENT AT SECTION 0-0 CARRIED BY EACH GIRDER, MODEL 2B (30<sup>0</sup>/47.4")

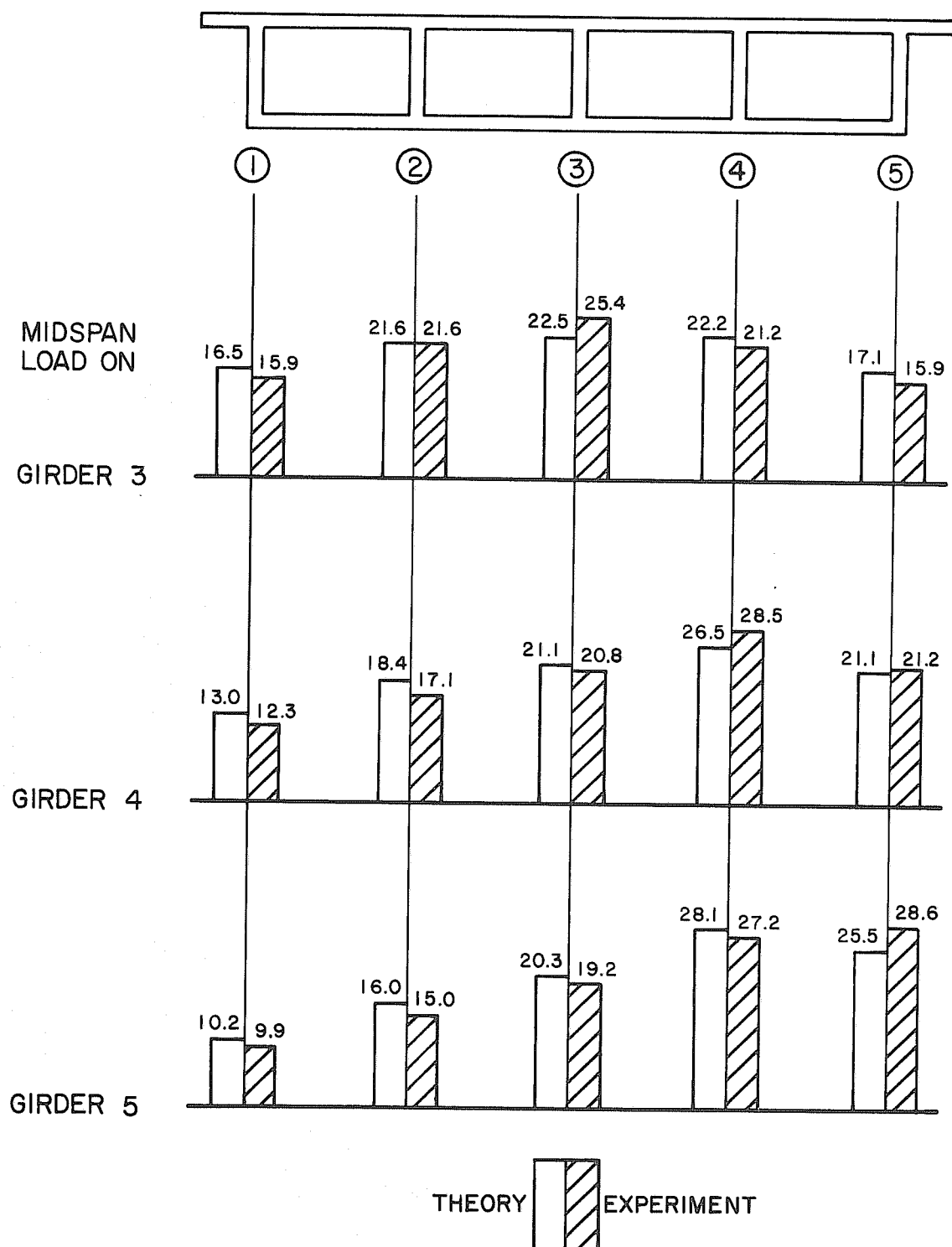


FIG. 3.33 PERCENTAGE OF TOTAL MOMENT AT SECTION 0-0 CARRIED BY EACH GIRDER, MODEL 3B (45°/35.5")

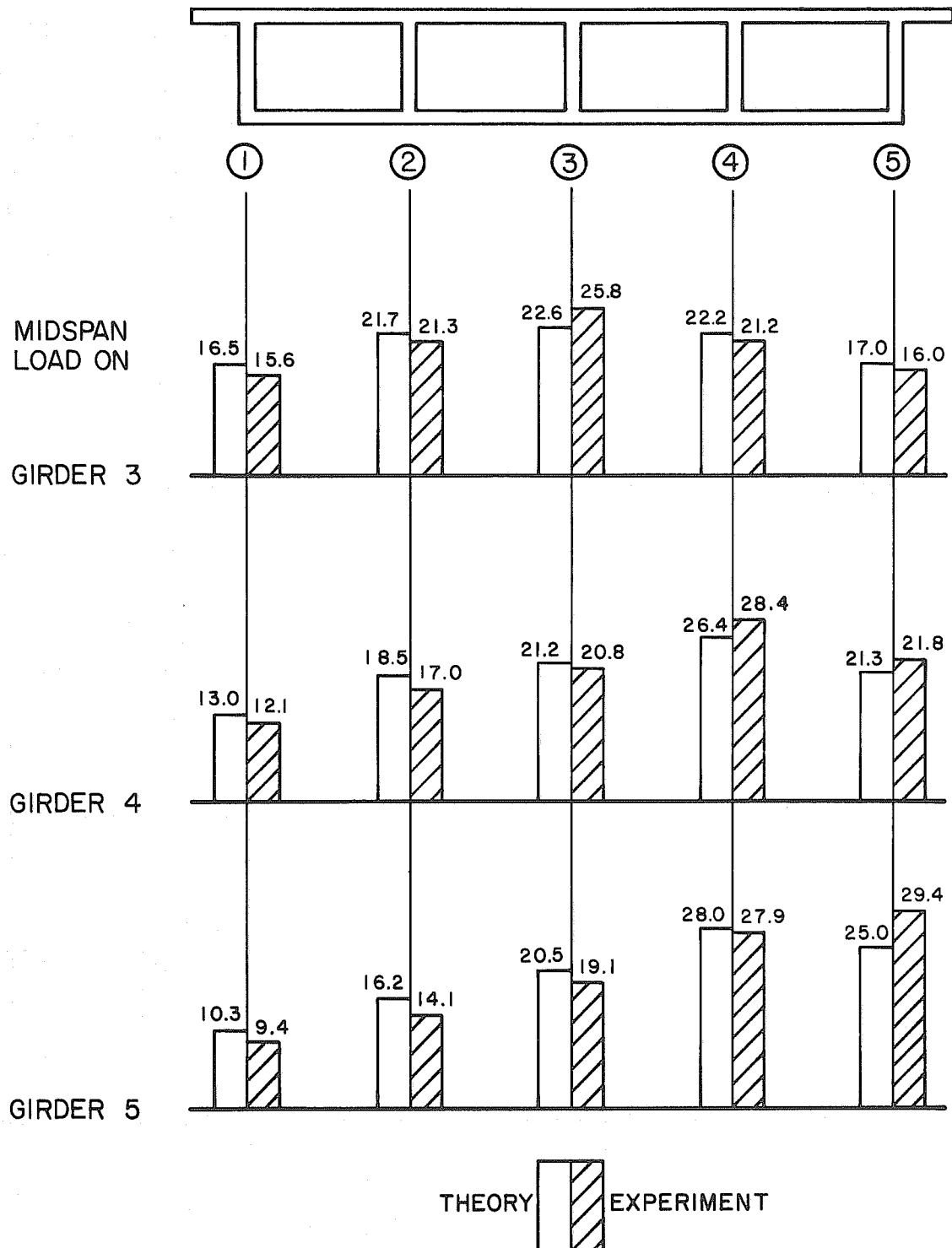


FIG. 3.34 PERCENTAGE OF TOTAL MOMENT AT SECTION 0-0 CARRIED BY EACH GIRDER, MODEL 4B (30°/29.7")

adequate for design purposes.

Table 3.4 presents a summary of the ratio of theoretical to experimental maximum percentages of the total moment at Section 0-0 taken by each individual girder. These maxima occur when the girder being considered has a midspan point load acting directly on it. It can be seen that for bridges without diaphragms the differences between theory and experiment range from 0 to 7% except for one case. For bridges with diaphragms the differences range from 0 to 15%.

For loads off the midspan section the agreement between theory and experiment is even better, as results for both approach a distribution of 15.8% for exterior girders and 22.8% for interior girders corresponding to a uniform stress distribution across the entire width of the bridge, as indicated in Fig. 2.6.

### 3.7 Transverse Bending Moments

Although the transverse plate bending moments are not tabulated in Appendix A, the values at Section 0-0 are presented graphically for models without diaphragms in Figs. 3.35 to 3.39 along with the experimental curves. The "CELL" output gave values at each intersection of a web and top or bottom deck. The variation of transverse moment in the top or bottom deck between webs is not necessarily linear. The experimental results show a linear trend, however. It is reasonable to expect a similar shape for the theoretical curve and the line connecting the values is drawn for purpose of comparison.

Theory and experiment compare fairly well except, perhaps, in Model 1A. Again, the divergence is probably attributable to the greater transverse flexibility of the experimental models discussed in

TABLE 3.4 RATIO OF THEORETICAL TO EXPERIMENTAL VALUES OF MAXIMUM PERCENTAGE OF TOTAL MOMENT AT SECTION 0-0 TAKEN BY EACH GIRDER DUE TO POINT LOADS AT THE MIDSPAN SECTION

Model	Girder				
	1	2	3	4	5
1A(45°/53.5")	.91	1.00	.98	1.03	.96
2A(30°/47.4")	.93	1.00	1.01	1.01	.97
3A(45°/35.5")	.96	1.03	1.06	1.04	.98
4A(30°/29.7")	.96	1.05	1.05	1.05	1.00
5A(0°/22.5")	.97	1.02	1.04	1.04	.97
OB(0°/69.0")	.99	.98	.96	.98	.99
1B(45/53.5")	1.03	.96	.92	.97	.89
2B(30°/47.4")	.85	.96	.92	.97	.89
3B(45°/35.5")	.89	.97	.89	1.00	.89
4B(30°/29.7")	.89	.96	.88	.99	.85

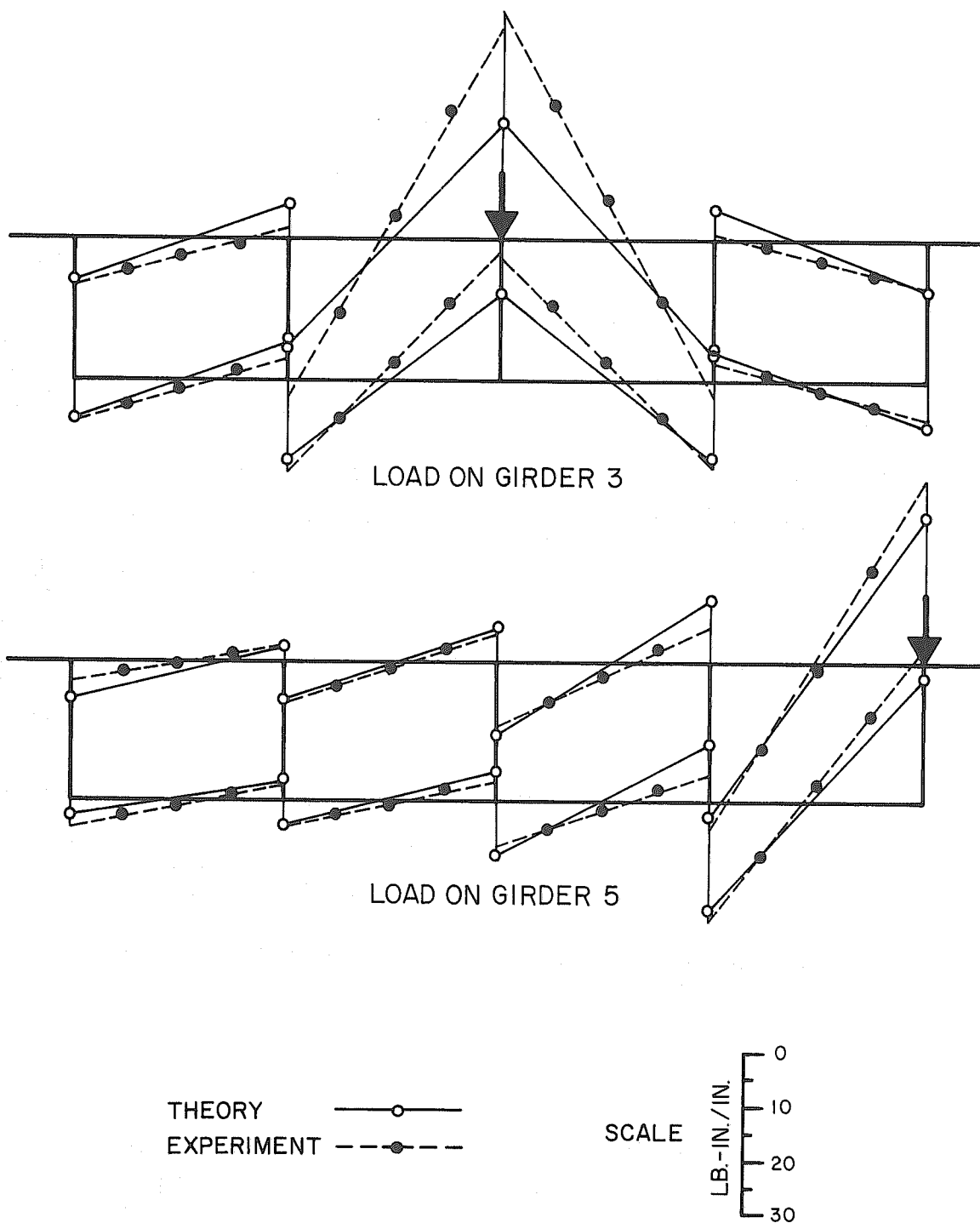
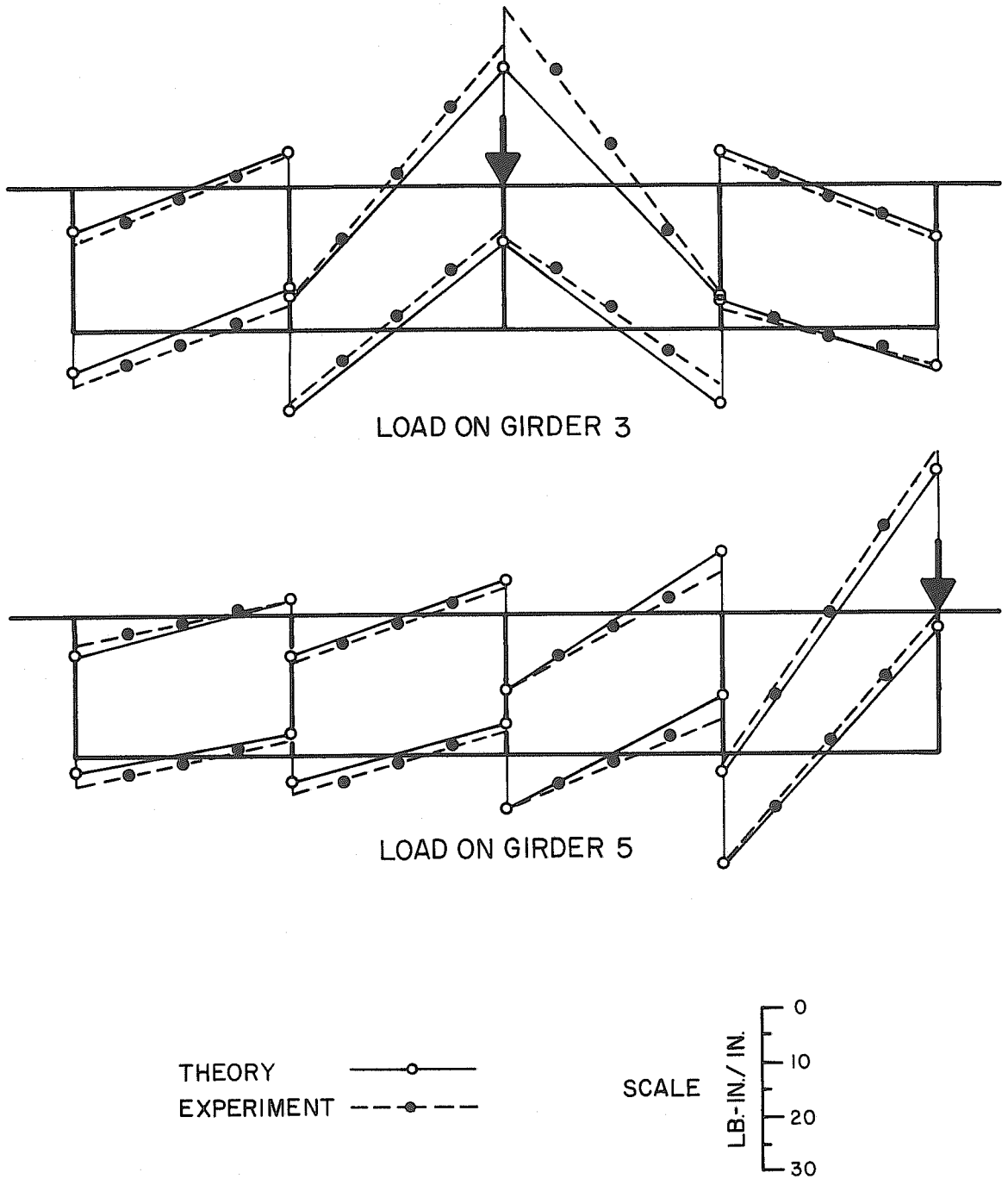


FIG. 3.35 THEORETICAL AND EXPERIMENTAL TRANSVERSE PLATE BENDING MOMENTS (IN.-LB./IN.), MODEL 1A (45°/53.5"), LOAD = 1000 LBS.



**FIG. 3.36 THEORETICAL AND EXPERIMENTAL TRANSVERSE PLATE BENDING MOMENTS (IN.-LB./IN.), MODEL 2A (30°/47.4"), LOAD = 1000 LBS.**

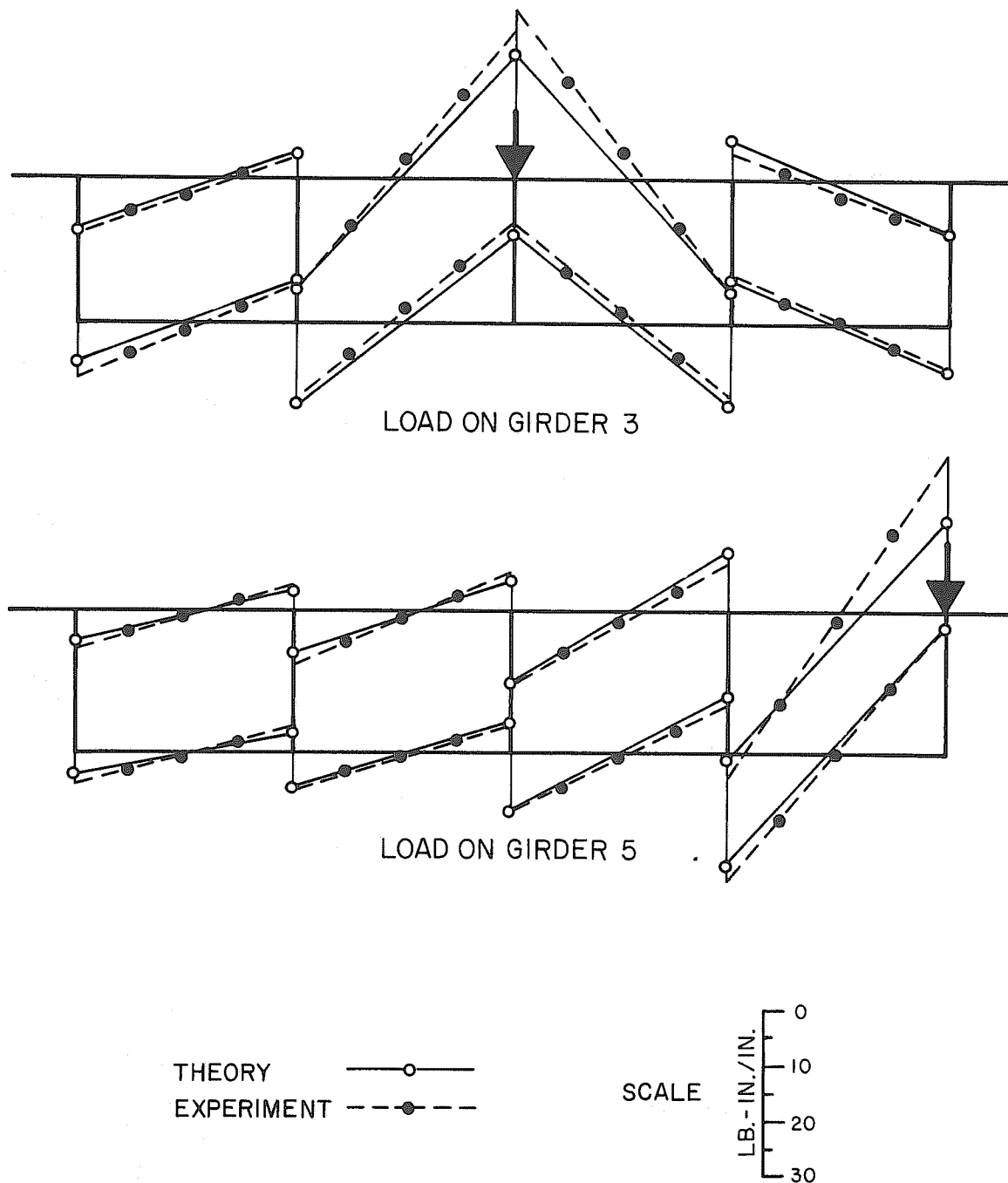


FIG. 3.37 THEORETICAL AND EXPERIMENTAL TRANSVERSE PLATE BENDING MOMENTS (IN.-LB./IN.), MODEL 3A (45°/35.5"), LOAD = 1000 LBS.



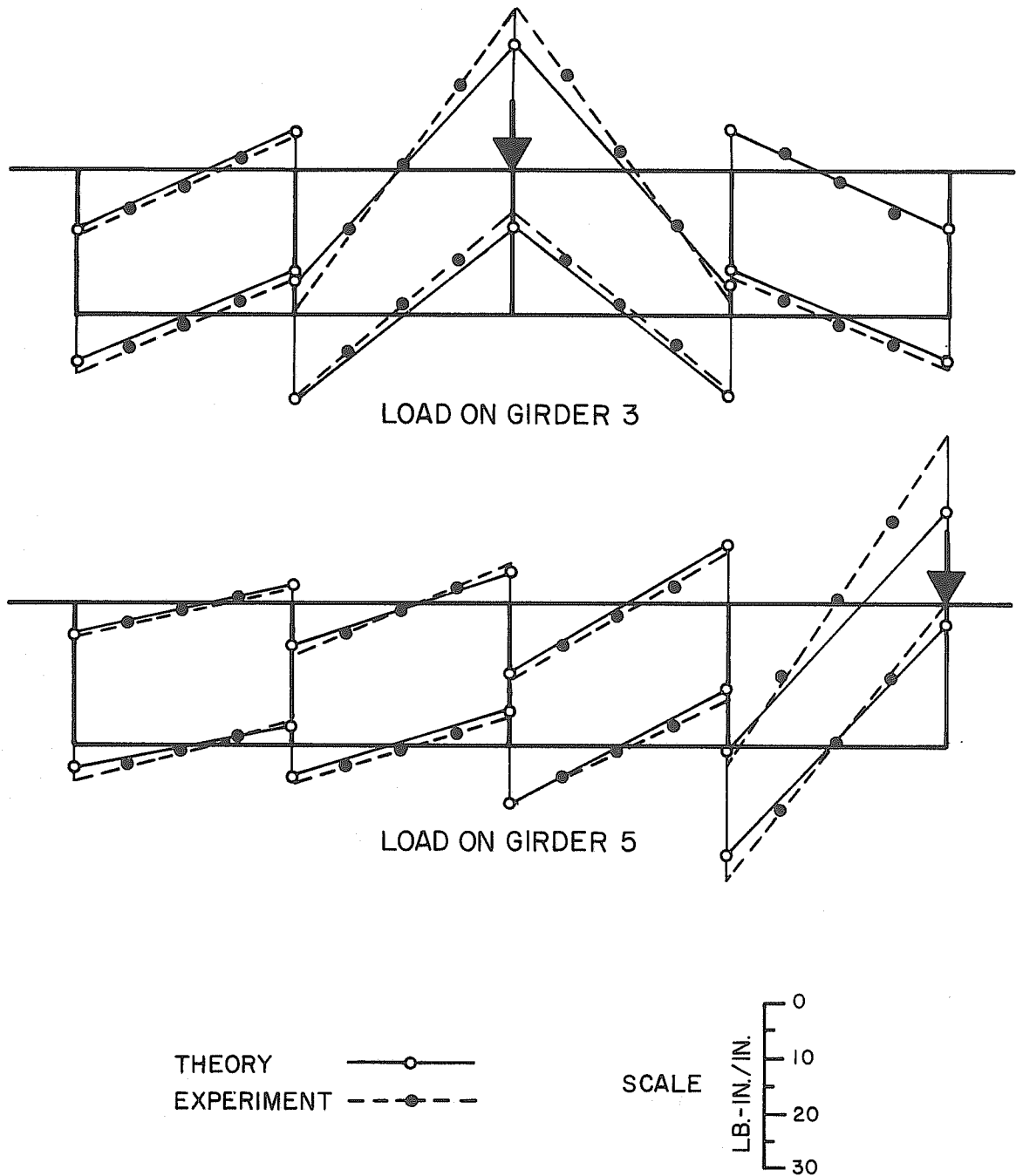
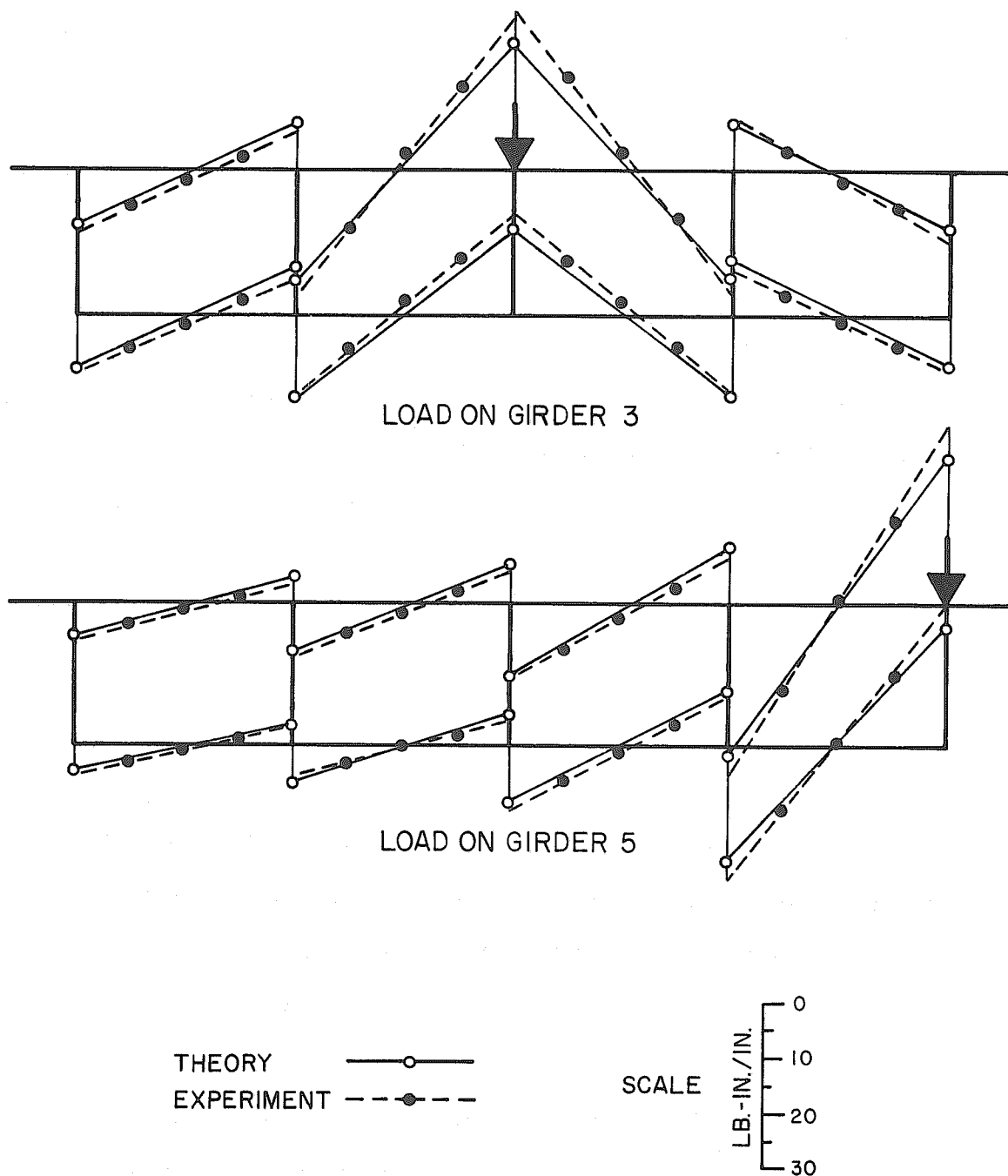


FIG. 3.38 THEORETICAL AND EXPERIMENTAL TRANSVERSE PLATE BENDING MOMENTS (IN.-LB./IN.), MODEL 4A (30°/29.7"), LOAD = 1000 LBS.



**FIG. 3.39 THEORETICAL AND EXPERIMENTAL TRANSVERSE PLATE BENDING MOMENTS (IN.-LB./IN.), MODEL 5A ( $0^{\circ}/22.5^{\circ}$ ), LOAD = 1000 LBS.**

Section 3.2. It is important to note from Figs. 3.35 to 3.39 that for theory as well as experiment the magnitudes and distribution of the transverse bending moments seem to be rather independent of span and angle of skew. Thus under point loads these moments are essentially a local effect.

### 3.8 Summary

In summary, four significant conclusions can be derived from the comparison of theoretical and experimental results.

- 1) Theory adequately predicts the external reactions and total moments at a section found in the experimental models for arbitrary point loads. Although in some cases the theoretical reactions appear to be slightly different than the experimental values, the effect on the external total midspan moment is minimal.
- 2) Theory predicts quite well the distribution of internal forces at a section found in the experimental model. This includes the longitudinal plate forces and the distribution of the total longitudinal moment to the individual girders.
- 3) Theoretical transverse plate bending moments are somewhat more divergent from experimental values but the agreement can still be considered satisfactory. The differences can be explained in terms of the greater flexibility of the experimental model compared to the analytical model.
- 4) Theory does not predict the magnitude of the deflections found in the experimental model within an acceptable range of differences. Although the general distribution of deflections was similar, differences in magnitudes of from 8 to 27% were found, with the theoretical model being

stiffer in all cases. Considerable evidence exists from the tests run on component parts of the bridge which suggests that part of the disagreement between theory and experiment is due to the greater flexibility of the screwed connections utilized in the experimental models. In a prototype monolithic structure, these increased flexibilities would not exist and thus the prototype would be closer to the analytical model. Also, there may have been some slippage in the experimental testing frame which contributed to the larger experimental deflection values.

Finally, it is important to note that even with the differences in the flexibilities of the experimental and theoretical models cited above, the agreement between theory and experiment for the magnitude and distribution of reactions, internal forces and moments was still quite good. This tends to indicate that moderate changes in the stiffness properties of a reinforced concrete bridge occasioned by cracking may not be a dominant factor in changing the load distribution behavior of skew box girder bridges.

#### 4. GENERAL BEHAVIOR AND PROPOSED APPROXIMATE ANALYSIS

##### 4.1 General

The comparisons presented in the preceding chapter between the theoretical results obtained with the finite element computer program CELL and the experimental results from the aluminum models have established the general validity of the theory for the elastic analysis of skew box girder bridges. Such an accurate analysis by the finite element method can always be made for a specific case, however, it can become very time consuming and expensive in terms of computer costs. If possible, for design purposes, it is advantageous to have a simplified approximate method of analysis, which can yield satisfactory answers for the usual design cases encountered.

Of prime interest from a design standpoint are two basic questions which must be answered for a given loading on a simple span, skew box girder bridge.

- (1) What is the total longitudinal moment on any section normal to the longitudinal axis of the bridge?
- (2) What is the transverse distribution of this total moment across the cross-section to each individual longitudinal girder?

In this chapter, the general behavior of the skew bridge models is scrutinized in order to develop an approximate method of analysis for answering these two basic questions. The results of the finite element analyses are reviewed and the effects of the various parameters (span, skew angle, etc.) on the reactions and moments are isolated. From this information an approximate method of determining external reactions and

total moments at a section due to arbitrary point loads is developed to answer the first question posed above. The transverse distribution of longitudinal internal forces and moments under various loading conditions is also examined and important conclusions emerge to provide an answer to the second question posed above. Various other behavioral characteristics important to design are also investigated.

#### 4.2 Reactions and Total Midspan Moment for Point Loads at the Midspan Section.

With a point load at the midspan center of a simple span straight bridge, the moment coefficient in terms of  $WL$  is 0.250. As the end supports become skewed this coefficient begins to decrease in magnitude. This effect was discussed in Section 3.3 and was found to be the result of the difference in the two reactions  $R_1$  and  $R_2$  at the end of the bridge, which must always total  $W/2$ . Figure 3.14 illustrates the effect of the couple caused by this difference. Since the analysis of a skew bridge on four supports is externally indeterminate to the first degree, the difference between the reactions  $R_1$  and  $R_2$  cannot be found directly from statics. However, some definite trends can be observed by studying the results of the finite element analyses.

As shown in Table 4.1 the angle of skew,  $\theta$ , has a significant effect on the reduction of the midspan moment coefficient from 0.250. For example, the moment coefficient for Model 2A with a skew angle of  $30^\circ$  is 0.214 for a point load at midspan center (position 3). This is 86% of the corresponding value for a straight bridge, 0B or 5A.

For model 1A with a skew angle of  $45^\circ$ , the moment coefficient drops to 0.178 which is 71% of that for the straight bridge. The

same behavior is evident in the shorter skew models 3A and 4A. There are two reasons for this effect of the skew angle.

First, for a given span, as the angle of skew decreases, the difference in the distances between the center point load and the two end reaction support points,  $R_1$  and  $R_2$ , also decreases. Thus the larger reaction  $R_2$  at the near obtuse corner decreases and the reaction  $R_1$  at the far acute corner increases. When the skew angle  $\theta$  reaches zero the reactions equalize,  $R_1 = R_2 = W/2$ .

Second, and more significant, however, is the change in lever arm for the reaction couple,  $(b/2)\tan \theta$ . Since in the four cell models considered the width of the bridge,  $b$ , is constant only the  $\tan \theta$  changes. The larger angle of skew yields the longer lever arm, and as a result the greater reduction in midspan moment.

Another parameter which affects the solution seems to be the plan "aspect ratio,"  $b/L$ . The effect of this measure of the slenderness of the bridge in plan can be observed by comparing the longer and shorter models having the same skew angle. For a load at midpoint position 3, the shorter  $45^\circ$  model, 3A, yields a midspan moment coefficient some 6% less than the longer model 1A, as the aspect ratio increases from .22 to .38. For a similar change in aspect ratio, .25 to .40, the  $30^\circ$  models 2A to 4A exhibit only a 3% decrease in midspan moment. For angles less than  $30^\circ$  the effect of the aspect ratio is probably even smaller.

A study of the available data on two and four cell bridges indicates that the midspan moment coefficient for a point load at midspan center of a skew bridge can be accurately estimated by the empirical relationship  $0.25 \cos \theta$ . Figure 4.1 illustrates this

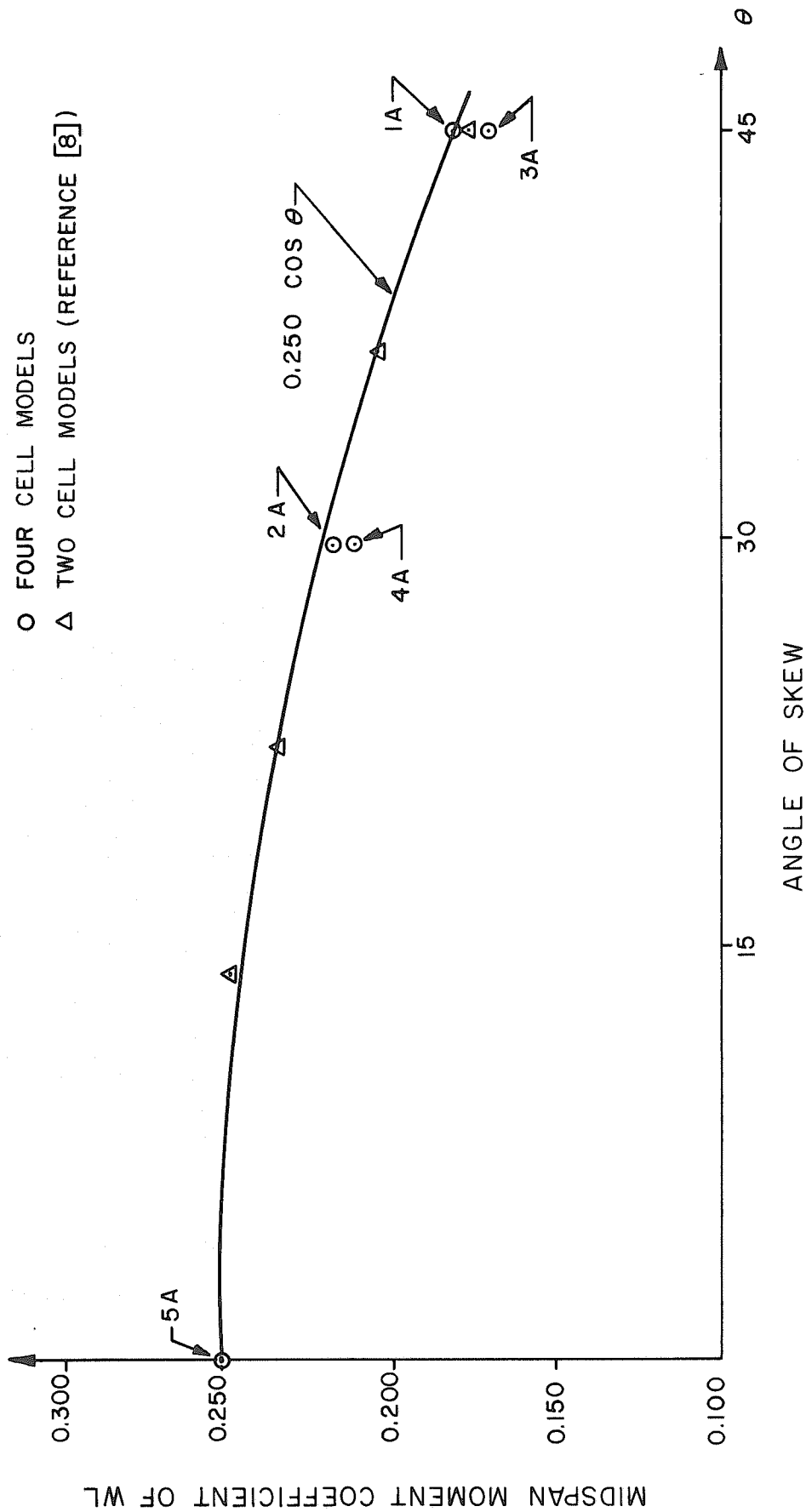


FIG. 4.1 TOTAL MOMENT AT MIDSPAN FOR A POINT LOAD AT MIDSPAN CENTER OF THE BRIDGE



approximation graphically. Included on this plot in addition to the values for the four cell bridges are values obtained by Sisodiya, et al, [8] from a finite element analysis of a series of two cell skew box girder bridges. The accuracy of this empirical formula is summarized in Table 4.1

TABLE 4.1 COMPARISON OF THEORETICAL AND APPROXIMATE TOTAL MIDSPAN MOMENT COEFFICIENTS FOR A POINT LOAD W AT MIDSPAN CENTER

Model	$M_{TH}$	$M_{AP}$	$M_{AP}/M_{TH}$
OB(0°/69.0")	.250	.250	1.00
1A(45°/53.5")	.178	.177	.99
2A(30°/47.4")	.214	.217	1.01
3A(45°/35.5")	.168	.177	1.05
4A(30°/29.6")	.209	.217	1.04
5A(0°/22.5")	.250	.250	1.00

$M_{TH}$  = Theoretical moment coefficient of WL  
obtained from finite element analysis

$M_{AP}$  = Approximate moment coefficient =  $0.25 \cos \theta$

The results of the finite element analyses also indicate the interesting fact that if the point load W is placed anywhere across the width of the midspan section normal to the longitudinal axis, the total moment coefficient remains essentially the same as that for the load acting at the midspan center of the bridge. The reactions, however, change quite considerably. The sum of R1 and R2 increases as the load is moved towards the R2 side. The reason for this is

obvious when moments are taken about the skew axis defined by R3 and R4. For the sum R1 and R2 to remain constant the load must be moved along a line parallel to the skewed supports. However, if the load is transferred along the right section at midspan, R2 increases and R1 decreases. Thus their difference increases, causing a couple which exactly offsets the effect of their larger sum on the total midspan moment. As illustrated in Figs. 3.12 and 3.13 the changes in R1 and R2 are linear as are those for R3 and R4 by symmetry. An interesting consequence of this linearity is that the sum of R2 and R3 and the sum of R1 and R4 are constants for a point load acting anywhere on the midspan cross-section.

One other significant peculiarity of skew bridges is the possibility of negative reactions at the acute corner supports, Table 4.2. This tendency is more pronounced in the longer span bridges. The greatest negative reaction with a load at the midspan section occurs when the load is on the exterior girder on the opposite side from the acute corner. Notice, however, in Table 4.2 that for all models except 2A slightly larger maximum negative reactions for R4 occur with a load at position 10 which is not on the midspan section.

Since for dead load only, Table 4.6, the reaction  $R4 = R1$  is always positive, it is unlikely that combined dead and live load will produce a net negative reaction at R4. However, this possibility should always be checked and if it occurs either a reaction tie-down would have to be provided or the effect of a lift off of the reaction support would have to be considered in calculating the other reactions and the section moments.

TABLE 4.2 MAXIMUM NEGATIVE REACTION, R4,  
DUE TO POINT LOAD W

Model	Load on Midspan Section		Load not on Midspan Section	
	Load Position	R4	Load Position	R4
1A (45°/53.5")	5	-.217 W	10	-.280 W
2A (30°/47.4")	5	-.215 W	10	-.205 W
3A (45°/35.5")	5	-.165 W	10	-.187 W
4A (30°/29.6")	5	-.127 W	10	-.133 W

1. See Appendix A for load position locations.

#### 4.3 Reactions and Total Moments for Point Loads Along the Longitudinal Centerline of Bridge.

As the load is moved longitudinally off of the right section at midspan the midspan moment coefficient naturally decreases. The influence lines for the midspan moment shown in Fig. 3.15 are typical of all models and show that as the load moves along center girder 3, the moment coefficient varies not quite linearly as it does in a straight bridge. However, the sum of any end reaction pair (R1 + R2 or R3 + R4) changes exactly linearly as required by statics. The moment coefficient does not behave linearly because the difference between reactions at the acute and obtuse corners changes slightly at first and then very radically as the load approaches the supports. With the load near the center of the bridge this difference is comparatively large. Near the ends of the bridge, however, the load is more evenly distributed to the two reactions and their difference decreases accordingly.

An interesting comparison between skew and straight bridges can be found by examining the moment coefficient for a right section at the point of application of the load along girder 3, Fig. 4.2. For a straight bridge the moment,  $M_{ST}$ , at the loaded cross-section is  $Wcd/L$  which gives a moment coefficient in terms of WL of  $cd/L^2$ . These moment coefficients are tabulated in Table 4.3.

TABLE 4.3 COMPARISON OF COEFFICIENTS FOR TOTAL MOMENT AT LOADED CROSS-SECTION DUE TO A POINT LOAD W ON SKEW BRIDGES AND STRAIGHT BRIDGES

MODEL	LP	c/L	$M_{SK}$	$M_{ST}$	$M_{SK}/M_{ST}$
1A(45°/53.5")	3	.50	.178	.250	.71
	8	.31	.151	.214	.71
	11	.13	.079	.113	.70
2A(30°/47.4")	3	.50	.214	.250	.86
	8	.29	.174	.206	.84
	11	.07	.055	.065	.85
3A(45°/35.5")	3	.50	.168	.250	.67
	8	.33	.149	.221	.67
	11	.17	.087	.141	.62
4A(30°/29.6")	3	.50	.209	.250	.84
	8	.31	.177	.214	.83
	11	.12	.081	.106	.76

LP = Load position, see Appendix A for location

c/L = Longitudinal location of load in terms of overall length, L, see Fig. 4.2

$M_{SK}$  = Moment coefficient of WL at loaded section for skew bridge.

$M_{ST}$  = Moment coefficient of WL at loaded section for load at corresponding location on a straight bridge.

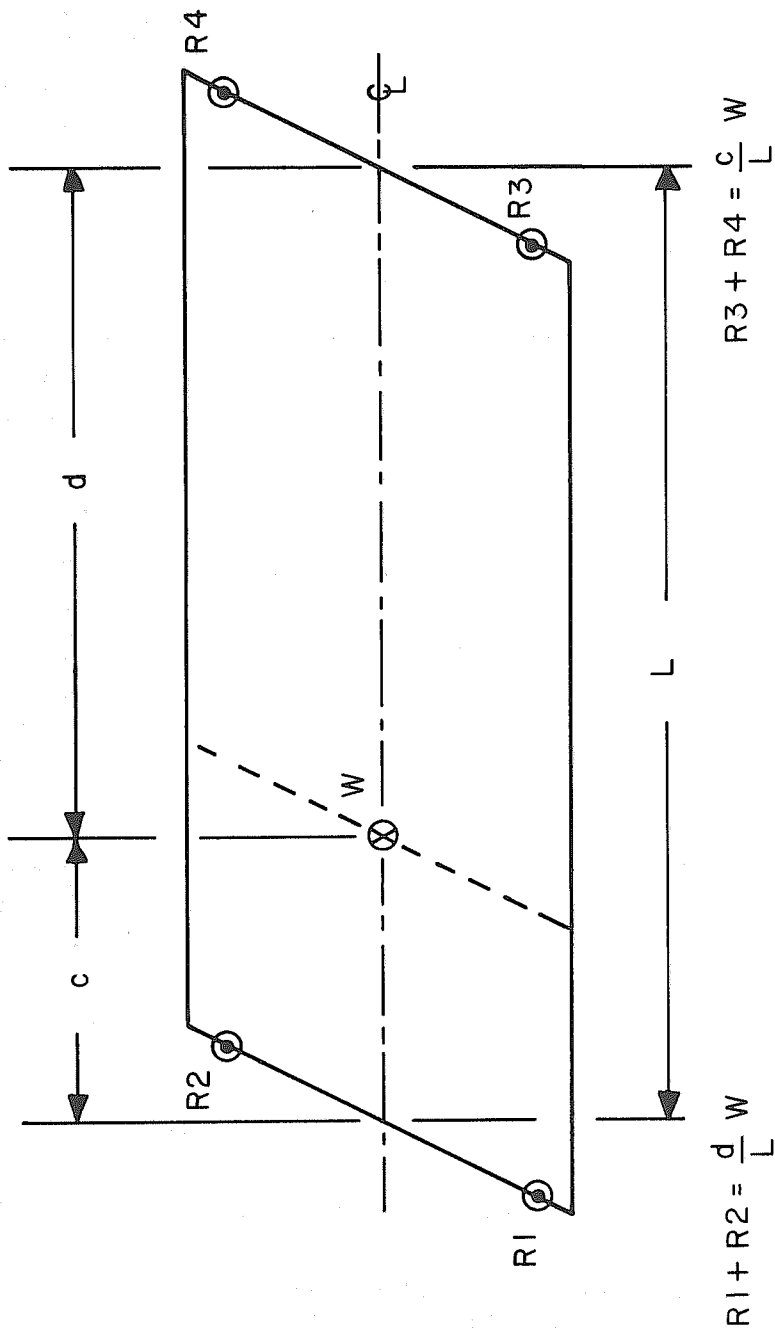


FIG. 4.2 POINT LOAD ON LONGITUDINAL CENTERLINE OF BRIDGE

Also shown in Table 4.3 are the corresponding values of moment coefficients for the skew models,  $M_{SK}$ . Note that the ratio of moment coefficients for the skew vs. straight bridge is nearly the same on all load positions for a given skew angle of  $30^\circ$  or  $45^\circ$ . Indeed, the ratio of skew coefficient to straight coefficient is very close to the cosine of the skew angle. This suggests that the moment coefficient at any loaded section may be approximated by  $(cd/L^2)\cos \theta$  if the load is on the longitudinal centerline of the bridge. At midspan this empirical approximation yields the previously discussed coefficient  $0.250 \cos \theta$ .

Once this moment coefficient is established the external reactions can be found from statics as follows, Fig. 4.2

$$R1 + R2 = \frac{dW}{L} \quad (4.1)$$

$$(R1 + R2)c - (R2 - R1) \frac{b \tan \theta}{2} = \frac{cdW}{L} \cos \theta \quad (4.2)$$

Substituting  $R2$  from Eq. (4.1) into (4.2)

$$R1 = \frac{cdW}{Lb \tan \theta} (\cos \theta - 1) + \frac{dW}{2L} \quad (4.3)$$

$$R2 = \frac{cdW}{Lb \tan \theta} (1 - \cos \theta) + \frac{dW}{2L} \quad (4.4)$$

$R3$  and  $R4$  can then be found from

$$R1 + R3 = 0.5 \quad (4.5)$$

$$R2 + R4 = 0.5 \quad (4.6)$$

It has been shown in Figs. 3.12 and 3.13 that a transverse movement of a point load across a right section anywhere on the bridge causes a linear variation in all reactions. As discussed before, the sum of each reaction pair is defined by statics. Again, the difference between the reactions at the acute and obtuse corners is indeterminate. Unlike the midspan section, transfer of the load off of the longitudinal centerline at any other section causes a variation in the midspan moment coefficient. This change is roughly linear with the moment coefficient increasing as the load moves closer to an acute corner and decreasing if it moves toward an obtuse corner. However, the magnitude of these changes cannot be precisely predicted empirically.

#### 4.4 Approximate Analysis for Arbitrary Point Loads

A very good approximate solution for the indeterminate corner reactions in a solution for a skew bridge subjected to a point load  $W$  at an arbitrary position can be obtained in the following manner, Fig. 4.3a. This arbitrary loading may be replaced by the superposition of the two loadings shown in Figs. 4.3b and c. As pointed out previously, the load may be moved anywhere along the skewed line parallel to the support lines without changing the sum of  $R_1 + R_2$  as well as  $R_3 + R_4$ . If the load is shifted to the centerline Fig. 4.3b, the reactions  $R_1'$  through  $R_4'$  may be determined directly using Eqs. (4.1) to (4.6).

The effect of the couple illustrated in Fig. 4.3c must be determined and added to the centerline solution to obtain the total solution for the loading in Fig. 4.3a. This skewed couple must be

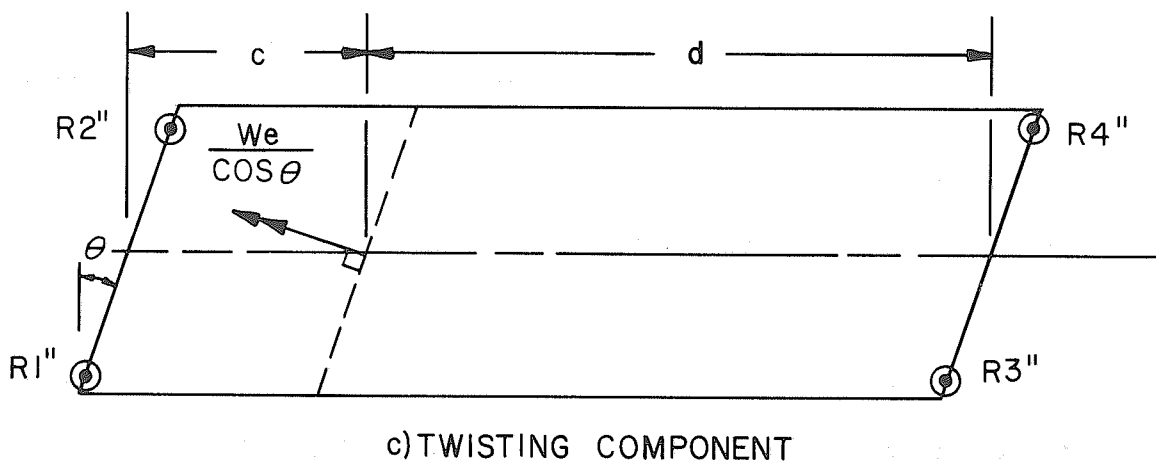
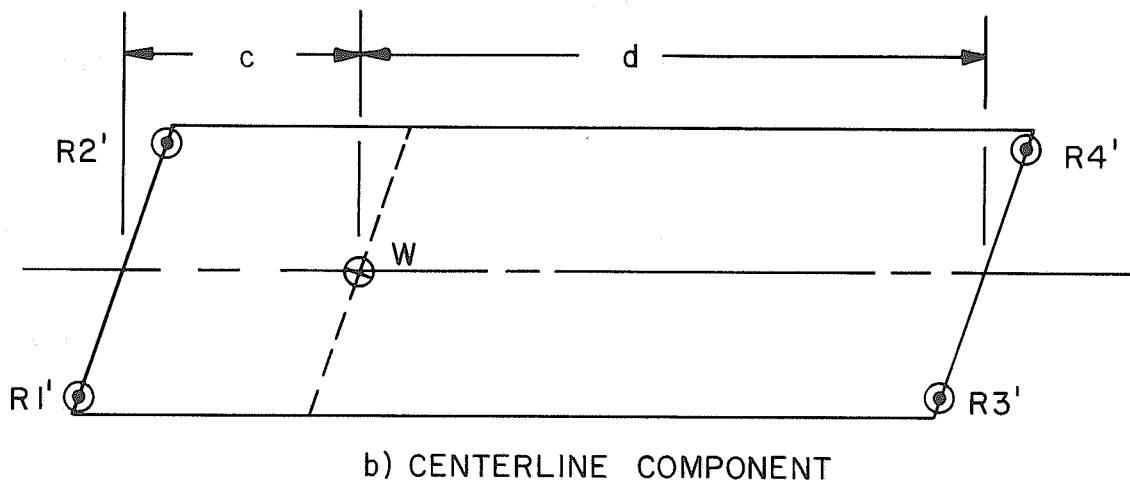
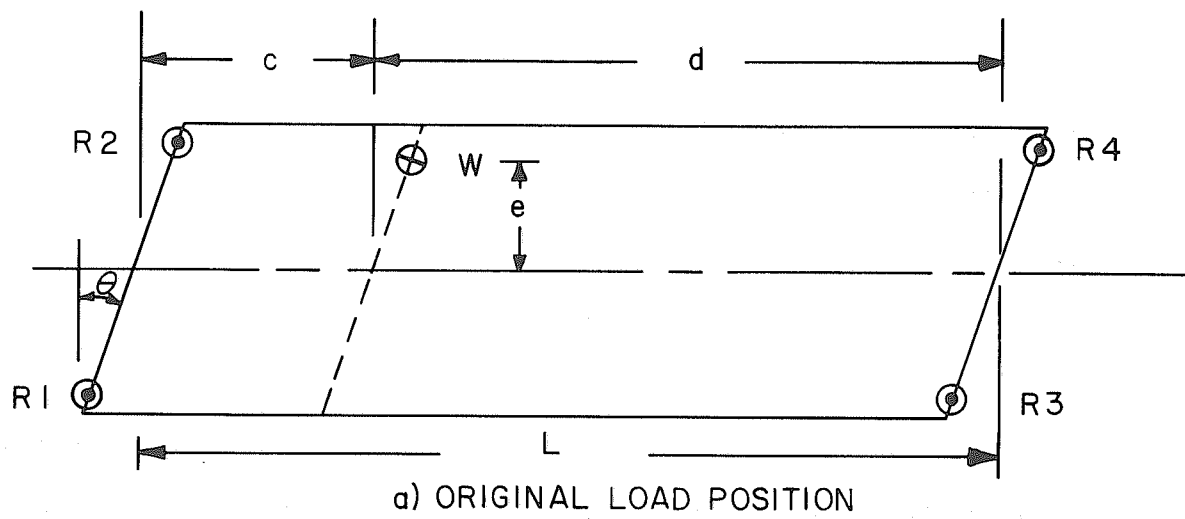


FIG. 4.3 POINT LOAD AT ARBITRARY POSITION ON SKEW BRIDGE



resisted by two reaction couples formed by each of the two end reaction pairs. Since the original couple is perpendicular to the end support lines, each of the reaction pairs must be self-equilibrating. That is

$$R1'' = -R2'' \text{ and } R3'' = -R4'' \quad (4.7)$$

The support conditions at each end of the bridge are identical. Therefore, the amount of the total torque resisted by each reaction pair may be approximated by the centerline location of the applied torque. Consequently,  $R1''$  and  $R2''$  resist  $d/L$  times the applied torque,  $We/\cos \theta$ . The reactions may then be determined as follows:

$$R2'' - R1'' = 2(R2'') \quad (4.8)$$

$$2(R2'') \left( \frac{b}{2c \cos \theta} \right) = \frac{We}{\cos \theta} \left( \frac{d}{L} \right) \quad (4.9)$$

$$R2'' = \frac{Wed}{bL} \quad (4.10)$$

$$R1'' = \frac{-Wed}{bL} \quad (4.11)$$

$R3''$  and  $R4''$  are similarly obtained

$$R3'' = \frac{Wec}{bL} \quad (4.12)$$

$$R4'' = \frac{-Wec}{bL} \quad (4.13)$$

If these reactions are then superimposed with those of the previous centerline solution, Fig. 4.3b

$$R_n = R_n' + R_n'' \quad (4.14)$$

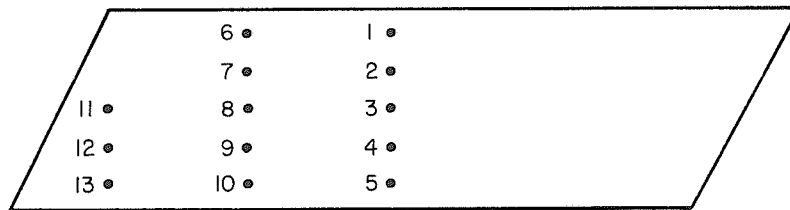
the resulting reactions are a very good approximation to the solution for the original arbitrary load position of Fig. 4.3a.

This approximate method of analysis was tested on all the skew models for all the load positions for which theoretical data from the finite element analyses was available. Table 4.4 shows these results for Models 1A, 2A, 3A and 4A in terms of the ratio of the approximate to the theoretical total moment coefficients for the midspan section. The comparison shows that the approximate method gives very acceptable results for all load positions except 11, 12, 13 which are very near the support reactions. The loadings of prime interest from a design standpoint are those which are somewhat removed from the support reactions since much larger total moments occur due to these loadings. Note also that the approximate results are generally conservative compared to theory. This is a desirable feature for an empirical approximate solution. This procedure is remarkably simple and can be easily applied. As will be discussed in the subsequent chapter this approximation could be very useful for design purposes. Its application, however, should be limited to bridges of similar proportions to those analyzed in this study. Preliminary results of finite element analyses for wider bridges with six and eight cells indicate that bridges that are wider and shorter than the four cell type used to develop the approximate method might behave somewhat differently.

#### 4.5 Transverse Distribution of Total Longitudinal Moment

Once the total moment on a section normal to the longitudinal axis is known, the transverse distribution of this moment to the individual girders, which is directly related to the transverse distribution of the longitudinal internal forces, must be determined.

TABLE 4.4 RATIO OF APPROXIMATE TO THEORETICAL MOMENT AT MIDSPAN SECTION FOR ALL POINT LOAD POSITIONS



Model	Load Position at Midspan Section				
	1	2	3	4	5
1A(45°/53.5")	.99	.99	.99	.99	.98
2A(30°/47.4")	1.01	1.01	1.01	1.01	1.01
3A(45°/35.5")	1.03	1.04	1.05	1.04	1.03
4A(30°/29.6")	1.02	1.03	1.04	1.03	1.02
	Load Position Near Quarter-Span				
	6	7	8	9	10
1A(45°/53.5")	.99	1.00	1.00	.98	.97
2A(30°/47.4")	1.02	1.03	1.03	1.02	1.01
3A(45°/35.5")	1.12	1.12	1.10	1.07	1.05
4A(30°/29.6")	1.05	1.06	1.07	1.06	1.04
	Load Position Near Support				
			11	12	13
1A(45°/53.5")			1.35	1.18	1.07
2A(30°/47.4")			1.13	1.09	1.04
3A(45°/35.5")			1.39	1.20	1.11
4A(30°/29.6")			1.25	1.15	1.07

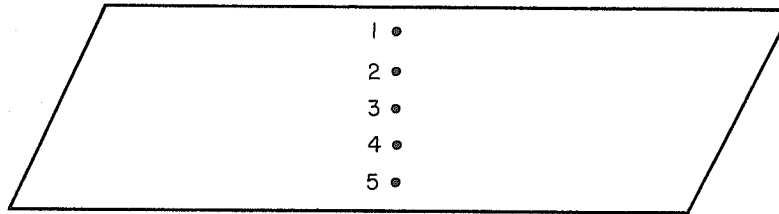
The theoretical data available in this study makes it possible to discuss the distribution of forces at Section 0-0. This section is close enough to midspan to give a rather accurate representation of the situation at midspan.

In Section 3.4 it was noted that the shape of the transverse distribution curve for longitudinal plate forces was essentially the same for all models for a given point load position and that it merely shifted up or down depending on the span. In models without the midspan diaphragm this resulted in a somewhat poorer distribution of moment to the individual girders for the shorter bridges. The effect in models with the diaphragm was somewhat less pronounced since the addition of the diaphragm itself produced a rather uniform distribution of moment.

The maximum percentage of the total longitudinal midspan moment taken by any girder always occurs with the point load applied at midspan on the girder being considered. Once the load is moved longitudinally away from the midspan section the distribution of moment at midspan quickly becomes very close to uniform. This is particularly interesting because the design truck live loads consist of several wheel loads some of which will always be somewhat removed from the midspan section where the maximum design moment occurs.

Tables 4.5a, b, c, d show the percentage distribution of the total moment at Section 0-0 to the individual girders for various combinations of point loads. The loadings shown in Tables 4.5a, b are similar to uniform live loads across the width of the bridge in the central portion

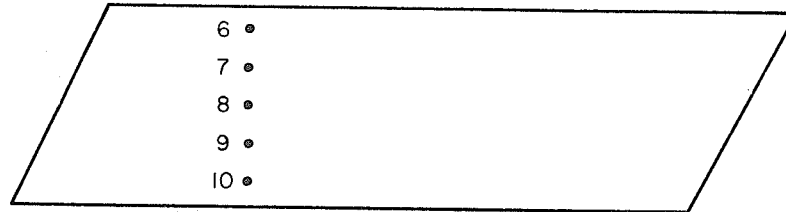
TABLE 4.5a PERCENTAGE OF TOTAL LONGITUDINAL MOMENT  
AT SECTION 0-0 TAKEN BY EACH GIRDER FOR  
EQUAL LOADS AT ALL FIVE POINTS SHOWN



Model	Girder				
	1	2	3	4	5
0B(0°/69.0")	16.0	22.7	22.5	22.7	16.0
1A(45°/53.5")	16.2	22.7	22.4	22.6	16.1
1B(45°/53.5")	16.5	22.7	22.1	22.5	16.4
2A(30°/47.4")	16.1	22.7	22.4	22.7	16.1
2B(30°/47.4")	16.4	22.6	22.2	22.5	16.5
3A(45°/35.5")	16.4	22.4	21.9	22.6	16.4
3B(45°/35.5")	17.2	22.0	21.0	22.3	17.5
4A(30°/29.6")	16.2	22.4	22.0	22.7	16.5
4B(30°/29.6")	17.0	22.0	21.2	22.4	17.3
5A(0°/22.5")	16.4	22.5	22.2	22.5	16.4

1. See Appendix A for location of load positions 1 to 5.

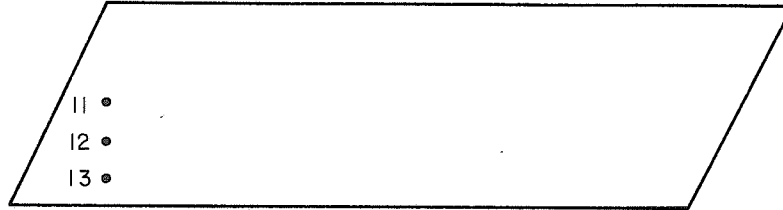
TABLE 4.5b PERCENTAGE OF TOTAL LONGITUDINAL MOMENT  
AT SECTION 0-0 TAKEN BY EACH GIRDER FOR  
EQUAL LOADS AT ALL FIVE POINTS SHOWN



Model	Girder				
	1	2	3	4	5
OB(0°/69.0")	15.9	22.8	22.7	22.8	15.9
1A(45°/53.5")	16.2	23.0	22.6	22.6	15.7
1B(45°/53.5")	16.6	22.9	22.2	22.4	16.0
2A(30°/47.4")	16.0	22.9	22.7	22.7	15.8
2B(30°/47.4")	16.5	22.9	22.3	22.4	16.0
3A(45°/35.5")	16.6	22.1	21.5	22.5	16.5
3B(45°/35.5")	17.4	22.1	20.9	22.3	17.4
4A(30°/29.6")	15.4	22.0	22.4	23.4	16.8
4B(30°/29.6")	17.0	22.0	21.1	22.6	17.4
5A(0°/22.5")	15.9	22.8	22.6	22.8	15.9

1. See Appendix A for location of load positions 6 to 10.

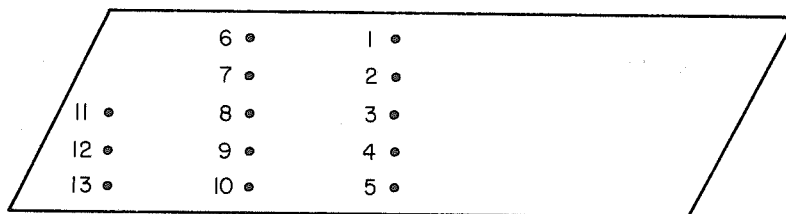
TABLE 4.5c PERCENTAGE OF TOTAL LONGITUDINAL MOMENT  
AT SECTION 0-0 TAKEN BY EACH GIRDER FOR  
EQUAL LOADS AT ALL THREE POINTS SHOWN



Model	Girder				
	1	2	3	4	5
0B(0°/69.0")	-	-	-	-	-
1A(45°/53.5")	18.4	24.7	22.1	20.8	14.0
1B(45°/53.5")	19.6	25.6	21.4	19.4	14.1
2A(30°/47.4")	17.9	24.1	22.1	21.3	14.6
2B(30°/47.4")	19.3	25.1	21.3	19.8	14.5
3A(45°/35.5")	14.0	20.2	21.6	25.1	19.1
3B(45°/35.5")	20.2	24.2	18.8	19.8	17.0
4A(30°/29.6")	12.3	18.9	21.9	26.4	20.5
4B(30°/29.6")	18.7	22.6	19.0	21.2	18.4
5A(0°/22.5")	-	-	-	-	-

1. See Appendix A for locations of load positions 11 to 13.

TABLE 4.5d PERCENTAGE OF TOTAL LONGITUDINAL MOMENT  
AT SECTION 0-0 TAKEN BY EACH GIRDER FOR  
EQUAL LOADS AT ALL THIRTEEN POINTS SHOWN



Model	Girder				
	1	2	3	4	5
0B(0°/69.0")	15.9	22.7	22.6	22.7	15.9
1A(45°/53.5")	16.3	22.9	22.4	22.5	15.8
1B(45°/53.5")	16.7	23.0	22.1	22.2	16.1
2A(30°/47.4")	16.2	22.8	22.5	22.6	15.9
2B(30°/47.4")	16.6	22.9	22.0	22.0	16.2
3A(45°/35.5")	16.3	22.1	21.7	22.8	16.7
3B(45°/35.5")	17.5	22.2	20.8	22.1	17.4
4A(30°/29.6")	16.1	22.0	22.1	23.3	16.9
4B(30°/29.6")	17.1	22.1	21.0	22.3	17.4
5A(0°/22.5")	16.2	22.6	22.3	22.6	16.2

1. See Appendix A for locations of load positions 1 to 13.



of the bridge, while the loading in Table 4.5d approximates the effect of a uniform load over the entire bridge. All three of these load combinations produce distributions of the total moment to the individual girders which approach the percentages associated with a uniform stress distribution across the section, therefore 15.8% for each exterior girder and 22.8% for each interior girder. These percentages for a uniform stress distribution can always be determined from the relative moments of inertia of the individual girders as shown in Fig. 2.6. Only the combination of three point loads at positions 11, 12, 13 near the end support, shown in Table 4.5c, produces a non-uniform stress distribution at midspan, but their contribution to the total midspan moment would be small compared to the other load combinations shown.

#### 4.6 Effect of Midspan Diaphragm

As noted several times throughout this report for a given point load the addition of a midspan diaphragm does not change the external reactions and moments for any of the bridges studied. However, the internal distribution of forces is affected rather significantly by the addition of a diaphragm. The longitudinal plate forces near midspan do not peak sharply near the load point in the B models with the diaphragm as they do in the A models without it. The maximum percentages of total longitudinal moment taken by any individual girder is much lower, in general, for the B models. While these differences are significant when discussing a single point load on the bridge, the more realistic design dead and live load situations to produce maximum design moments would consist of several loads

across the bridge width. Thus the same distribution of moments to the girders would occur regardless of whether or not the bridge had a midspan diaphragm (see Tables 4.5a, b, d). For this reason it is felt that the midspan diaphragm is not necessary in order to insure a more uniform stress distribution in a four cell skew bridge under working loads. This conclusion was previously expressed for two cell skew bridges by Sisodiya, et al [8].

Despite its unimportance in the response of the skew bridge under working loads the contribution of a midspan diaphragm to the response of a reinforced concrete skew box girder bridge under extremely heavy overloads and at ultimate capacity could be important. For example, if one of the girders sustains a extremely heavy overload and extensive cracking and possibly yielding of the steel reinforcement begins to occur, failure may be avoided if some structural mechanism can transfer the excess load to the other girders. The transverse bending stiffness of the box girder section may or may not be sufficient to insure this transfer. In the event that is not, the diaphragm is highly desirable since it would guarantee the transverse redistribution of forces.

#### 4.7 Dead Load Considerations

Experimentally, it was not possible to determine the response of the aluminum models to dead load. Theoretical results for external response due to self weight were obtained for models 1A - 5A and are presented in Table 4.6. Since the solutions for external reactions and total moments at a section due to an arbitrary point load was independent of whether or not a midspan diaphragm was included, the B series models were not analyzed for dead load.

The midspan moment coefficients follow the pattern established for point loads. The greater angle of skew produces a larger reduction in the midspan moment from the 0.125 WL for a straight bridge ( $W =$  total weight). The shorter skew models show a slightly smaller moment coefficient than their longer counterparts with the same angle of skew. This is also consistent with the previously observed response to point loads. The deflections beneath girders 1, 2, and 3 for Model 1A are represented in Figure 4.4. The deflection at midspan of the bridge is constant across the right cross-section. Girders 1 and 2 show slightly larger deflections at their individual midpoints than those at midspan of the bridge.

An empirical solution to the dead load problem is rather difficult to justify with the small amount of data available. With the information now available it seems that the midspan moment coefficient may be reasonably approximated by  $0.125 - 0.100 \sin^2 \theta$ . A plot of this curve with the data available is shown in Fig. 4.5. Two cell models analyzed by Sisodiya, et al [8], are again presented. Although the results appear to be very good, they must be regarded as inconclusive until more evidence is available. It may be possible to estimate the response of the skew bridge to dead load through some type of integration procedure utilizing the approximate method for point loads developed earlier in this chapter. However, results from such a scheme will undoubtedly be rather conservative due to the error in approximation near the supports.

Although information on the distribution of internal forces in models subjected to dead load is not readily available, there are

MIDSPAN OF BRIDGE

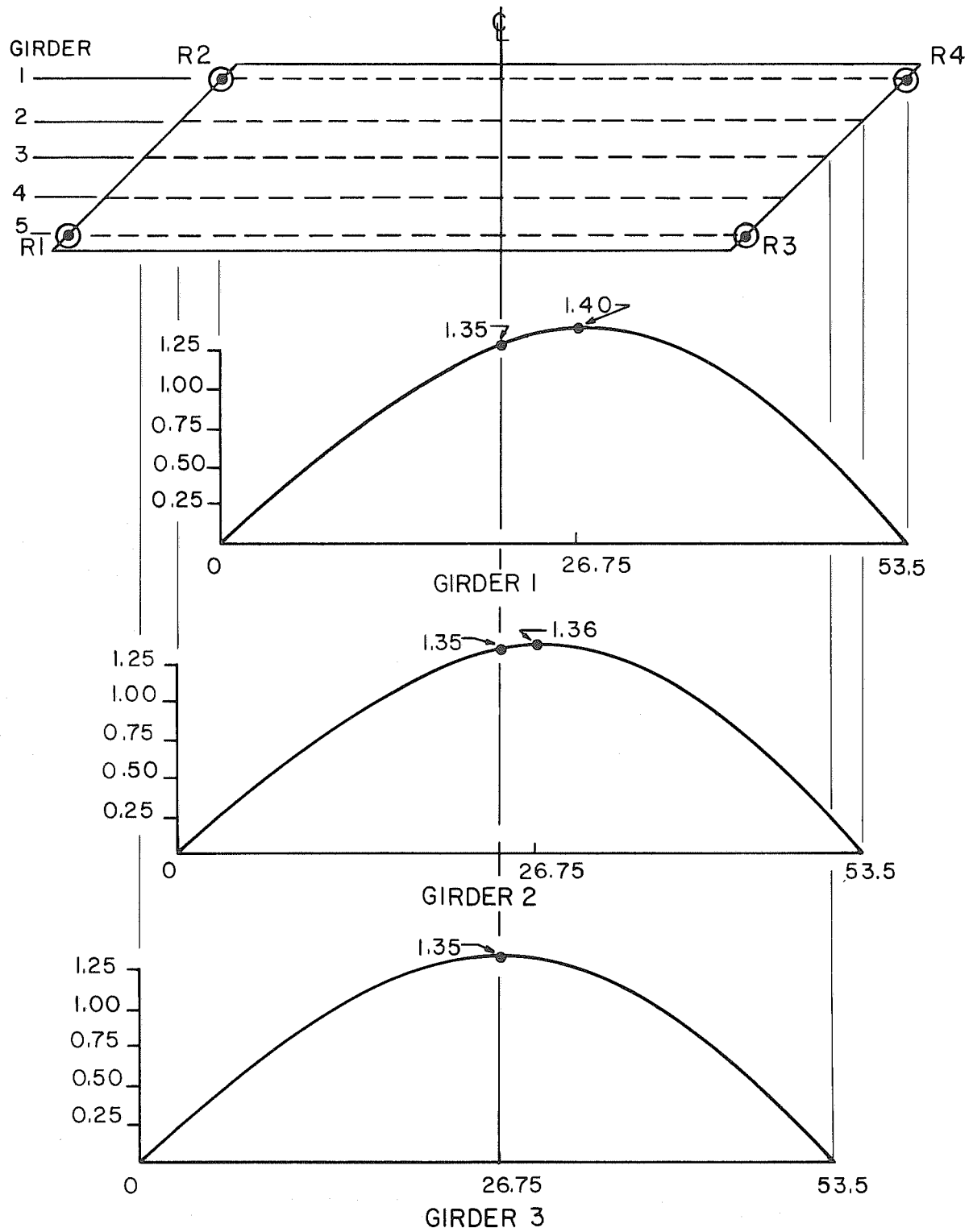


FIG. 4.4 DEFLECTION IN INCHES OF GIRDERS 1, 2, AND 3 IN MODEL 1A DUE TO DEAD LOAD, W = 63 KIPS

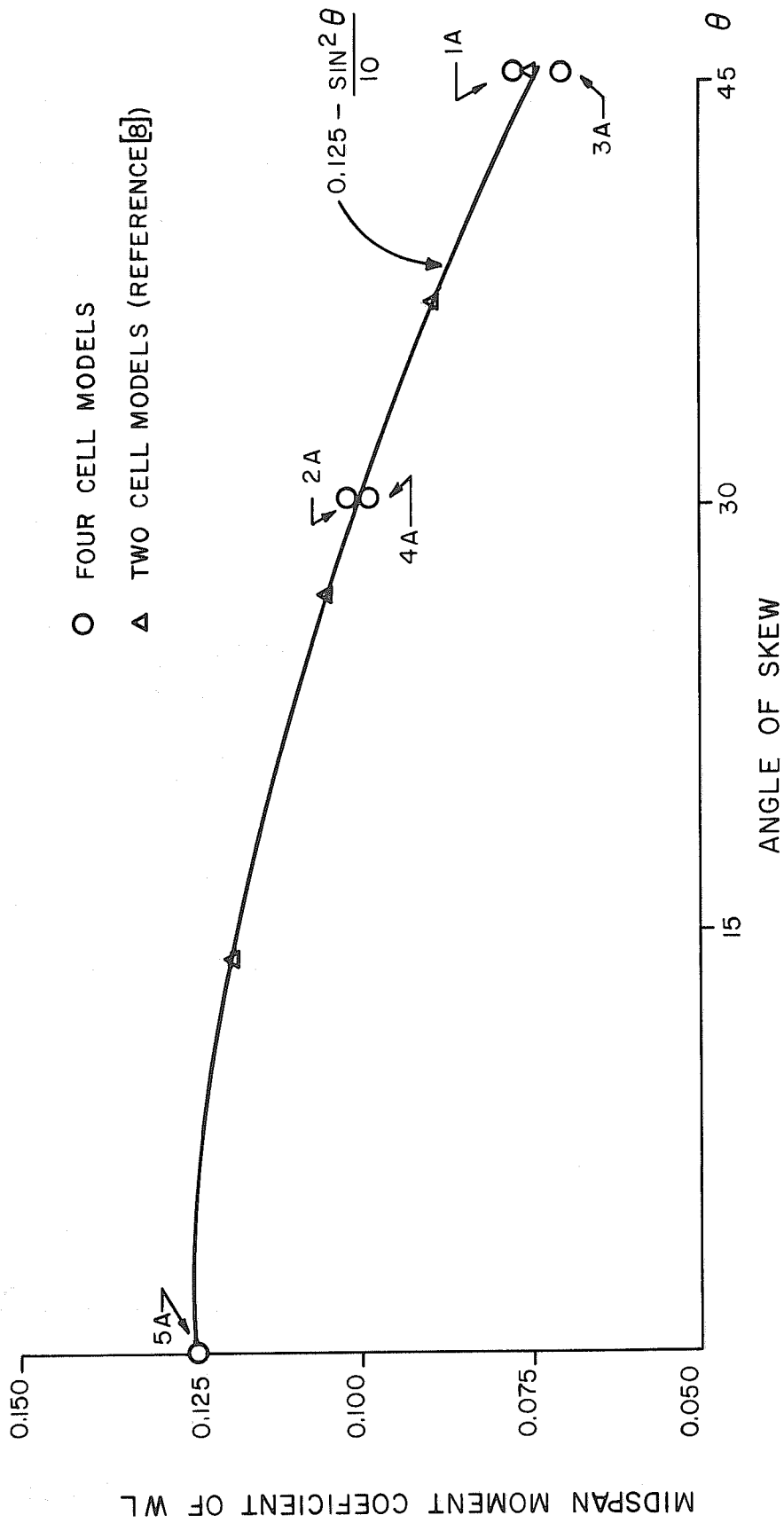


FIG. 4.5 DEAD LOAD MIDSPAN MOMENT COEFFICIENT AS A FUNCTION OF THE ANGLE OF SKEW,  $\theta$

definite indications that the distribution of longitudinal moment at midspan is nearly the same as for a uniform stress distribution.

If the percentage values for girders 1 and 5 and girders 2 and 4 in Table 4.5d are averaged, the resulting values along with that for girder 3 would be a rather accurate estimate for the distribution of the dead load total moment to the individual girders.

TABLE 4.6 DEAD LOAD REACTIONS IN TERMS OF TOTAL LOAD, W, AND MIDSPAN MOMENTS IN TERMS OF WL

Model	R1	R2	Moment
1A(45°/53.5")	.046	.454	.077
2A(30°/47.4")	.093	.407	.101
3A(45°/35.5")	.101	.399	.070
4A(30°/29.6")	.141	.359	.098
5A(0°/22.5")	.250	.250	.125

#### 4.8 Support Conditions

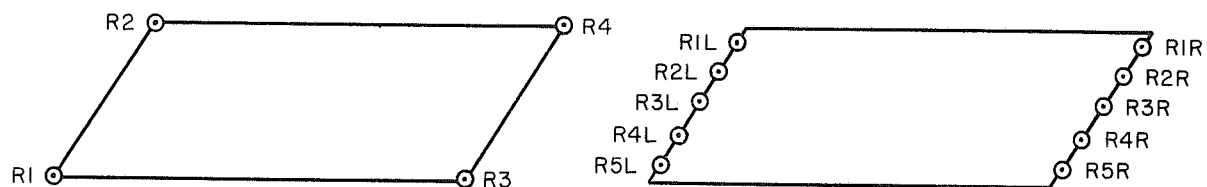
The support conditions of the models analyzed in this study differ somewhat from those usually found in practice. Normally a box girder bridge is supported at the ends beneath each girder. The models were supported only at the four corners, thus only at the ends of each exterior girder. At the ends of each model was a transverse diaphragm which transferred the load from the interior girders to the corner reaction supports. The deflections at the midpoint of the end diaphragms was generally an order of magnitude smaller than those beneath a load at midspan. For this reason it was felt that the response of bridges similar to the models, only supported beneath each girder, would be essentially the same as the models supported

only at the four corners. To verify this assumption, Model 1A and Model 3A were each analyzed by the finite element program CELL with supports beneath each girder at the ends of the models. Partial results of these analyses are presented in Tables 4.7a, b. For comparison, shown with the results for all girders supported is the data for the original model on four corner supports. This comparison shows that for a point load at midspan location 1, 2, or 3 or for dead load, the difference in support conditions has very little effect on the total midspan moment and the deflections at midspan.

Based on the above, it would appear that the total moment at any section for skew bridges, having aspect ratios equal to or less than the models, may be found by substituting for the actual supports under all girders, supports at the four corners only, to which the approximate method of analysis outlined in Section 4.4 then may be applied. It is reasonable also to expect that the transverse distribution of the total moment will be similar for the two support conditions.

From Tables 4.7a, b, it is evident that the total reactions at each end of the skew bridges are essentially identical for the two different support conditions studied. This, as previously mentioned, is a requirement of statics. No approximate method is available for determining the transverse distribution of the total end reactions for the cases in which the bridges are supported on all five girders. The distribution of these reactions is highly sensitive to the flexibility of each individual support assembly and small differences in these from the rigid supports assumed in the analysis

TABLE 4.7a COMPARISON OF RESULTS FOR MODEL 1A (45°/53.5") FOR SUPPORTS AT CORNERS ONLY VS. ALL GIRDERS SUPPORTED

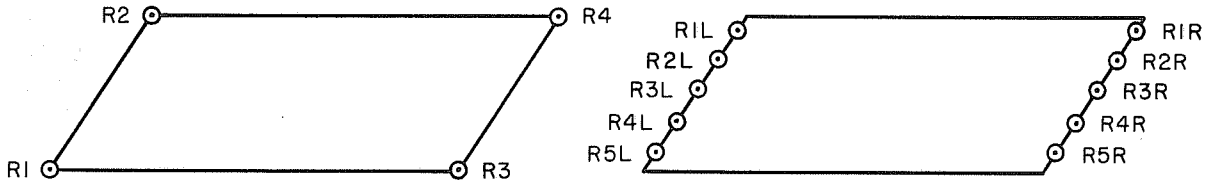


Supported at Corners Only					All Girders Supported				
	Load Case					Load Case			
	DL	1	2	3		DL	1	2	3
Reactions in Terms of Total Load W									
R1	.046	-.271	-.170	-.071	R1L	.417	1.172	.869	.602
R2	.454	.883	.726	.571	R2L	.002	-.294	-.135	-.043
					R3L	.058	-.067	-.037	.028
					R4L	.030	-.113	-.079	-.043
					R5L	-.007	-.085	-.062	-.045
$\Sigma R$	.500	.612	.556	.500	$\Sigma R$	.500	.613	.556	.500
Midspan Moments in Terms of WL									
M	.077	.177	.178	.178	M	.077	.176	.177	.177
Midspan Deflections in Terms of 1000 W/EL									
$\Delta_1$	11.34	27.89	22.36	18.61	$\Delta_1$	11.73	27.00	21.81	18.40
$\Delta_3$	11.34	18.61	19.37	21.41	$\Delta_3$	11.72	18.40	19.16	21.19
$\Delta_5$	11.34	13.94	15.91	18.61	$\Delta_5$	11.73	14.27	15.99	18.40

1. See Appendix A for locations of loads.
2. W = Total dead load for DL case or value of single point load for Cases 1, 2, or 3.



TABLE 4.7b COMPARISON OF RESULTS FOR MODEL 3A (45°/35.5") FOR SUPPORTS AT CORNERS ONLY VS. ALL GIRDERS SUPPORTED



Supported at Corners Only					All Girders Supported				
	Load Case					Load Case			
	DL	1	2	3		DL	1	2	3
Reactions in Terms of Total Load W									
R1	.101	-.165	-.076	.009	R1L	.297	1.078	.647	.359
R2	.399	.834	.661	.491	R2L	.048	-.270	.050	.099
					R3L	.081	-.048	-.045	.102
					R4L	.063	-.053	-.041	-.032
					R5L	.012	-.037	-.026	-.029
ΣR	.500	.669	.585	.500	ΣR	.501	.670	.585	.501
Midspan Moments in Terms of WL									
M	.070	.166	.168	.168	M	.073	.165	.171	.173
Midspan Deflections in Terms of 1000 W/EL									
Δ <sub>1</sub>	2.09	7.19	4.58	3.03	Δ <sub>1</sub>	2.21	6.85	4.42	3.06
Δ <sub>3</sub>	2.30	3.03	3.74	5.17	Δ <sub>3</sub>	2.28	3.03	3.67	5.06
Δ <sub>5</sub>	2.09	1.37	2.02	3.03	Δ <sub>5</sub>	2.21	1.67	2.20	3.06

1. See Appendix A for Locations of loads.
2. W = Total dead load for DL case or value of single point load for Cases 1, 2, or 3.

can change the distribution markedly, because of the high rigidity of the transverse end diaphragm.

One last point should be made in comparing the reactions for the two support conditions given in Tables 4.7 a, b. It appears that the possibility of a net negative reaction under dead load plus some eccentric live truck load combinations may be more likely at an individual reaction support point for the case of all girders supported than for the case of the supports at the four corners only. In general, however, the design live load for girder moment design will involve all lanes being loaded and under this loading, even though there may be a small net negative reaction at the acute corner, its effect on the total design moment at midspan should be small. The sensitivity of the distribution of the total end reaction to each of the support points demonstrates the fact that the individual reaction for which each support assembly is to be designed should be selected conservatively.

## 5. DESIGN CONSIDERATIONS

### 5.1 General

As noted in the previous chapter the design of a box girder bridge for longitudinal bending requires the answer to two basic questions.

- (1) For a given loading, what is the total longitudinal moment existing at any transverse section normal to the longitudinal axis of the bridge?
- (2) What is the transverse distribution of this total moment at the section in question?

For a reinforced concrete bridge the answers to these questions for dead and live load effects ultimately lead to a decision by the designer as to the total required amount of steel reinforcement at a section and the transverse distribution and arrangement of these reinforcing bars. Throughout this report particular emphasis has been placed on these two considerations as they apply to simply supported skew box girder bridges. Overall agreement between an analytical solution and experimental observation has been established on these points. Based on the results of these studies significant insight has been gained on the general behavior of skew box girder bridges. While many questions remain unanswered, certain tentative recommendations can be made for the design of skew box girder bridges.

Before making these recommendations, however, it is instructive to review the present design procedures for box girder bridges.

### 5.2 Present Design Procedures

The highway live loadings on bridges specified by AASHO consist of standard trucks or of lane loadings which are equivalent to truck

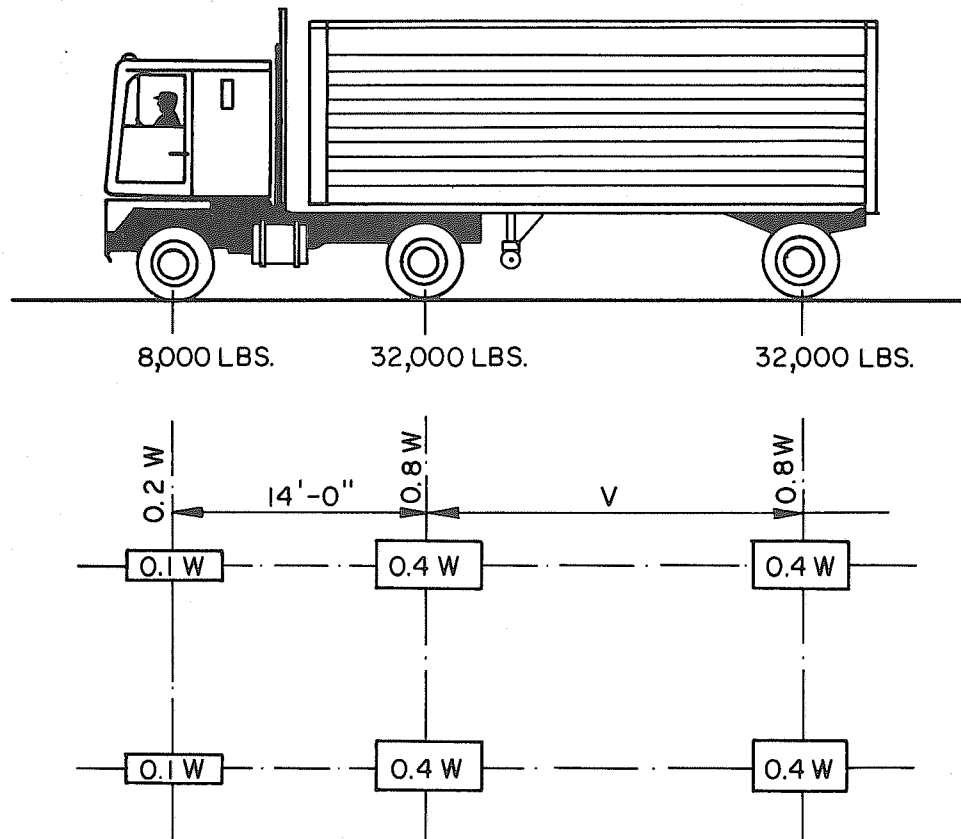
trains [11]. Except for long span box girder bridges the standard truck loadings govern the design rather than the lane loadings. In California, the HS 20-44 standard truck is used for design live loadings and it is assumed to occupy a width of 10 ft., (Fig. 5.1). In each span one such truck per traffic lane may occupy any position which will produce the maximum stress. Where maximum stresses are produced in any member by loading any number of traffic lanes simultaneously, the following percentages of the resultant live load stresses are used in view of the improbable coincident of maximum loading in all lanes:

One or two lanes	100%
Three lanes	90%
Four lanes or more	80%

The 1969 AASHTO specifications [11] specify a design procedure in which the bridge is assumed to consist of a number of similar interior I - girders plus two exterior girders. The division of the total cross-section of any bridge into these components is exactly the same as that done previously in this report for the four cell skew box girder bridge, Fig. 2.6. Each of these girders is designed as an independent member, separated from the rest of the bridge, by applying to it a fraction of a single longitudinal line of wheel loads from a standard truck. This fraction, defined as the "number of wheel loads,  $N_{WL}$ ," is determined as follows for two or more lanes of loading:

For interior girders,

$$N_{WL} = \frac{S}{7} \quad (5.1)$$



W = COMBINED WEIGHT ON THE FIRST TWO AXLES

V = VARIABLE SPACING - 14 FEET TO 30 FEET INCLUSIVE. IN THIS STUDY ASSUMED TO BE 14 FEET TO PRODUCE MAXIMUM STRESS

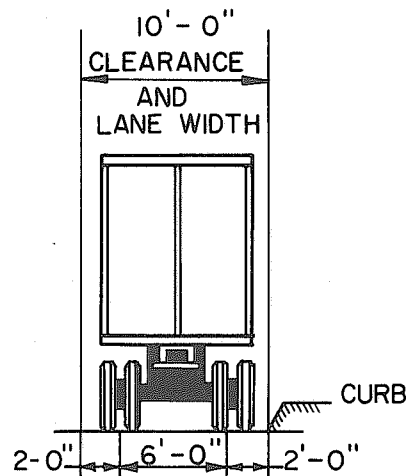


FIG. 5.1 STANDARD HS 20-44 TRUCK OF THE AMERICAN ASSOCIATION OF STATE HIGHWAY OFFICIALS (ASSHO)

For exterior girders,

$$N_{WL} = \frac{W_e}{7} \quad (5.2)$$

where  $N_{WL}$  = number of wheel loads taken by each girder

$S$  = average box width in feet

$W_e$  = top slab width in feet as measured from the midpoint between exterior and interior girder webs to outside face of slab overhang; the cantilever overhang is not to exceed  $S/2$ .

No limitations are stated in the AASHO specifications as to the applicability of these formulas to skew or curved box girder bridges. Although they were undoubtedly initially developed for straight bridges, these formulas are presently being used for the design of bridges of all types of plan layout and alignment.

In December 1967, a slightly different philosophical approach to the design of box girder bridges was adopted by the State of California Bridge Department. This method makes no distinction between interior and exterior girders. The entire cross-section is treated as a "whole width unit," in which the total number of wheel lines applied to the unit is determined as:

$$\text{Total } N_{WL} = \frac{\text{overall deck width in ft.}}{7} \quad (5.3)$$

The total moment developed at any section of the "whole width unit" under the loading given by Eq. (5.3) is assumed to be constant across the width of the bridge. Again, no difference is apparently recognized between straight, skew or curved box girder bridge behavior.

It is important to note that in using Eqs. (5.1) to (5.3) no reductions are to be made for live loads in more than two lanes, since this is

assumed to have been included in the development of these empirical equations.

Both of these procedures, based essentially on the web spacing as a single parameter, are oversimplified and involve some inconsistencies even in the design of straight box girder bridges. As pointed out in a previous report on straight box girder bridges additional parameters such as number of lanes per girder, number of cells, span and end boundary conditions affect load distribution in box girder bridges.

More important for the present discussion is the failure of these present methods of design to make any distinction between the behavior of skew and straight bridges. This raises some serious questions as to the validity of either method for the design of skew box girder bridges. Discussion in the foregoing chapters of this report points out a number of fundamental differences between the behavior of skew and straight box girder bridges.

For example, if one wished to design a four cell bridge similar to the models considered in this study by the AASHO method, each girder would be removed from the bridge and analyzed as an independent simply supported girder subjected to the number of wheel loads per girder determined by Eqs. 5.1 or 5.2.

The longitudinal position of this train of truck wheel loads to produce maximum moments in each girder would be the same for all girders. For a straight bridge, when these individually loaded girders are assembled to form the total bridge the longitudinal wheel load positions would be consistent with the true position of actual trucks on the straight bridge, which produce the maximum total moment on a particular section.

However, this would not be true for a skew bridge, since when the individually loaded girders are assembled to form the total bridge the longitudinal wheel load positions would form a staggered pattern, which would be inconsistent with the true position of actual trucks on the skew bridge needed to produce maximum total moment on a particular section. Thus it is physically inconsistent to design a skew box girder bridge by analyzing it as a set of individual girder components each subjected to a train of wheel load magnitudes given by the AASHO Eqs. 5.1 and 5.2.

The "whole width unit" method is an improvement over the AASHO method for designing skew box girder bridges since it does not separate the bridge into individual girders. However, no provision is made in this method for determining the total moment at any transverse section of a skew bridge for a given loading. As discussed in Chapter 3, this moment cannot be as readily determined for a skew bridge as it can for a straight bridge. Also, in a straight bridge the transverse location of an arbitrary point load does not affect the total longitudinal moment at any right section. This is not so for a skew bridge as described in Chapters 3 and 4. Consequently, while the "whole width unit" method is a philosophical improvement over the AASHO method, its application to skew box girder bridges must be accompanied by a rational approach to the determination of the total moment to be resisted at any right transverse section.

In addition some specification for the transverse distribution of the total longitudinal moment at any section should be made. Such a transverse distribution specification is ignored in the "whole width unit" method presently being used by the State of California Bridge Department.



### 5.3 Tentative Recommended Design Procedure for Live Load

In light of the observations made in this investigation about the overall behavior of skew box girder bridges, it is felt that the "whole width unit" should be considered at any right transverse section for the purpose of design. Once this general approach is adopted the two fundamental questions as to the total longitudinal moment at any section and its transverse distribution remain to be answered.

#### 5.3.1 Determination of Critical Total Design Moment at Any Section

The first consideration which must be made in determining the total live load design moments for a skew bridge is the top deck layout and number of traffic lanes to be carried. The number of lanes on the bridge corresponds to the maximum number of trucks which the bridge will be expected to carry across its width at any section.

With this defined for a specific skew bridge the problem then is the determination of the envelope of the maximum total moments at several design right transverse sections and their transverse distribution. This can be done accurately by using the CELL finite element program to establish the necessary influence surfaces, however, computer costs would be relatively high, since many analyses would be required. Nevertheless, for unusual bridge layouts this may be necessary. Also as part of a long range development program, it might be worthwhile to use the CELL program to develop and tabulate the necessary design information for a wide range of commonly encountered bridges in terms of parameters such as skew angle, number of cells, span, and end boundary conditions. While this would be an expensive and tedious job, the cost spread over the large number of skew bridges encountered in present highway

construction would not be great and the possible savings in more economical designs as well as a better understanding of the behavior of these bridges could warrant the effort.

In the absence of such accurate data, the approximate method described in the preceding chapter can be used as a satisfactory simplified design method for skew box girder bridges of four cells or less, having plan width to span ratios equal to or less than those studied in this investigation. It has been demonstrated that, in the determination of the total design moment at a section, bridges supported beneath all girders may be idealized as supported only at the four corners of the bridge beneath the exterior girders. Once the corner reactions for a point load anywhere in the bridge are found by the approximate method described in Chapter 4, the total longitudinal moment at any section may be determined directly by simple statics. Since a truck load is merely a set of arbitrary point loads the approximate method can be used to find the reactions of a skew bridge on four supports due to a truck anywhere on its deck. A solution is obtained for each of the point wheel loads and the effects of each are superimposed to determine the total response.

To determine the critical design moment at any section, one truck in each traffic lane must be positioned on the top deck of the bridge so as to produce the maximum total moment on the section being considered. This always occurs with all lanes loaded and for practical design purposes may be assumed to occur with the trucks (Fig. 5.1) positioned longitudinally in each lane so that the central heavy axle wheel load of each truck is directly over the section being considered and the second

heavy axle wheel load is positioned on the side of the section nearest midspan. The total moment at a midspan section is not highly sensitive to the transverse position of the trucks in each of the lanes, when all lanes are loaded as above. However, at other sections, somewhat higher total section moments will generally occur when the trucks are positioned transversely so that the resultant of all the wheel loads of each truck is closest to the nearest acute corner of the bridge. Thus this latter transverse positioning is recommended for all cases.

If desired a more accurate determination of the truck positions for maximum total moment on a section may be made by using the approximate method to determine reactions and total moments due to unit loads at various points on the top deck of the bridge. By recording these values on a plan diagram of the bridge and interpolating where necessary, it is possible to generate the contour lines representing the influence surface for the total moment at any right transverse section. A typical influence surface is shown in Fig. 5.2 for Model 4A. Using the customary trial and error procedure, the trucks can then be positioned to give the maximum total moment in the section being considered.

It should be re-emphasized here that the approximate method is rather conservative for loads at sections near the end supports. Generally these are of secondary importance compared to loads and sections near the larger interior portion of the bridge, where the approximate method will yield results quite close to those obtained by a more accurate solution based on a finite element analysis using the CELL program.

Once the maximum total live load moment at each section has been determined, as described earlier, the following percentages of it are

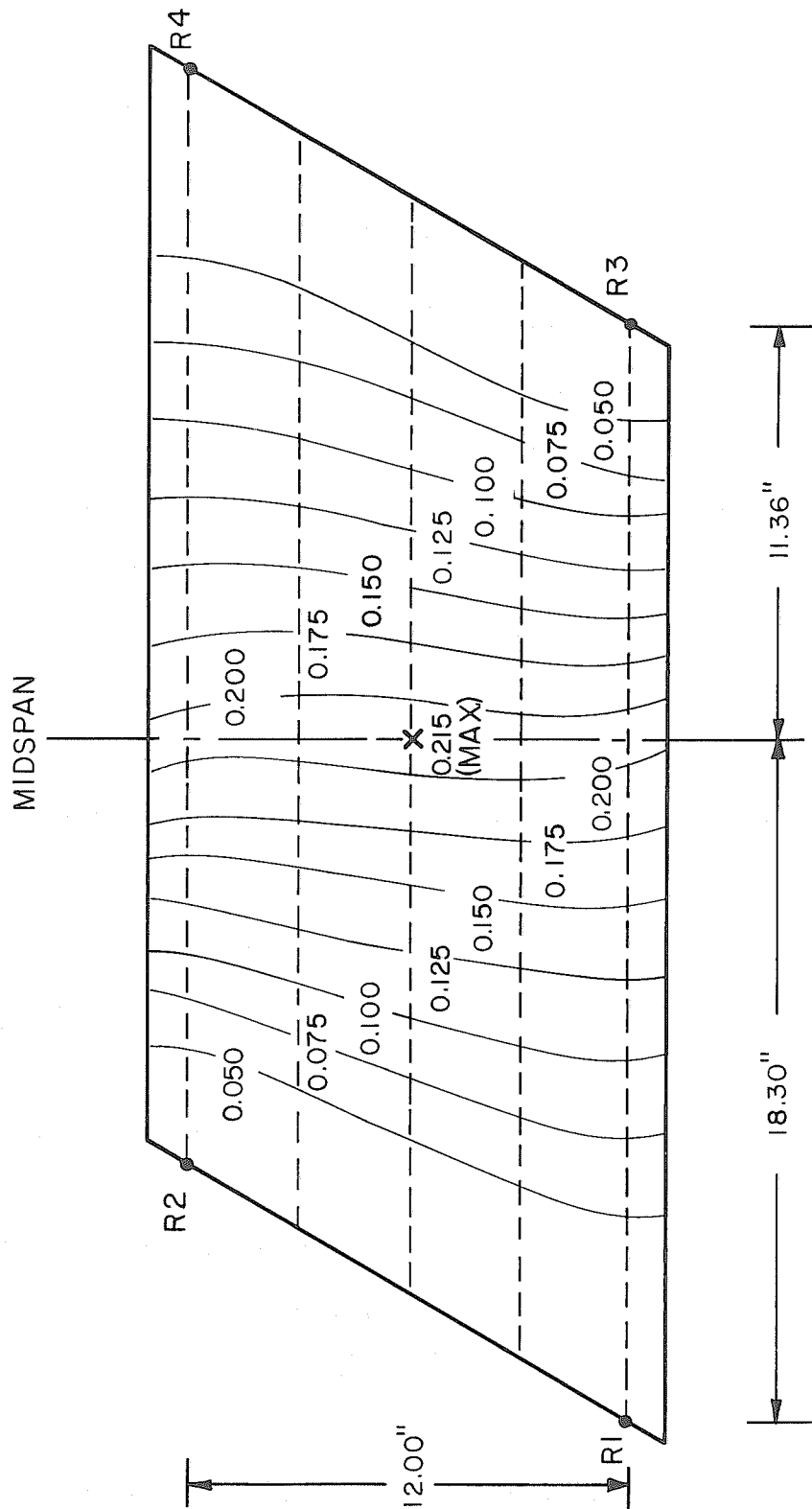


FIG. 5.2 TYPICAL INFLUENCE SURFACE FOR MIDSPAN MOMENT  
IN MODEL 4A

used as a design moment depending on the number of loaded lanes: 100% for one or two lanes; 90% for three lanes; and 80% for four lanes or more. The next step is the determination of the transverse distribution of these total design live load moments at a section.

### 5.3.2 Transverse Distribution of Total Moment at a Section

In the previous chapter on the general behavior of the bridge models it was noted that the transverse distribution of the total moment at section 0-0, very near midspan, was essentially the same as the optimum uniform stress case, Fig. 2.6, for various combinations of point loads, Fig. 4.5 a to d. However, in virtually all instances the exterior girders resisted a slightly higher percentage of the total moment than the 15.8% found for the uniform stress case. This condition is in part due to the end conditions of the various girders in the models. The exterior girders in the models studied are directly centered over the corner supports and are slightly stiffer than the interior girders, whose ends are supported by an end diaphragm which spans between corner supports. In a bridge with all girders supported it is expected that this slight divergence from the uniform stress case would become insignificant.

One inconsistency which may arise in treating the "whole width unit" is the possibility that although a certain arrangement of the truck loads will produce a maximum total moment at a section a slightly different arrangement might cause a slightly larger moment in an individual girder. For example, if the trucks are shifted the total moment may decrease very slightly. However, the percentage of the total moment taken by an individual girder may increase such that

the moment taken by that girder is larger than when the maximum total moment existed at the section. In this sense, the "whole width unit" method represents a lower bound solution, and if any local yielding occurs there would have to be a transverse redistribution of stress to adequately resist the total section moment.

The discrepancy should be small. Nevertheless, to account for this factor it is recommended that a skew bridge be designed for a slight excess (say 5%) above the maximum total design live load moment at a section. At the midspan section the reinforcement required for the design moment should be distributed uniformly across the section. The reinforcement required for the excess (say 5%) should be concentrated in the two exterior girders since their percentages of total moment tend to be slightly higher than the uniform stress case and are the most affected by a slight movement of the critical truck load positions.

With the information available at this time it is not possible to determine the distribution of the maximum total moment at a right transverse section other than at midspan. For sections near midspan, the distribution is probably close to the optimum uniform stress case. However, near the end supports this assumption cannot be made since in this region local effects due to the skewed supports greatly influence the distribution of internal stresses.

#### 5.4 Design for Dead Load Moments

Depending upon the span and plan dimensions of a box girder bridge, the dead load may produce as much as half or more of the total dead load plus live load moment to be resisted at a particular section.

An accurate determination of the dead load moments and their transverse distribution can always be found in a skew bridge using the CELL finite element program. However, if desired, for a simplified design method for bridges of four cells or less having plan width to span ratios equal to or less than those studied in this investigation, the total dead load moment at the midspan section may be adequately predicted by the empirical formula presented in Chapter 4. The dead load moment at midspan will always be less for a skew bridge than for a straight bridge of the same span, however, additional data is needed to determine the amount of this reduction for bridges outside of the range of those indicated above.

As shown in Table 4.5d, the transverse distribution of the dead load moment at midspan is very close to that for the uniform stress case. At sections other than midspan, no data is available to make a definitive statement on the total moment or its transverse distribution.

### 5.5 Transverse Slab Moments

In Section 3.7 and Figs. 3.35 to 3.39 it was noted that the magnitude and distribution of the transverse plate bending moments at midspan as found by the CELL program were essentially a function of local loading and were independent of span and angle of skew. A similar conclusion was determined in studies [1,2] of these moments in straight bridges of various spans, number of cells and load positions. Thus no distinction appears necessary between skew and straight bridges with respect to the design for transverse slab moments due to live loads in the central portion of the bridge. However, when these live loads act near the end supports differences undoubtedly occur and further study is necessary on this subject to determine whether these differences are important.

## 5.6 Other Design Considerations

The present investigation was not intended to develop a comprehensive set of design recommendations. In the total design of a skew box girder bridge a number of additional factors have to be considered beyond those already described.

The present investigation dealt primarily with the total longitudinal moment and its distribution at the midspan section. While the total moment at other sections can be found by the approximate method described, its distribution at other sections especially near the end supports cannot. Longitudinal moments in this region will undoubtedly be small and can be taken care of by nominal steel in simple span reinforced concrete skew box girder bridges. For prestressed bridges, cable profiles in each girder are dependent on a knowledge of the longitudinal distribution of the maximum moment envelope in each girder. For design purposes, knowing the midspan condition, reasonable approximations may be satisfactory for this longitudinal distribution. However, it is suggested that the CELL program be used wherever there is any doubt.

No attempt has been made in this investigation to study maximum girder web shears at the end supports. For the bridges, supported at the four corners only, which were studied in this investigation it has been shown that a larger reaction occurs at the obtuse corner than at the acute corner for dead load and live loads in the central portion of the bridge. This indicates that the web shears near the obtuse corner will be larger than at the acute corner and should be accounted for. Maximum web shears will occur with truck live loads placed near the end supports, a condition which was not studied in this investigation.



For skew bridges supported under all girders the transverse distribution of the total reactions at each end to individual reaction supports and of the web shears can only be found using the CELL program. However, it should be emphasized that because of the relatively stiff end diaphragms this distribution is highly dependent on the type and manner of the actual installation of the supports. The distribution is difficult to predict by theory unless the spring constant of each individual support is accurately known. Thus reaction assemblies should be designed conservatively, perhaps considering the case of the bridge on only four corner supports as an upper bound solution for guidance.

The effect of cracking on the load distribution in reinforced concrete skew bridges has not been considered in this study. Tests on a large scale reinforced concrete model of a straight box girder bridge [4] have indicated that at the working stress level cracking is not an important factor in determining the total moment at a section and its transverse distribution. Thus results from analyses of uncracked homogeneous elastic systems can be used for these straight simple or continuous bridges to determine load distribution. The effect of cracking remains to be studied for curved and skew reinforced concrete bridges. Intuitively, it would appear that the load distribution in highly skew bridges would be the most sensitive to cracking and changes in stiffness. However, contradicting this to some extent is the fact that, while there were significant differences between the stiffnesses of the experimental aluminum models and the analytical models studied with the CELL program, the results for total moments and their transverse distribution were almost the same.

The present investigation was confined to single span, simply supported, skew bridges. For continuous bridges of two or more spans with skew supports, the CELL finite element program can be used to obtain an accurate solution for dead and live load distribution. No approximate design method can be recommended for these bridges at this time.

## 6. CONCLUSIONS AND RECOMMENDATIONS FOR IMPLEMENTATION AND FURTHER STUDY

A detailed presentation of the reduction, analysis and interpretation of theoretical results obtained for a series of single span, simply supported, four cell, skew box girder bridges having varying angles of skew and span lengths has been given. Each bridge was studied first without and then with a midspan diaphragm. The theoretical results were based on a finite element computer program CELL, which treats the bridge as an uncracked, homogeneous and elastic system made up of interconnected plate elements. Both membrane and plate bending action in each plate element are accounted for in the finite element analysis.

Theoretical results were compared with experimental results from a previous study on aluminum models of identical dimensions. On the basis of this comparison and the interpretation of the data, an approximate simplified method of analysis was proposed and finally some tentative recommendations for the design of skew box bridges were made.

The most important conclusions from this study are summarized below.

1. The finite element computer program CELL can be used to accurately predict external reactions, the total longitudinal moments at any section and its transverse distribution in terms of longitudinal plate forces or moments taken by individual girders.

2. The shape of the midspan transverse distribution curve of longitudinal plate forces  $N_{xx}$  for any given concentrated point load position at the midspan section is essentially independent of the span of the bridge or its skew angle. The departure from a uniform transverse distribution is thus a function of local bending rather than span or skew angle.

3. Under a single point load on a bridge the addition of a midspan diaphragm does not change the external reactions or total moments at a section, but it does result in a more uniform transverse distribution of the longitudinal forces  $N_{xx}$  than for the case without a midspan diaphragm. However, for realistic design truck live loads involving several loads across the bridge width or for dead load there is little difference, with essentially a uniform transverse distribution of longitudinal forces  $N_{xx}$  existing at midspan for bridges with or without a midspan diaphragm.

4. The total moment at any section for skew bridges, having plan aspect ratios equal to or less than the models studied, may be found by substituting for a condition of actual supports under all girders, supports at the four corners only, to which the approximate method of analysis outlined in Section 4.4 may then be applied as a simplified design method.

5. For skew bridges similar to those studied the midspan coefficient for the total dead load moment as a fraction of the total dead load times the span length may be adequately predicted by the empirical expression  $0.125 - 0.100 \sin^2 \theta$ , where  $\theta$  is the angle of skew.

6. The present AASHO method of design or the "whole width unit" method used by the State of California Bridge Department, which do not differentiate between straight and skew bridges should be reviewed because definite differences do exist which should be accounted for. Since it has been shown in this report that the total design moment at any section in a skew bridge is less than in a straight bridge, a more accurate design method than those used at present could result in more economical skew bridge structures.

For implementation, based on the results of the present investigation, it is recommended that the CELL finite element program be used as an accurate method of analysis of skew bridges of any plan configuration. The approximate design method described in Chapter 4 should in the strictest sense be used only for bridges similar to the four cell models studied in this investigation. However, available theoretical data for bridges with fewer cells and smaller plan aspect ratios (width to span) indicate the approximate method is also applicable to these bridges. Limited preliminary studies of six and eight cell bridges with larger aspect ratios indicate that the approximate method might have to be modified somewhat to account for differences in their behavior.

Recommendations for further study include the following:

1. Analysis of additional cases with the CELL program in which the parameters would include the number of cells, plan aspect ratio, and continuous as well as simple spans.
2. A detailed study using the results from the CELL program, of maximum girder shears for design dead and live loads on box girder bridges with various angles of skew.
3. Experimental study on a large scale reinforced concrete skew box girder bridge model to determine the effects of cracking and overloads on load distribution and also to observe the ultimate strength behavior during a final loading to failure.

## 7. ACKNOWLEDGEMENTS

This investigation was sponsored by the Division of Highways, Department of Public Works, State of California, and the Federal Highway Administration, United States Department of Transportation.

The contents of this report reflect the views of the authors who are responsible for the facts and the accuracy of the data presented herein. The contents do not necessarily reflect the official policies of the State of California or the Federal Highway Administration. This report does not constitute a standard, specification, or regulation.

Mr. G. D. Mancarti, Assistant Bridge Engineer, and Mr. R. E. Davis, Senior Bridge Engineer, of the Research and Development Section, provided close liaison from the Bridge Department, Division of Highways, State of California. Their cooperation and assistance is gratefully acknowledged.

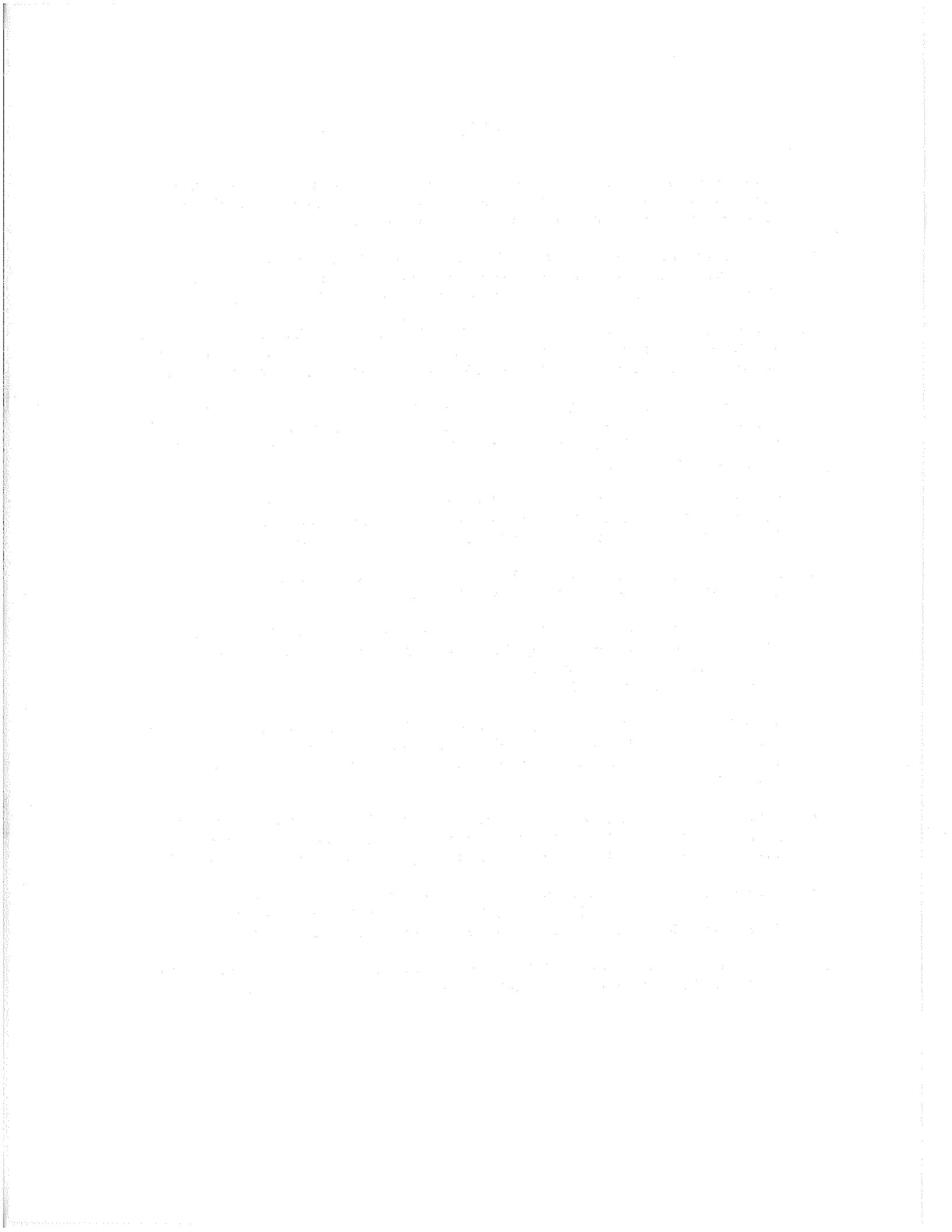
Special acknowledgements are due to Mr. Y. J. Kang and Mr. A. R. Nene, Research Assistants in the Division of Structural Engineering and Structural Mechanics of the University of California. Mr. Kang carried out all of the computer analyses using the CELL program and participated in reduction and the plotting of the data. Mr. Nene participated in the interpretation of the data and the development of some of the approximate analysis procedures.



8. REFERENCES

1. Scordelis, A. C., Analysis of Simply Supported Box Girder Bridges," Structural Engineering and Structural Mechanics Report No. 66-17, University of California, Berkeley, October 1966.
2. Scordelis, A.C., Analysis of Continuous Box Girder Bridges," Structural Engineering and Structural Mechanics Report No. 67-25, University of California, Berkeley, November 1967.
3. Scordelis, A. C., and Meyer, C., "Wheel Load Distribution in Concrete Box Girder Bridges," Structural Engineering and Structural Mechanics Report No. 69-1, University of California, Berkeley, January 1969.
4. Scordelis, A. C., Bouwkamp, J. G., and Wasti, S. T., "Structural Behavior of a Two Span Reinforced Concrete Box Girder Bridge Model," Vol. 1, UC-SESM Report No. 71-5, Vol. 2, UC-SESM Report No. 71-16, Vol. 3, UC-SESM Report No. 71-17.
5. Godden, W. G., and Aslam, M., "Model Studies of Skew Box Girder Bridges," Structural Engineering and Structural Mechanics Report No. 71-26, University of California, Berkeley, December 1971.
6. Zienkiewicz, O. C., "The Finite Element Method in Engineering Science," McGraw-Hill Publishing Co., Ltd., London, 1971.
7. Willam, K. J. and Scordelis, A. C., "Computer Program for Cellular Structures of Arbitrary Plan Geometry," Structural Engineering and Structural Mechanics Report No. 70-10, University of California, Berkeley, September 1970.
8. Sisodiya, R. G., Ghali, A., and Cheung, Y. K., "Diaphragms in Single and Double Cell Box Girder Bridges with Varying Angle of Skew," Journal of American Concrete Institute, Proceedings V. 69, No. 7, July 1972.
9. William, K. J., and Scordelis, A. C., "Cellular Structures of Arbitrary Plan Geometry," Journal of the Structural Division, Proceedings of the American Society of Civil Engineers, Vol. 98, No. ST7, July 1972.
10. Clough, R. W., and Felippa, C. A., "A Refined Quadrilateral for Analysis of Plate Bending," 2nd Conference on Matrix Methods in Structural Mechanics, Wright-Patterson Air Force Base, Ohio, October 1968.
11. "Standard Specifications for Highway Bridges," American Association of State Highway Officials (AASHO), Tenth Edition, Washington, D.C., 1969.





APPENDIX A

Theoretical Results from CELL Program

MODEL A: WITHOUT MID DIAPHRAGM  
 MODEL B: WITH MID DIAPHRAGM

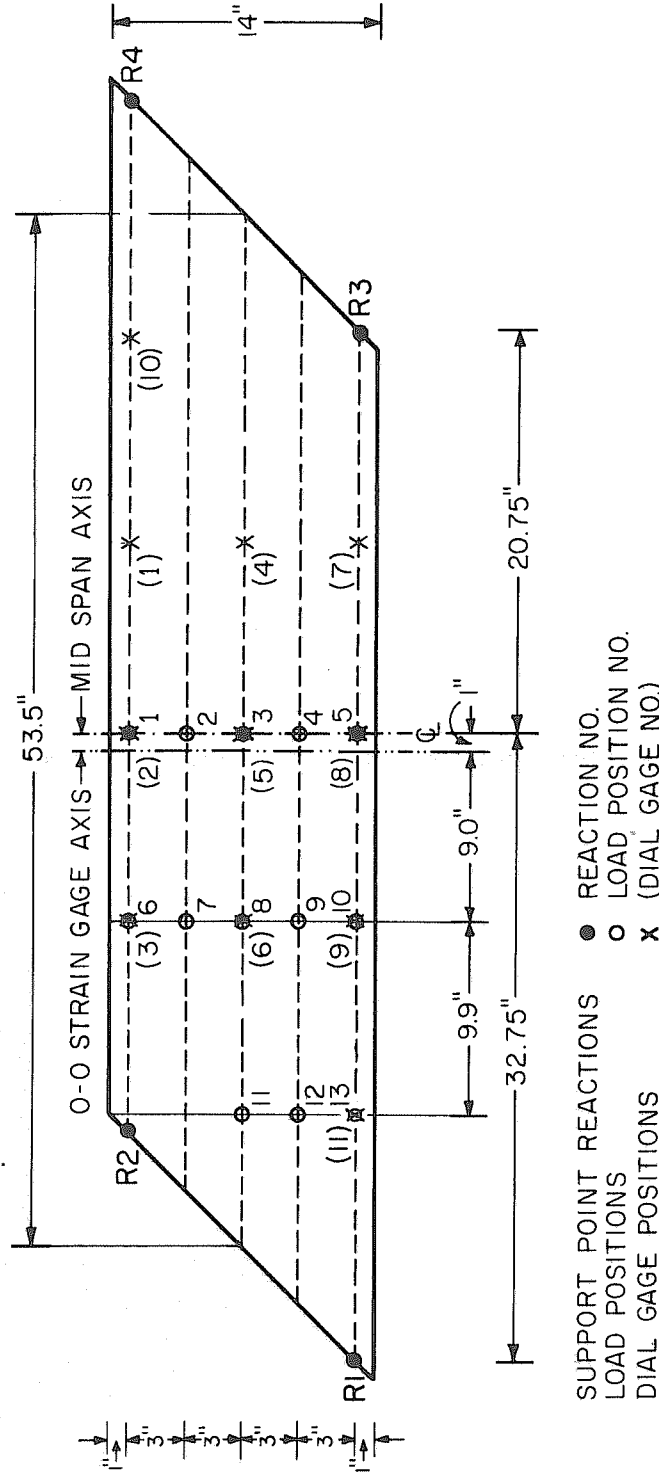


FIG. A.1 SKEW BOX GIRDER BRIDGE MODEL NO. 1,  
 SPAN = 53.5 INCHES, SKEW ANGLE = 45°



\*\*\*\*\*  
 ALUMINIUM BOX GIRDER BRIDGE MODEL STUDY  
 \*\*\*\*\*

MODEL N3 = 1A / SPAN = 53.50 INCHES / SKEW ANGLE = 45 DEGREES / MIDSPAN DIAPHRAGM = NO  
 THEORETICAL RESULTS WITH MESH SIZE 6X28

NXX FORCES \*\*\* LONGITUDINAL PLATE FORCES PER UNIT WIDTH AT SECTION O-O  
 COEFFICIENTS OF W/L

S/R	L O A D P O S I T I O N												
	1	2	3	4	5	6	7	8	9	10	11	12	13
	T O P P L A T E												
00/14	-26.13	-16.21	-13.21	-11.97	-11.51	-8.25	-10.61	-10.97	-10.80	-11.06	-3.02	-4.46	-5.57
01/14	-30.50	-17.58	-14.04	-12.41	-11.69	-8.52	-10.77	-10.93	-10.73	-10.83	-3.03	-4.35	-5.37
04/14	-17.69	-25.11	-15.92	-13.47	-12.48	-9.80	-8.80	-10.39	-10.80	-11.02	-2.57	-4.04	-5.22
07/14	-13.91	-15.77	-24.26	-15.99	-14.34	-9.18	-9.61	-8.85	-10.84	-11.65	-2.07	-3.57	-4.91
10/14	-12.04	-13.25	-15.91	-25.31	-18.10	-8.39	-9.44	-10.28	-9.88	-12.06	-2.42	-3.11	-4.39
13/14	-11.22	-12.17	-14.01	-17.75	-30.87	-8.08	-9.28	-10.72	-11.71	-10.57	-2.76	-3.36	-3.75
14/14	-11.04	-11.71	-13.17	-16.36	-26.47	-8.23	-9.27	-10.69	-11.48	-10.22	-2.65	-3.17	-3.60
	B O T T O M P L A T E												
01/14	37.37	19.10	15.06	12.97	11.68	8.50	11.77	11.90	11.45	11.43	3.29	4.73	5.83
04/14	18.93	26.44	16.48	13.91	12.79	10.41	9.45	10.94	11.26	11.47	2.74	4.29	5.52
07/14	14.51	16.24	25.15	16.47	14.97	9.63	10.05	9.30	11.34	12.21	2.24	3.78	5.13
10/14	12.32	13.67	16.48	26.66	19.36	8.68	9.82	10.82	10.57	12.77	2.59	3.29	4.54
13/14	11.18	12.69	15.01	19.26	37.74	8.45	9.85	11.61	12.68	10.55	2.91	3.45	3.70





\*\*\*\*\*  
 ALUMINUM BOX GIRDER BRIDGE MODEL STUDY  
 \*\*\*\*\*

MODEL NO = 1B / SPAN = 53.50 INCHES / SKEW ANGLE = 45 DEGREES / MIDSPAN DIAPHRAGM = YES  
 THEORETICAL RESULTS WITH MESH SIZE 6X28

NXX FORCES \*\*\* LONGITUDINAL PLATE FORCES PER UNIT WIDTH AT SECTION 0-0  
 COEFFICIENTS OF W/L

		L O A D P O S I T I O N												
		1	2	3	4	5	6	7	8	9	10	11	12	13
		T O P P L A T E												
S/R														
00/14		-15.33	-18.70	-17.17	-15.67	-14.24	-5.26	-11.11	-12.83	-12.66	-12.14	-3.74	-4.92	-5.50
01/14		-22.79	-19.69	-17.08	-15.00	-13.37	-6.15	-11.21	-12.32	-12.00	-11.43	-3.57	-4.66	-5.24
04/14		-18.82	-18.70	-16.89	-15.51	-14.44	-9.68	-6.72	-10.47	-11.78	-12.02	-2.61	-4.32	-5.47
07/14		-15.90	-16.63	-17.69	-16.85	-16.33	-9.90	-9.51	-6.65	-10.76	-12.40	-1.52	-3.44	-5.12
10/14		-14.00	-15.29	-16.88	-18.91	-19.24	-9.27	-10.30	-10.24	-7.69	-11.87	-2.21	-2.57	-4.32
13/14		-12.91	-14.76	-17.05	-19.87	-23.18	-8.68	-10.49	-12.02	-12.07	-8.11	-3.10	-3.55	-3.42
14/14		-13.76	-15.40	-17.11	-18.83	-16.67	-9.25	-11.03	-12.41	-11.86	-7.11	-3.06	-3.40	-3.21
		B O T T O M P L A T E												
S/R														
01/14		26.20	22.07	19.47	16.39	14.16	5.27	12.38	13.83	13.16	12.31	4.03	5.15	5.65
04/14		19.72	19.59	17.39	15.90	14.77	10.20	7.39	11.00	12.21	12.43	2.79	4.55	5.75
07/14		16.33	17.07	18.40	17.30	16.79	10.27	9.96	7.24	11.27	12.89	1.72	3.66	5.32
10/14		14.30	15.66	17.39	19.81	20.16	9.54	10.66	10.76	8.40	12.47	2.38	2.75	4.45
13/14		13.67	16.11	19.42	22.23	26.58	9.32	11.48	13.41	13.18	7.21	3.37	3.71	3.26





MODEL A: WITHOUT MID DIAPHRAGM  
 MODEL B: WITH MID DIAPHRAGM

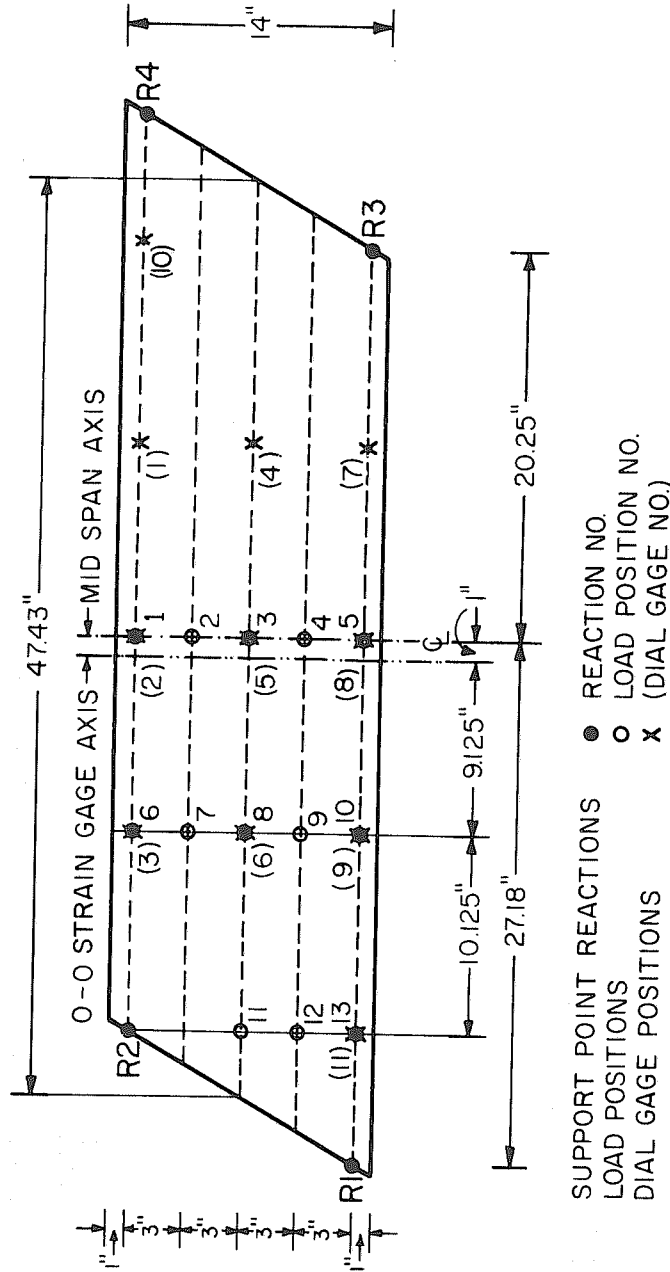


FIG.A.2 SKEW BOX GIRDER BRIDGE MODEL NO.2,  
 SPAN=47.43 INCHES, SKEW ANGLE = 30°



\*\*\*\*\*  
 ALUMINUM BOX GIRDER BRIDGE MODEL STUDY  
 \*\*\*\*\*

MODEL NO = 2A / SPAN = 47.44 INCHES / SKEW ANGLE = 30 DEGREES / MIDSPAN DIAPHRAGM = NO  
 THEORETICAL RESULTS WITH MESH SIZE 6X28

NXX FORCES \*\*\* LONGITUDINAL PLATE FORCES PER UNIT WIDTH AT SECTION 0-0  
 COEFFICIENTS OF W/L

S/B	L O A D P O S I T I O N												
	1	2	3	4	5	6	7	8	9	10	11	12	13
00/14	-24.27	-15.45	-12.77	-11.67	-11.28	-7.78	-9.81	-10.18	-10.05	-10.33	-2.37	-3.52	-4.50
01/14	-28.17	-16.66	-13.50	-12.05	-11.43	-8.02	-9.97	-10.15	-9.99	-10.12	-2.39	-3.45	-4.34
04/14	-16.83	-23.37	-15.17	-12.99	-12.13	-9.19	-8.31	-9.65	-10.04	-10.29	-2.02	-3.22	-4.25
07/14	-13.52	-15.10	-22.59	-15.22	-13.77	-8.75	-9.03	-8.34	-10.07	-10.83	-1.65	-2.90	-4.08
10/14	-11.88	-12.87	-15.18	-23.50	-17.08	-8.10	-8.94	-9.61	-9.26	-11.12	-2.00	-2.61	-3.71
13/14	-11.17	-11.92	-13.50	-16.78	-28.40	-7.86	-8.85	-10.07	-10.84	-9.78	-2.36	-2.91	-3.16
14/14	-11.02	-11.53	-12.76	-15.56	-24.48	-8.01	-8.86	-10.06	-10.63	-9.48	-2.29	-2.77	-3.05

T O P P L A T E

B O T T O M P L A T E

01/14	34.31	18.06	14.46	12.60	11.48	8.02	10.84	11.01	10.65	10.69	2.59	3.74	4.70
04/14	17.99	24.61	15.73	13.43	12.46	9.74	8.90	10.16	10.47	10.71	2.15	3.41	4.48
07/14	14.12	15.57	23.43	15.70	14.38	9.17	9.45	8.78	10.54	11.35	1.79	3.08	4.27
10/14	12.20	13.31	15.74	24.74	18.25	8.40	9.32	10.12	9.90	11.76	2.15	2.78	3.85
13/14	11.20	12.46	14.45	18.17	34.53	8.25	9.41	10.89	11.70	9.79	2.52	3.01	3.13





\*\*\*\*\*  
 ALUMINUM BOX GIRDER BRIDGE MODEL STUDY  
 \*\*\*\*\*

MODEL NJ = 28 / SPAN = 47.44 INCHES / SKEW ANGLE = 30 DEGREES / MIDSPAN DIAPHRAGM = YES  
 THEORETICAL RESULTS WITH MESH SIZE 6X28

NXX FORCES \*\*\* LONGITUDINAL PLATE FORCES PER UNIT WIDTH AT SECTION 0-0  
 COEFFICIENTS OF W/L

S/B	L O A D P O S I T I O N												
	1	2	3	4	5	6	7	8	9	10	11	12	13
	T O P P L A T E												
00/14	-15.60	-17.65	-16.28	-14.95	-13.70	-5.24	-10.25	-11.81	-11.69	-11.26	-3.02	-3.99	-4.49
01/14	-21.32	-18.53	-16.19	-14.34	-12.91	-5.99	-10.35	-11.35	-11.10	-10.62	-2.89	-3.78	-4.26
04/14	-17.83	-17.68	-16.04	-14.81	-13.87	-9.07	-6.53	-9.71	-10.89	-11.16	-2.03	-3.44	-4.48
07/14	-15.29	-15.88	-16.77	-16.00	-15.54	-9.36	-8.93	-6.46	-10.00	-11.49	-1.17	-2.78	-4.28
10/14	-13.63	-14.69	-16.05	-17.81	-18.08	-8.88	-9.68	-9.57	-7.37	-10.95	-1.82	-2.14	-3.66
13/14	-12.66	-14.22	-16.19	-18.64	-21.56	-8.37	-9.90	-11.17	-11.12	-7.64	-2.67	-3.06	-2.79
14/14	-13.44	-14.81	-16.26	-17.74	-15.80	-8.89	-10.39	-11.53	-10.93	-6.80	-2.67	-2.94	-2.61
	B O T T O M P L A T E												
01/14	24.39	20.68	18.36	15.62	13.67	5.26	11.37	12.69	12.14	11.43	3.27	4.18	4.61
04/14	18.68	18.52	16.54	15.20	14.21	9.54	7.14	10.20	11.29	11.55	2.16	3.62	4.69
07/14	15.73	16.32	17.45	16.45	16.00	9.72	9.36	7.01	10.48	11.95	1.34	2.96	4.44
10/14	13.96	15.08	16.55	18.65	18.95	9.15	10.04	10.07	8.03	11.49	1.97	2.32	3.78
13/14	13.40	15.49	18.35	20.79	24.62	8.98	10.82	12.43	12.09	6.88	2.94	3.22	2.64





MODEL A: WITHOUT MID DIAPHRAGM  
 MODEL B: WITH MID DIAPHRAGM

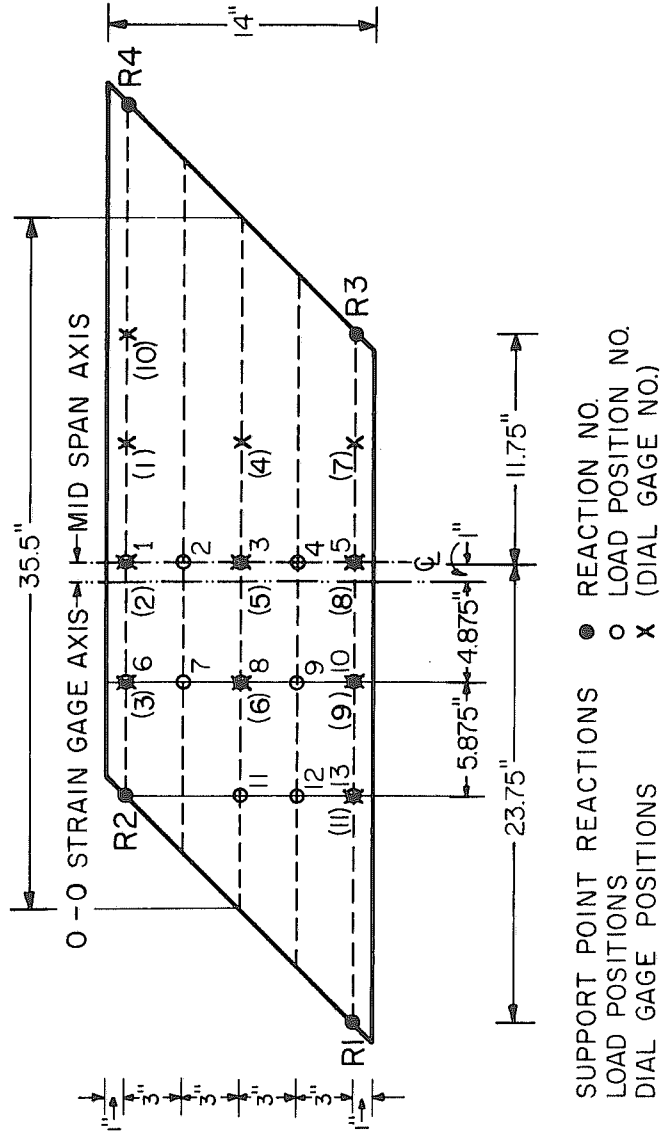


FIG.A.3 SKEW BOX GIRDER BRIDGE MODEL NO.3,  
 SPAN= 35.5 INCHES, SKEW ANGLE =45°



\*\*\*\*\*  
 ALUMINUM BOX GIRDER RF IDG MODEL STUDY  
 \*\*\*\*\*

MODEL NO = 34 / SPAN = 35.50 INCHES / SKIN ANGLE = 45 DEGREES / MIDSPAN DIAPHRAGM = NO  
 THEORETICAL RESULTS WITH MESH SIZE 6X24

NXX FORCES \*\* LONGITUDINAL FLATE FORCES PER UNIT WIDTH AT SECTION 0-0  
 (COEFFICIENTS OF 4/L)

S/B	L O A D P O S I T I O N												
	1	2	3	4	5	6	7	8	9	10	11	12	13
	-12.94	-6.25	-4.19	-3.31	-2.98	-6.00	-5.40	-3.76	-3.18	-3.26	-1.51	-1.98	-2.64
00/14	-15.78	-7.18	-4.77	-3.64	-3.14	-5.75	-5.50	-4.01	-3.34	-3.28	-1.56	-1.96	-2.49
01/14	-7.07	-12.09	-6.01	-4.36	-3.71	-4.95	-4.35	-4.72	-3.94	-3.78	-1.36	-2.10	-2.73
04/14	-4.57	-5.94	-11.61	-6.15	-5.02	-3.19	-4.42	-4.38	-5.28	-4.97	-.88	-2.30	-3.21
07/14	-3.43	-4.30	-6.18	-12.46	-7.67	-2.28	-3.42	-5.10	-5.44	-6.87	-1.92	-2.03	-3.38
10/14	-2.96	-3.69	-5.04	-7.64	-16.39	-1.95	-3.05	-4.66	-6.79	-7.33	-2.57	-3.20	-2.54
13/14	-2.80	-3.37	-4.49	-6.73	-13.55	-1.85	-2.89	-4.44	-6.71	-7.53	-2.58	-3.09	-2.42

T O P P L A T E

B O T T O M P L A T E

01/14	20.13	7.93	5.21	3.76	2.86	6.31	6.58	4.50	3.49	3.20	1.79	2.12	2.66
04/14	7.67	12.73	6.13	4.39	3.65	5.51	4.51	4.79	3.95	3.76	1.37	2.09	2.76
07/14	4.78	6.03	11.97	6.25	5.22	3.34	4.49	4.38	5.39	5.17	.95	2.40	3.33
10/14	3.39	4.36	6.33	13.14	8.31	2.25	3.48	5.28	5.74	7.56	2.10	2.30	3.60
13/14	2.63	3.84	5.55	8.52	20.82	1.75	3.25	5.27	7.99	7.91	3.00	3.60	2.42





\*\*\*  
 ALUMINUM BOX STUDY BRIDGE MODEL STUDY  
 \*\*\*

MODEL #1 = 39 / SPAN = 39.50 INCHES / SKEW ANGLE = 45 DEGREES / MIDSPAN DIAPHRAGM = YES  
 THEORETICAL RESULTS WITH MESH SIZE 6X24

\*\*\*  
 NXX FORCES \*\*\* LONGITUDINAL PLATE FORCES PER UNIT WIDTH AT SECTION D-D  
 COEFFICIENTS OF W/L  
 \*\*\*

S/R	1	2	3	4	5	6	7	8	9	10	11	12	13
	L O A D P O S I T I O N												
	T O P P L A T E												
00/14	-6.66	-8.14	-7.02	-5.90	-4.82	-2.94	-6.42	-5.96	-5.30	-4.66	-2.99	-3.30	-3.26
01/14	-10.89	-8.78	-6.93	-5.53	-4.36	-3.38	-6.36	-5.71	-4.88	-4.21	-2.70	-2.92	-2.87
04/14	-7.79	-7.76	-6.58	-5.65	-4.92	-5.02	-2.05	-4.88	-4.91	-4.76	-1.46	-2.67	-3.31
07/14	-5.75	-6.31	-7.07	-6.53	-6.19	-3.77	-4.25	-1.74	-5.21	-5.71	.34	-2.12	-3.59
10/14	-4.04	-5.59	-6.74	-8.14	-8.39	-2.98	-4.13	-5.04	-2.90	-6.83	-1.62	-.78	-3.20
13/14	-4.19	-5.57	-7.24	-9.23	-11.53	-2.70	-4.34	-6.04	-7.29	-4.40	-3.16	-3.29	-1.24
14/14	-4.65	-5.95	-7.23	-8.59	-7.29	-2.95	-4.65	-6.20	-7.22	-3.74	-3.30	-3.13	-.73

S/R

	B O T T O M P L A T E												
01/14	13.04	10.21	8.39	6.24	4.63	3.05	7.75	6.85	5.54	4.52	3.35	3.40	3.21
04/14	5.17	8.13	6.68	5.67	4.90	5.48	2.26	4.97	4.93	4.76	1.49	2.68	3.34
07/14	5.86	6.41	7.34	6.63	6.30	3.88	4.36	1.92	5.35	5.84	-.19	2.25	3.68
10/14	4.64	5.54	6.38	8.55	8.32	2.97	4.20	5.24	3.25	7.39	1.81	1.06	3.36
13/14	4.46	6.31	8.70	10.73	13.76	2.81	4.96	7.18	8.65	3.89	3.80	3.73	.64



MODEL A: WITHOUT MID DIAPHRAGM  
 MODEL B: WITH MID DIAPHRAGM

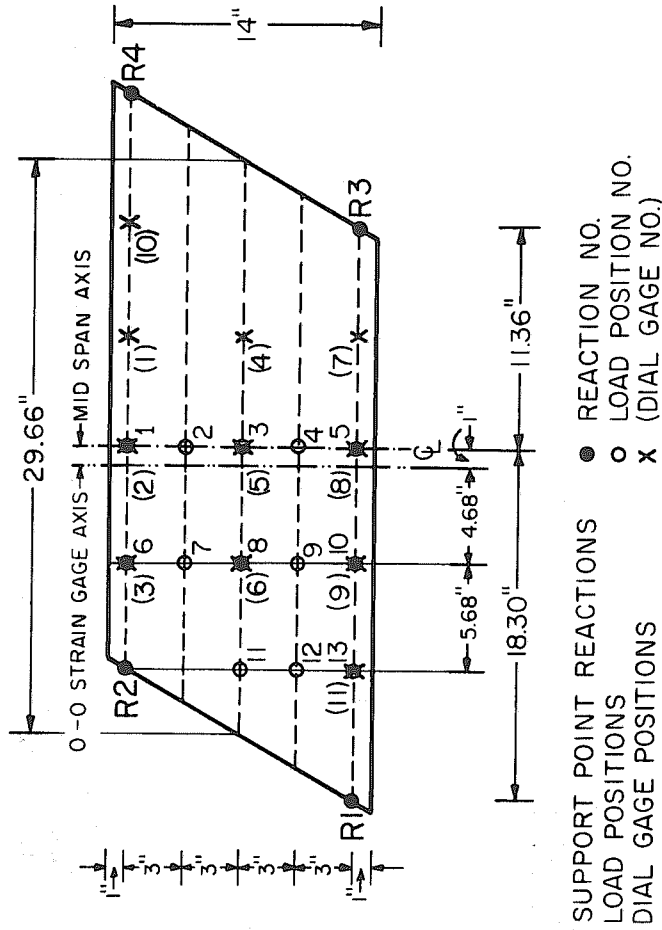


FIG.A.4 SKEW BOX GIRDER BRIDGE MODEL NO. 4,  
 SPAN=29.66 INCHES, SKEW ANGLE = 30°





ALUMINUM BOX RIGID BRIDGE MODEL STUDY

MODEL NO = +A / SPAN = 20.64 INCHES / SKEN ANGLE = 30 DEGREES / MIDSPAN DIAPHRAGM = ND

THEORETICAL RESULTS WITH MESH SIZE 6X24

NXX FORCES \*\*\* LONGITUDINAL PLATE FORCES PER UNIT WIDTH AT SECTION 0-0  
COEFFICIENTS OF W/L

		L O A D P O S I T I O N												
		1	2	3	4	5	6	7	8	9	10	11	12	13
S/B														
00/14		-11.22	-5.55	-3.68	-2.82	-2.55	-5.56	-4.73	-3.14	-2.54	-2.59	-1.02	-1.29	-1.80
01/14		-13.59	-6.32	-4.16	-3.12	-2.70	-5.32	-4.84	-3.39	-2.72	-2.66	-1.10	-1.33	-1.74
04/14		-6.31	-10.45	-5.26	-3.79	-3.24	-4.49	-4.05	-4.12	-3.32	-3.17	-1.04	-1.53	-2.02
07/14		-4.15	-5.25	-9.98	-5.38	-4.42	-2.88	-3.95	-4.02	-4.61	-4.29	-.78	-1.83	-2.57
10/14		-3.10	-3.78	-5.37	-10.68	-6.69	-2.06	-2.96	-4.44	-4.91	-6.59	-1.50	-1.72	-2.89
13/14		-2.65	-3.19	-4.37	-6.64	-13.97	-1.75	-2.58	-3.99	-5.96	-6.59	-1.99	-2.73	-2.27
14/14		-2.51	-2.91	-3.91	-5.89	-11.62	-1.65	-2.42	-3.80	-5.88	-6.82	-2.00	-2.68	-2.20

T O P P L A T E

B O T T O M P L A T E

01/14		17.26	7.04	4.57	3.22	2.46	5.88	5.79	3.80	2.82	2.54	1.28	1.41	1.81
04/14		6.85	11.01	5.36	3.80	3.18	5.00	4.18	4.17	3.31	3.13	1.03	1.51	2.02
07/14		4.32	5.32	10.27	5.44	4.59	3.02	3.99	3.99	4.68	4.46	.81	1.89	2.65
10/14		3.07	3.81	5.50	11.27	7.26	2.03	3.00	4.58	5.16	6.66	1.62	1.93	3.10
13/14		2.41	3.33	4.33	7.42	17.71	1.57	2.76	4.54	7.04	7.19	2.38	3.14	2.23



\*\*\*\*\*  
 ALUMINUM BOX GIRDER BRIDGE MODEL STUDY  
 \*\*\*\*\*

MODEL NO = 4B / SPAN = 29.64 INCHES / SKEW ANGLE = 30 DEGREES / MIDSPAN DIAPHRAGM = YES  
 THEORETICAL RESULTS WITH MESH SIZE 6X24

STATIC CHECKS

(1) RATIO OF APPLIED LOAD TO REACTIONS  
 (2) RATIO OF LONGITUDINAL TENSION TO COMPRESSION FORCE AT SECTION 0-0  
 (3) RATIO OF INTERNAL TO EXTERNAL MOMENT AT SECTION 0-0

	1	2	3	4	5	6	7	8	9	10	11	12	13
	L O A D P O S I T I O N												
(1)	1.000	1.000	1.000	1.000	1.000	1.000	1.000	1.000	1.000	1.000	1.000	1.000	1.000
(2)	1.016	.999	1.008	.999	1.015	.998	.998	1.001	.998	.997	1.004	.999	1.000
(3)	.997	.994	.997	.994	.998	1.000	.998	1.000	.998	1.000	.998	.997	1.001

REACTIONS \*\*\* COEFFICIENTS OF W

	1	2	3	4	5	6	7	8	9	10	11	12	13
	L O A D P O S I T I O N												
R1	-.126	-.025	.073	.167	.257	-.081	.057	.189	.318	.443	.347	.510	.670
R2	.743	.533	.427	.275	.126	.890	.693	.502	.315	.132	.536	.315	.097
R3	.126	.275	.427	.593	.743	.081	.193	.311	.432	.557	.153	.240	.330
R4	.257	.167	.073	-.025	-.126	.110	.057	-.002	-.065	-.132	-.036	-.065	-.097
TOTAL	1.000	1.000	1.000	1.000	1.000	1.000	1.000	1.000	1.000	1.000	1.000	1.000	1.000

\*\*\*\*\*  
 ALUMINUM BOX GIRDER BRIDGE MODEL STUDY  
 \*\*\*\*\*

MODEL NO = 4B / SPAN = 29.64 INCHES / SKEW ANGLE = 30 DEGREES / MIDSPAN DIAPHRAGM = YES  
 THEORETICAL RESULTS WITH MESH SIZE 6X24

NXX FORCES \*\*\* LONGITUDINAL PLATE FORCES PER UNIT WIDTH AT SECTION 0-0  
 COEFFICIENTS OF W/L

S/B	L O A D P O S I T I O N												
	1	2	3	4	5	6	7	8	9	10	11	12	13
00/14	-5.80	-7.01	-6.05	-5.10	-4.21	-2.82	-5.51	-4.99	-4.38	-3.87	-2.20	-2.37	-2.35
01/14	-9.37	-7.56	-6.02	-4.79	-3.82	-3.18	-5.50	-4.81	-4.06	-3.51	-2.01	-2.13	-2.09
04/14	-6.85	-6.78	-5.73	-4.92	-4.32	-4.52	-2.06	-4.23	-4.15	-4.04	-1.05	-1.95	-2.49
07/14	-5.16	-5.58	-6.18	-5.70	-5.42	-3.40	-3.80	-1.78	-4.55	-4.96	.21	-1.65	-2.91
10/14	-4.18	-4.91	-5.84	-7.02	-7.22	-2.71	-3.60	-4.41	-2.73	-5.99	-1.26	-.71	-2.78
13/14	-3.77	-4.86	-6.22	-7.87	-9.78	-2.45	-3.76	-5.20	-6.33	-3.96	-2.56	-2.85	-1.10
14/14	-4.17	-5.18	-6.26	-7.34	-6.22	-2.68	-4.02	-5.35	-6.28	-3.43	-2.71	-2.78	-.69

S/B	B O T T O M P L A T E												
	01/14	11.16	8.78	7.23	5.40	4.07	2.95	6.69	5.77	4.61	3.75	2.52	2.48
04/14	7.19	7.10	5.82	4.94	4.31	4.92	2.23	4.30	4.16	4.03	1.07	1.94	2.49
07/14	5.24	5.65	6.39	5.77	5.50	3.50	3.88	1.90	4.65	5.06	-.11	1.73	2.96
10/14	4.19	4.95	5.96	7.37	7.59	2.70	3.65	4.56	3.02	6.48	1.39	.94	2.93
13/14	4.03	5.50	7.47	9.14	11.64	2.57	4.31	6.21	7.55	3.59	3.16	3.31	.64

ALUMINUM BOX GIRDER BRIDGES MODEL STUDY

MODEL NO = 45 / SPAN = 29.64 INCHES / SKEN ANGLE = 30 DEGREES / MIDSPAN DIAPHRAGM = YES  
 THEORETICAL RESULTS WITH MESH SIZE 6X24

DEFLECTIONS \*\*\* DGP = DIAL GAGE POSITION  
 COEFFICIENTS OF 1000W/EL

DGP	1	2	3	4	5	6	7	8	9	10	11	12	13
1	4.03	3.13	2.37	1.79	1.36	2.06	1.85	1.62	1.40	1.22	.52	.63	.70
2	4.32	3.30	2.52	1.94	1.50	2.52	2.14	1.81	1.55	1.36	.61	.72	.79
3	2.51	1.95	1.50	1.19	.97	2.44	1.43	1.09	.94	.86	.33	.42	.51
4	2.22	2.26	2.28	2.05	1.81	1.28	1.45	1.58	1.63	1.62	.66	.86	.98
5	2.52	2.66	2.85	2.65	2.52	1.50	1.91	2.29	2.36	2.37	1.08	1.35	1.50
6	1.81	2.05	2.28	2.26	2.22	1.09	1.78	2.95	2.37	2.23	1.69	1.61	1.49
7	.97	1.19	1.50	1.95	2.51	.63	.92	1.28	1.67	2.06	.64	.96	1.27
8	1.50	1.94	2.52	3.30	4.32	.97	1.53	2.22	3.08	4.03	1.18	1.87	2.56
9	1.36	1.79	2.37	3.13	4.03	.86	1.44	2.23	3.39	5.41	1.27	2.29	3.75
10	2.56	2.90	1.50	1.10	.79	1.27	1.13	.98	.83	.70	.29	.35	.38
11	.79	1.10	1.50	2.00	2.56	.51	.91	1.49	2.40	3.75	.98	1.82	3.82

TOTAL LONGITUDINAL BENDING MOMENT AT MIDSPAN \*\*\* COEFFICIENTS OF WL

	1	2	3	4	5	6	7	8	9	10	11	12	13
	.207	.208	.209	.208	.207	.099	.109	.118	.125	.132	.036	.052	.067

DISTRIBUTION OF LONGITUDINAL MOMENT AT SECTION 0-0 AMONG BEAMS \*\*\* PERCENTAGE OF TOTAL MOMENT CARRIED BY EACH BEAM

BEAM NO	1	2	3	4	5	6	7	8	9	10	11	12	13
1	24.9	20.4	16.5	13.0	10.3	15.7	22.5	19.5	15.5	12.6	25.0	19.2	15.0
2	27.7	26.0	21.7	19.5	16.2	29.9	16.8	22.6	21.8	20.0	18.2	23.9	24.0
3	20.4	21.2	22.6	21.2	20.5	23.8	21.7	13.1	22.4	24.6	1.9	19.7	27.6
4	15.4	18.9	22.2	26.4	23.0	18.7	22.3	23.8	18.2	28.6	23.2	14.4	25.4
5	10.6	13.5	17.0	20.3	25.0	12.0	16.7	21.0	22.2	14.2	31.7	22.7	8.0
TOTAL	100.0	100.0	100.0	100.0	100.0	100.0	100.0	100.0	100.0	100.0	100.0	100.0	100.0

MODEL A: WITHOUT MID DIAPHRAGM

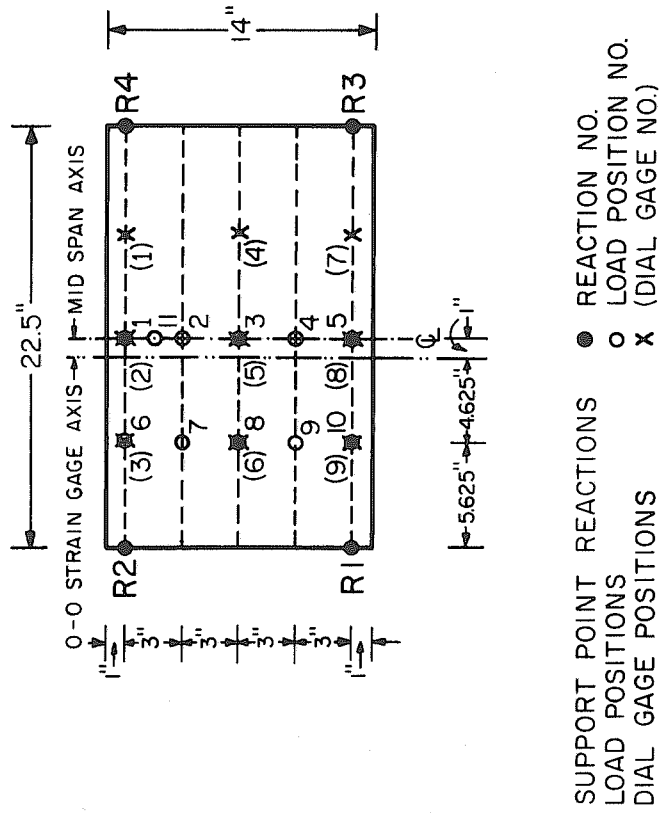


FIG. A.5 RECTANGULAR BOX GIRDER BRIDGE MODEL NO. 5,  
SPAN = 22.5 INCHES, SKEW ANGLE = 0°





\*\*\*\*\*  
 ALUMINUM BOX GIRDER BRIDGE MODEL STUDY  
 \*\*\*\*\*

MODEL NO = 5A / SPAN = 22.50 INCHES / SKEW ANGLE = 0 DEGREES / MIDSPAN DIAPHRAGM = NO  
 THEORETICAL RESULTS WITH MESH SIZE 6X16

NXX FORCES \*\*\* LONGITUDINAL PLATE FORCES PER UNIT WIDTH AT SECTION 0-0  
 COEFFICIENTS OF W/L

S/B	L O A D P O S I T I O N									
	1	2	3	4	5	6	7	8	9	10
00714	-8.66	-4.04	-2.24	-1.38	-1.18	-4.56	-3.48	-1.79	-0.99	-0.83
01714	-10.40	-4.59	-2.64	-1.67	-1.36	-4.32	-3.54	-2.01	-1.20	-0.95
04714	-4.71	-7.78	-3.60	-2.32	-1.82	-3.57	-3.02	-2.68	-1.72	-1.31
07714	-2.82	-3.67	-7.34	-3.67	-2.82	-2.11	-2.75	-2.76	-2.75	-2.11
10714	-1.82	-2.32	-3.60	-7.78	-4.71	-1.31	-1.72	-2.68	-3.02	-3.57
13714	-1.36	-1.67	-2.64	-4.59	-10.40	-0.95	-1.20	-2.01	-3.54	-4.32
14714	-1.18	-1.38	-2.24	-4.04	-8.66	-0.83	-0.99	-1.79	-3.48	-4.56

S/B	B O T T O M P L A T E									
	1	2	3	4	5	6	7	8	9	10
01714	13.31	5.24	3.00	1.73	1.09	4.88	4.37	2.37	1.25	0.77
04714	5.14	8.18	3.63	2.27	1.74	3.99	3.11	2.68	1.68	1.24
07714	2.90	3.65	7.47	3.65	2.90	2.18	2.72	2.65	2.72	2.18
10714	1.74	2.27	3.63	8.18	5.14	1.24	1.68	2.68	3.11	3.99
13714	1.09	1.73	3.00	5.24	13.31	0.77	1.25	2.37	4.37	4.88

\*\*\*\*\*  
 ALUMINUM BOX GIRDER BRIDGE MODEL STUDY  
 \*\*\*\*\*

MODEL NO = 5A / SPAN = 22.50 INCHES / SKEW ANGLE = 0 DEGREES / MIDSPAN DIAPHRAGM = NO  
 THEORETICAL RESULTS WITH MESH SIZE 6X16

DEFLECTIONS \*\*\* DGP = DIAL GAGE POSITION  
 COEFFICIENTS OF 1000K/EL

DGP	1	2	3	4	5	6	7	8	9	10
1	1.84	1.07	.60	.36	.28	1.03	.69	.42	.27	.21
2	2.91	1.53	.85	.52	.39	1.84	1.08	.61	.37	.28
3	1.84	1.07	.60	.36	.28	1.92	.85	.42	.24	.19
4	.61	1.03	1.53	1.03	.61	.42	.69	.93	.69	.42
5	.86	1.35	2.25	1.35	.86	.60	1.03	1.53	1.03	.60
6	.61	1.03	1.53	1.03	.61	.42	.69	1.77	.96	.42
7	.28	.36	.60	1.07	1.84	.21	.27	.42	.69	1.03
8	.39	.52	.85	1.53	2.91	.28	.37	.61	1.08	1.84
9	.28	.36	.60	1.07	1.84	.19	.24	.42	.85	1.92

TOTAL LONGITUDINAL BENDING MOMENT AT MIDSPAN \*\*\* COEFFICIENTS OF WL

	1	2	3	4	5	6	7	8	9	10
	.250	.250	.250	.250	.250	.125	.125	.125	.125	.125

DISTRIBUTION OF LONGITUDINAL MOMENT AT SECTION 0-0 AMONG BEAMS \*\*\* PERCENTAGE OF TOTAL MOMENT CARRIED BY EACH BEAM

BEAM NO	1	2	3	4	5	6	7	8	9	10
1	39.6	20.1	10.8	6.5	4.9	28.5	23.6	13.9	7.9	5.7
2	29.7	39.2	21.3	12.7	9.8	33.7	28.8	23.7	15.8	11.9
3	16.0	21.5	35.9	21.5	16.0	20.2	24.0	24.8	24.0	20.2
4	9.8	12.7	21.3	39.2	29.7	11.9	15.8	23.7	28.8	33.7
5	4.9	6.5	10.8	20.1	39.6	5.7	7.9	13.9	23.6	28.5
TOTAL	100.0	100.0	100.0	100.0	100.0	100.0	100.0	100.0	100.0	100.0





\*\*\*\*\*  
 ALUMINUM BOX GIRDER BRIDGE MODEL STUDY  
 \*\*\*\*\*

MODEL NO = 08 / SPAN = 69.00 INCHES / SKEW ANGLE = 0 DEGREES / MIDSPAN DIAPHRAGM = YES  
 THEORETICAL RESULTS WITH MESH SIZE 6X22

\*\*\* NXX FORCES \*\*\* LONGITUDINAL PLATE FORCES PER UNIT WIDTH AT SECTION 0-0  
 COEFFICIENTS OF W/L

1 2 3 4 5 6 7 8 9 10

S/B	T O P P L A T E									
00/14	-40.19	-42.50	-40.28	-38.49	-36.89	-19.40	-21.94	-23.40	-23.64	-23.07
01/14	-47.27	-43.48	-40.22	-37.49	-35.59	-19.60	-21.95	-23.13	-23.12	-22.48
04/14	-42.93	-42.69	-40.48	-38.59	-37.18	-21.58	-20.25	-21.92	-22.90	-22.99
07/14	-39.64	-40.51	-41.56	-40.51	-39.64	-22.78	-21.85	-20.25	-21.85	-22.78
10/14	-37.18	-38.59	-40.48	-42.69	-42.93	-22.99	-22.90	-21.92	-20.25	-21.58
13/14	-35.59	-37.49	-40.22	-43.48	-47.27	-22.48	-23.12	-23.13	-21.95	-19.60
14/14	-36.89	-38.49	-40.28	-42.50	-40.19	-23.07	-23.64	-23.40	-21.94	-19.40

S/B	B O T T O M P L A T E									
01/14	52.53	47.35	43.98	40.16	37.50	20.02	23.13	24.66	24.63	23.89
04/14	45.03	44.73	42.04	40.02	38.52	22.48	21.33	23.06	24.02	24.09
07/14	41.19	42.06	43.47	42.06	41.19	23.82	23.02	21.47	23.02	23.82
10/14	38.52	40.02	42.04	44.73	45.03	24.09	24.02	23.06	21.33	22.48
13/14	37.50	40.16	43.98	47.35	52.53	23.89	24.63	24.66	23.13	20.02

\*\*\*\*\*  
 ALUMINUM BOX GIRDER BRIDGE MODEL STUDY  
 \*\*\*\*\*

MODEL NO = 08 / SPAN = 69.00 INCHES / SKEW ANGLE = 0 DEGREES / MIDSPAN DIAPHRAGM = YES  
 THEORETICAL RESULTS WITH MESH SIZE 6X22

DEFLECTIONS \*\*\* DGP = DIAL GAGE POSITION  
 COEFFICIENTS OF 1000W/EL

DGP	1	2	3	4	5	6	7	8	9	10
1	70.55	68.22	65.84	63.89	62.35	44.35	43.05	41.93	40.96	40.14
2	105.48	100.10	95.70	92.31	89.73	70.95	68.29	65.92	63.92	62.35
3	70.95	68.22	65.84	63.89	62.35	63.76	57.25	53.16	50.50	48.93
4	65.92	65.56	65.47	65.56	65.92	41.93	41.72	41.66	41.72	41.93
5	95.71	95.32	95.49	95.32	95.71	65.84	65.53	65.48	65.53	65.84
6	65.92	65.56	65.47	65.56	65.92	53.16	53.91	56.42	53.91	53.16
7	62.35	63.89	65.84	68.22	70.95	40.14	40.96	41.93	43.05	44.35
8	89.73	92.31	95.70	100.10	105.48	62.35	63.92	65.92	68.29	70.95
9	62.35	63.89	65.84	68.22	70.95	48.93	50.50	53.16	57.25	63.76

TOTAL LONGITUDINAL BENDING MOMENT AT MIDSPAN \*\*\* COEFFICIENTS OF WL

	1	2	3	4	5	6	7	8	9	10
	.250	.250	.250	.250	.250	.125	.125	.125	.125	.125

DISTRIBUTION OF LONGITUDINAL MOMENT AT SECTION O-O AMONG BEAMS \*\*\* PERCENTAGE OF TOTAL MOMENT CARRIED BY EACH BEAM

BEAM NO	1	2	3	4	5	6	7	8	9	10
1	18.3	17.0	15.8	14.8	14.0	14.2	15.6	16.6	16.7	16.3
2	24.4	23.9	22.6	21.7	20.9	22.2	21.4	22.7	23.7	23.8
3	22.3	22.6	23.0	22.6	22.3	23.5	22.6	21.5	22.6	23.5
4	20.9	21.7	22.6	23.9	24.4	23.8	23.7	22.7	21.4	22.2
5	14.0	14.8	15.8	17.0	18.3	16.3	16.7	16.6	15.6	14.2
TOTAL	100.0	100.0	100.0	100.0	100.0	100.0	100.0	100.0	100.0	100.0